NASA TECHNICAL NOTE

NASA TN D-7664

NASA TN D-7664

EXPERIMENTAL INVESTIGATION OF THE LANDING DYNAMICS OF THREE-LEGGED SPACECRAFT MODELS

by Sandy M. Stubbs

Langley Research Center
Hampton, Va. 23665

NATIONAL AERONAUTICS AND SPACE ADMINISTRATION • WASHINGTON, D. C. • SEPTEMBER 1974

1. Report No.	2. Government Accession No.	3. Recipient's Catalog No.
NASA TN D-7664		

4. Title and Subtitle	5. Report Date
EXPERIMENTAL INVESTIGATION OF THE LANDING DYNAMICS OF THREE-LEGGED SPACECRAFT MODELS	September 1974
	6. Performing Organization Code
7. Author(s)	8. Performing Organization Report No.
Sandy M. Stubbs	L-9499
	10. Work Unit No.
9. Performing Organization Name and Address	501-38-18-02
NASA Langley Research Center Hampton, Va. 23665	11. Contract or Grant No.
	13. Type of Report and Period Covered
12. Sponsoring Agency Name and Address	Technical Note
National Aeronautics and Space Administration Washington, D.C. 20546	14. Sponsoring Agency Code

15. Supplementary Notes

Technical film supplement L-1151 is available on request.

16. Abstract

An experimental investigation was conducted to obtain accurate data from two three-legged spacecraft landing systems for purposes of validating current and future computer programs for legged landers. Two landing-gear systems were investigated: an inverted tripod system and a cantilever system. Tests were conducted for eight landing conditions chosen to obtain stability data, maximum loads, and maximum strokes for correlation with analytical results. Data from the two models are not directly comparable because of geometry and mass differences, but both are considered to be typical models of the respective landing-gear systems.

Results indicate that maximum accelerations for both models, which occurred during a nearly flat landing on a horizontal surface, were nearly the same (approximately -18g). Maximum primary strut forces occurred for landings into a 20° slope and were 40 kN (9000 lbf) and 47 kN (10 500 lbf) for the inverted tripod and cantilever models, respectively; and maximum primary strut strokes for both models were 19 cm (7.4 in.). The inverted tripod model was slightly more stable than the cantilever model because of a larger ratio of footpad radius to center-of-gravity height.

17. Key Words (Suggested by Author(s))	18. Distribution Statement
Spacecraft landing Computer program validation Three-legged landing gear systems	Unclassified – Unlimited STAR Category 02

19. Security Classif. (of this report)	20. Security Classif. (of this page)	21. No. of Pages	22. Price*
Unclassified	Unclassified	78	$4.00

*For sale by the National Technical Information Service, Springfield, Virginia 22151

EXPERIMENTAL INVESTIGATION OF THE LANDING DYNAMICS OF THREE-LEGGED SPACECRAFT MODELS

By Sandy M. Stubbs
Langley Research Center

SUMMARY

An experimental investigation was conducted to obtain accurate data from two three-legged spacecraft landing systems for purposes of validating current and future computer programs for legged landers. Two landing-gear systems were investigated: an inverted tripod system and a cantilever system. Tests were conducted for eight landing conditions chosen to obtain stability data, maximum loads, and maximum strokes for correlation with analytical results. Data from the two models are not directly comparable because of geometry and mass differences, but both are considered to be typical models of the respective landing-gear systems.

Results indicate that maximum accelerations for both models, which occurred during a nearly flat landing on a horizontal surface, were nearly the same (approximately -18g). Maximum primary strut forces occurred for landings into a 20° slope and were 40 kN (9000 lbf) and 47 kN (10 500 lbf) for the inverted tripod and cantilever models, respectively; and maximum primary strut strokes for both models were 19 cm (7.4 in.). The inverted tripod model was slightly more stable than the cantilever model because of a larger ratio of footpad radius to center-of-gravity height.

INTRODUCTION

In the past, legged lander computer programs were developed to analyze a specific landing-gear design. Although these programs were adequate in predicting results for a specific vehicle, they were limited in their ability to analyze other landing system configurations. Accurate experimental data are needed on a variety of legged landing systems to evaluate existing legged lander analytical programs and to validate future more comprehensive landing dynamics programs. Although investigations have been previously made of three-, four-, and five-legged vehicles for use in planetary exploration (refs. 1 to 8), little quantitative data have been published for three-legged landing systems which use inverted tripod or cantilever landing-gear systems with shock-absorbing capability in all three of the strut members. Although there is a need for systematic quantitative data on several

landing systems for computer program validation, the two systems reported herein were chosen because they were proposed landing systems for early versions of the Viking spacecraft.

The primary purpose of this investigation was to obtain accurate quantitative experimental data for computer program correlation. The secondary purpose was to obtain data to aid in the design of the Viking spacecraft. Inverted tripod and cantilever landing-gear systems were tested on 3/8-scale models of the proposed Viking spacecraft at eight widely varying landing conditions chosen to validate stability results, maximum loads, and maximum strokes. Time history data are presented as well as maximum value data, and a film supplement (L-1151) is also available on request. A request card and a description of the film will be found at the back of this paper. The accurate experimental results from this investigation provide a part of a data base for validating the adequacy and accuracy of present and future analytical landing programs.

SYMBOLS

The units used for the physical quantities defined in this paper are given first in the International System of Units and parenthetically in the U.S. Customary Units. Measurements and calculations were made in the U.S. Customary Units.

A	area, m^2 (ft^2)
a	acceleration, m/s^2 (ft/s^2)
F	force, N (lbf)
g	gravitational acceleration, 9.81 m/s^2 (32.2 ft/s^2)
I	inertia, kg-m^2 (slug-ft^2)
I_X	roll moment of inertia, kg-m^2 (slug-ft^2)
I_Y	pitch moment of inertia, kg-m^2 (slug-ft^2)
I_Z	yaw moment of inertia, kg-m^2 (slug-ft^2)
k	spring constant, MN/m (lbf/in.)
l	length, m (ft)

m	mass, kg (slugs)
t	time, s
V_h	horizontal velocity, m/s (ft/s)
V_v	vertical velocity, m/s (ft/s)
v	velocity, m/s (ft/s)
X,Y,Z	body axes
β	gravity ratio
λ	geometric scale factor
σ	stress, N/m^2 (lbf/in^2)
μ	friction coefficient

DESCRIPTION OF MODELS

Two dynamic models of unmanned legged lander spacecraft were used in the investigation. One model consisted of a center body equipped with an inverted tripod landing gear and the other consisted of the same center body but with a cantilever landing gear attached. These landing systems were selected because they were being considered early in the design phase as landing-gear designs for the Viking spacecraft.

Scaling Laws

The scale relationships pertinent to the investigation are presented in table I, and measured parameters for the model and full-scale vehicle are given in tables II and III. Both models used the same scale relationships. The scale factors for the quantities shown with the double asterisk (table I) were chosen to provide a suitable model for small-scale testing. The geometric scale factor $\left(\lambda = \frac{3}{8} = \frac{1}{2.66}\right)$ was selected to facilitate construction, size, and mass requirements and also for convenience in performing the tests. Since the tests were to be conducted in the Earth gravity environment, and it was desirable to convert data to values that would result from a full-scale vehicle landing on Mars, accelerations vary as the ratio of Earth gravity to Mars gravity (designated β). Force was chosen to vary as the cube of the scale factor, that is, λ^3. With these three scale relationships fixed, other pertinent scale relationships were derived from the laws of physics.

Test Model Body

Photographs of the two models are shown in figure 1. The coordinate system shown in the figure is a body-fixed coordinate system. The primary structural frame was the same for both models and was made of welded aluminum tubing, sufficiently light to allow additional ballast weight for obtaining the correct masses, center-of-gravity location, and moments of inertia. The structural frame was designed to minimize effects of center-body elasticity. The center of gravity for both models was established at the same location within the body structure, but because of different landing-gear geometries, the height of the center of gravity above the ground line was different.

Landing Gear

The general arrangements of the inverted tripod model and cantilever model are shown in figures 2 and 3, respectively; and landing-gear strut designations (1A, 1B, etc.) are shown. Dimensional values given are full scale. More detailed photographs of a single landing-gear leg for the inverted tripod and cantilever models are presented in figure 4. The following sections describe these gears in detail.

Inverted tripod.- A single inverted tripod landing leg consisted of a primary strut and two secondary struts all connected at a footpad interface. All struts were attached to the model body with universal joint fittings. At the apex of the inverted tripod, one secondary strut was attached with a universal joint and the other secondary strut was attached with a single pivot connection to an apex fitting. (See fig. 4(a).) These attachments allow complete freedom of motion of the footpad.

A stiff flat-bottom, non-shock-absorbing footpad was attached to the bottom of the tripod by a ball joint which allowed the pad free pitching movements and 360° of rotation. All landing-gear components, except the ball joints, sockets, and attachment fittings, were made of 6061-T6 aluminum. The ball joints, sockets, and fittings were made of 17-4 PH steel.

The primary strut shock absorber for this gear was a simple piston-cylinder arrangement as shown by the sketch in figure 5. The cylinder had a centering rod held in place at the top of the strut by a thin disk. The centering rod, which positioned and held crushable honeycomb elements, passed freely through a hole in the center of the piston. Four aluminum honeycomb, energy-absorbing cartridges were used in each primary strut separated by thin disks to insure proper crushing of each stage. These cartridges were crushed in compression (accordionlike column failure) by the landing loads imposed upon the telescoping landing-gear strut. Each cartridge was designed to crush at a predetermined force level which remained approximately constant during the strut stroke. A typical dynamic force-stroke history of the staged crush loads obtained during

an actual model landing is also presented in figure 5. The solid line was obtained from a primary strut and includes strut friction forces. The dashed curve was the nominal force stroke curve obtained from preliminary experimental testing.

The secondary struts were equipped with two aluminum honeycomb cartridges: one for compression and the other for tension force attenuation. Details of the secondary strut shock absorber are presented in figure 6. The compression cartridge was held in place by recesses in the piston and cylinder heads and the tension cartridge completely filled its cylinder cavity. Typical force time histories for both cartridges are also presented in the figure. Force is presented here as a function of time instead of stroke since the latter was not measured on these struts. The tension force time history was obtained by dropping a 4.64 kg (0.318 slug) at mass 1.5 m/s (5.0 ft/s) onto the bare honeycomb cartridge. The compression force time history was obtained by dropping a 11.3 kg (0.776 slug) at mass 2.86 m/s (9.37 ft/s) onto the vertically oriented assembled strut in which the honeycomb cartridge had been previously installed. Thus, strut friction forces are included in the axially applied compression force time history.

Nominal crush loads and strokes for both the primary and secondary struts of the inverted tripod model gear are given in table II.

Cantilever.- The cantilever landing-gear leg consisted of a primary strut and two secondary struts that interfaced with the primary strut at the lower end of its cylinder so that the piston rod was cantilevered with a non-shock-absorbing footpad on the end. (See fig. 4(b).) All the struts were attached to the body with a swivel and pin arrangement that allowed three-dimensional stroking of the leg. The secondary struts were attached to the primary strut with a pinned ball joint connection allowing sufficient freedom of motion for maximum stroking of the leg assembly. The footpad was attached to the end of the cantilever strut by a ball joint. Additional details and photographs of the cantilever gear can be found in reference 4.

Typical force-stroke histories for the two-stage compressive primary strut obtained from actual model landing tests are shown in figure 7(a). The solid line was obtained from experimental data, and the dashed line presents nominal values of force and stroke obtained from preliminary tests. Typical experimentally determined compression and tension secondary strut force-stroke histories are shown in figures 7(b) and 7(c), respectively, along with nominal values (dashed lines). All experimental data shown in figure 7 have strut friction forces included with honeycomb crush forces. Nominal crush loads and strokes for both the primary and secondary struts of the cantilever model are given in table III. The crushable honeycomb cartridges, used in both models, were precrushed a small distance prior to installation in the landing gears to alleviate the peak load associated with initiation of crushing.

APPARATUS AND PROCEDURE

Launch Equipment

A sketch illustrating operation of the pendulum launch apparatus is shown in figure 8. The pendulum launcher, with the model installed at the desired attitude, was released from a predetermined pullback height to produce the desired horizontal velocity at the lowest point of the swing when the model was released. The predetermined free-fall height produced the desired vertical velocity at model touchdown. A photograph of the launch apparatus is shown in figure 9. The experimental tests were conducted in the Langley impacting structures facility.

Landing Surface

The landing surface, shown sloped 20° in figure 10, was of stiff wood frame construction covered with smooth plywood 1.9 cm (0.75 in.) thick, 1.8 m (6 ft) wide, and 3.7 m (12 ft) long. One end of the surface was raised to obtain various slope conditions. Surface slopes are considered to be negative when the slope of the landing surface is in the same general direction as the slope of the resultant velocity vector.

The friction coefficients at the footpad-surface interface were determined by sliding a single footpad, loaded to approximately the weight of the model, on a flat plywood surface similar to that of the landing surface. The friction coefficient was computed by dividing the total weight of the footpad into the horizontal force necessary to slide the footpad at a slow, relatively constant, velocity once static friction had been overcome. The coefficients obtained by this method were later verified by sliding the model down the inclined landing surface. A nominal coefficient of friction of approximately 0.4 was obtained with the aluminum footpad sliding on a plywood surface. A higher friction coefficient, nominally 0.8, was obtained on the plywood when the bottom of the footpad was covered with a thin sheet of rubber.

Test Parameters

Sketches which identify the vehicle axes, acceleration directions, attitudes, and flight path are presented in figure 11. Accelerations in the direction of the negative axes are considered as negative accelerations. Both vertical and horizontal velocities are treated as positive even though the horizontal velocity component is sometimes in the direction of the negative Z-axis. The principal forces and strokes in the primary shock-absorbing struts are compression and are considered to be positive. In the secondary struts, however, tension forces and strokes are considered as positive and compression forces and strokes as negative.

The procedure used for setting up the vehicle attitude for a test was as follows: With the model X-axis alined with the gravity vector and leg 1 pointing in the direction of the horizontal velocity, the model was rolled about the X-axis to the desired roll attitude. The model was then pitched about the Y-axis with leg 1 down being negative pitch and leg 1 up being positive pitch. Finally, the yaw angle was set with leg 2 down being right yaw and leg 2 up being left yaw.

Landings were made at touchdown pitch attitudes ranging from -16° to 15°. Nominal pitch conditions were -15°, 0°, and 15°. Roll attitudes with one exception were either 0° or 180°. Measurements show a scatter of yaw attitudes from 2° left yaw to 2° right yaw. Nominal vertical impact velocity was 7 m/s (23 ft/s) and nominal horizontal velocity was 0 or 2 m/s (0 or 6 ft/s). Landings were made on slopes of 0°, -20°, and 20°. Two different nominal friction coefficients were used in the investigation: 0.4 and 0.8. It was difficult to obtain identical runs for the two models, but most runs had only small differences in test conditions.

The reading accuracies of the various landing condition parameters are as follows:

Pitch, roll, and yaw attitudes	$\pm 0.5^{\circ}$
Vertical and horizontal velocities	± 0.03 m/s (± 0.1 ft/s)
Landing surface slope	$0^{\circ} \pm 10'$
Friction coefficient (estimated)	± 0.1

Instrumentation and Data Reduction

Normal, longitudinal, and transverse accelerations were measured at or near the model center of gravity by rigidly mounted piezoresistive strain-gage accelerometers. Three additional accelerometers were used at remote locations. Table IV gives the coordinates and a description of the various accelerometers. The strokes of the primary struts of both models and secondary strut of the cantilever model were measured by means of linear potentiometers. Only maximum stroke data were obtained for the secondary struts of the inverted tripod model by measuring the crushed honeycomb elements after each run. All struts of each leg of both models were equipped with strain gages calibrated to measure force. The signals from the accelerometers, potentiometers, and strain gages were transmitted through trailing cables to frequency-modulated magnetic tape recorders. The limiting flat frequency response of the accelerometers and potentiometers with the associated recording equipment was 1000 Hz. The limiting response for the strain-gage force measurements was 5000 Hz. In the process of data reduction, the acceleration and stroke data were passed through 300-Hz low-pass filters and the force data through 880-Hz low-pass filters to eliminate undesirable high-frequency structural oscillations. The data were digitized by using a sample rate of 2000 samples per second and stored on tapes which were processed to obtain printouts and plots of the data.

Motion pictures (taken at 64 and 200 frames per second) were used to determine landing attitudes, touchdown velocities, and motions. A video camera, tape recorder, and video receiver were used to obtain an immediate review of the test conditions and landing behavior.

RESULTS AND DISCUSSION

The data obtained in this investigation are presented as time histories in figures 12 to 18 for the inverted tripod model and in figures 19 to 25 for the cantilever model. These histories include the accelerations at the center of gravity, force in the primary and secondary struts of each leg, and stroke in all primary and some secondary struts. The maximum values of these parameters are summarized in tables V and VI together with comments relative to the stability characteristics of the models at each test condition. To aid in understanding these histories, one for each model has been selected for discussion. General comments on model impact loads and landing behavior are presented in subsequent sections. All data are presented in full-scale values.

Time History Data

Typical acceleration, stroke, and force time histories are shown in figure 26 for the inverted tripod and in figure 27 for the cantilever model. The data are presented for both models landing at run 4 conditions (tables V and VI): nominally at a vertical velocity of 6.85 m/s (22.5 ft/s); horizontal velocity of 2 m/s (6 ft/s); pitch, -15°; roll, 180°, and slight right yaw. The friction coefficient was approximately 0.4, and the models were landed on a -20° slope.

For the inverted tripod model, the force and stroke data indicated that leg 1 (the trailing leg) hit initially. During the crushing of the no. 1 gear, compression forces occurred in secondary struts 1B and 1C. (See fig. 26(b).) After leg 1 crushed, the model rebounded slightly so that leg 1 was clear of the surface; and the model rotated downward with legs 2 and 3 hitting at a time of approximately 0.22 second. The dashed lines for primary struts 2A and 3A illustrate that for this run, three stages of honeycomb cartridges in legs 2 and 3 crushed, and the force was rising to the fourth-stage crush level before the impact energy was absorbed. The dashed lines are used here to indicate only the nominal force of the various stages. Maximum accelerations, maximum forces, and strokes for this test occurred when legs 2 and 3 hit.

As indicated by the sketches in figure 27, the cantilever model had a landing sequence of events similar to those of the inverted tripod model. The maximum normal and longitudinal accelerations for this case were -9g and -5g, respectively, and occurred when legs 2 and 3 hit. The spikes at the beginning of each primary strut force curve (fig. 27(c) and (c) part of figs. 19 to 25) are attributed to friction in the cantilevered

primary strut. Typical fairings of the force data for the cantilever primary struts are shown in the figure, and the faired values are presented in table VI. After the initial spike in the force curves, the force drops off to the crush level of the first-stage honeycomb element and then rises toward the end of the force curve as the first honeycomb element bottoms and the load builds toward second-stage crushing. Typical secondary strut action is shown by strut 3B. (See figs. 27(b) and 27(c).) For the condition being discussed (run 4), strut 3B reaches a maximum tension force of 13 kN (3000 lbf) and strokes of 3.8 cm (1.5 in.). Secondary strut 3C shows a similar trend but in a negative (compression) direction.

Landing Accelerations and Forces

Maximum center-of-gravity accelerations as given in tables V and VI are summarized in figures 28 and 29 for both the inverted tripod and the cantilever models, respectively. The figures show that for similar test conditions, the maximum normal accelerations incurred by the cantilever model were approximately the same as those of the inverted tripod. The highest normal acceleration, -20g for the cantilever and -18g for the inverted tripod, occurred for the case where the model lands nearly flat on a hard horizontal surface. Longitudinal and lateral accelerations had maximum values that were both positive and negative. The maximum longitudinal accelerations for the inverted tripod model ranged from -9g to 7g and for the cantilever model, -7g to 7g. The maximum lateral accelerations ranged from -6g to 8g for the inverted tripod model and from -8g to 6g for the cantilever model.

The maximum landing-gear forces which were limited by the crush force of the shock-absorbing elements are summarized in figures 30 and 31 for the inverted tripod and cantilever models, respectively. These forces were obtained from data which were faired (see fig. 27(c)) and strut 1A data (fig. 26(b)) to negate obvious structural elastic responses. Maximum primary strut forces experienced by the inverted tripod model ranged from 16 kN to 40 kN (3600 lbf to 9000 lbf); and those for the cantilever model were somewhat higher and ranged between 27 kN and 47 kN (6000 lbf and 10 500 lbf) because of the friction spikes. The secondary struts had both positive and negative forces which ranged between ±22 kN (±5000 lbf) for the inverted tripod model and between ±16 kN (±3600 lbf) for the cantilever model.

Landing Behavior

Maximum landing-gear stroke data for both models are presented in figures 32 and 33 for the inverted tripod and cantilever models, respectively. For the eight landing conditions examined, the maximum primary strut strokes for the inverted tripod model ranged from 6.6 cm to 19 cm (2.6 in. to 7.5 in.) and those for the cantilever model from

6.4 cm to 19 cm (2.5 in. to 7.5 in.). Although the ranges of values for the two models were about the same, this is not meant to imply that the magnitudes were comparable for each test condition. The secondary strut strokes for the inverted tripod model were ±3 cm (±1.2 in.) or less except for cases 7 and 8 where the vehicle landed into a 20° slope. For cases 7 and 8, maximum secondary strut stroking was -14 cm (-5.6 in.) and -15 cm (-5.8 in.), respectively. Maximum secondary strut strokes for the cantilever model ranged from ±8 cm (±3 in.). Here again the maximum values occurred for cases 7 and 8 with the vehicle landing into a 20° slope.

The inverted tripod model was stable for all conditions tested. The cantilever model was stable for all conditions except when landed downslope with a friction coefficient of 0.8, one gear trailing, and pitched down 15° (case 5). A test made at nearly the same conditions as that of case 5, but with the friction coefficient reduced to 0.4, resulted in a stable run. A pitch time history plot for each model tested at case 5 conditions is presented in figure 34, together with sketches which illustrate the attitude of the models with respect to the landing surface. For both models, the trailing leg (leg 1) initially impacted the surface and the vehicle pitched to approximately 25° in approximately 0.25 second, and legs 2 and 3 then impacted the surface with leg 1 in the air. The model pitch direction changed as the legs stroked, and the trailing leg (leg 1) again contacted the surface at the times identified by the arrows (0.3 sec and 0.36 sec, respectively, for the cantilever and inverted tripod models). The pitch attitude for the inverted tripod model did not change appreciably as the model slid down the 20° slope and maintained an attitude of approximately 22°. The cantilever model, however, showed a slight pitch oscillation as it slid down the 20° slope, and then the sliding friction caused the trailing gear to lift free of the surface and a turnover occurred. One explanation for the better stability exhibited by the inverted tripod model is its larger ratio of footpad radius to center-of-gravity height (2.29 as compared with 1.73 for the cantilever model).

CONCLUDING REMARKS

Accurate results are presented from dynamic model studies of inverted tripod and cantilever landing-gear systems tested at eight widely varying landing conditions in order to obtain data for computer correlation. Data from the two models are not directly comparable because of geometry and mass differences, but both models are considered to be typical models of their respective landing-gear systems.

Results indicate that maximum accelerations for both models were nearly the same (approximately -18g) which occurred during a nearly flat landing on a horizontal surface. Maximum primary strut forces occurred for landings into a 20° slope and were 40 kN

(9000 lbf) and 47 kN (10 500 lbf) for the inverted tripod and cantilever models, respectively; and maximum primary strut strokes for both models were 19 cm (7.4 in.).

The inverted tripod model was more stable than the cantilever model because of a larger ratio of footpad radius to center-of-gravity height.

Langley Research Center,
National Aeronautics and Space Administration,
Hampton, Va., April 16, 1974.

REFERENCES

1. Blanchard, Ulysse J.: Characteristics of a Lunar Landing Configuration Having Various Multiple-Leg Landing-Gear Arrangements. NASA TN D-2027, 1964.

2. Herr, Robert W.; and Leonard, H. Wayne: Dynamic Model Investigation of Touchdown Stability of Lunar-Landing Vehicles. NASA TN D-4215, 1967.

3. Blanchard, Ulysse J.: Evaluation of a Full-Scale Lunar-Gravity Simulator by Comparison of Landing-Impact Tests of a Full-Scale and a 1/6-Scale Model. NASA TN D-4474, 1968.

4. Anon.: Lunar Module (LM) Soil Mechanics Study. Vol. II. AM-68-1 (Contract No. NAS 9-5759), Bendix Corp., May 1, 1968. (Available as NASA CR-92215.)

5. Blanchard, Ulysse J.; and Stubbs, Sandy M.: Martian Gravity Simulator for Full-Scale Viking Landing Tests. Space Simulation, NASA SP-298, 1972, pp. 629-646.

6. McGehee, John R.; and Stubbs, Sandy M.: Experimental Validation of a Landing Dynamics Computer Program for Legged Spacecraft Landers. NASA TN D-7301, 1973.

7. Deitrick, R. E.; and Jones, R. H.: Surveyor Spacecraft System – Touchdown Dynamics Study (Preliminary Report). SSD 3030R (JPL) 950056), Hughes Aircraft Co., Jan. 1963.

8. Stubbs, Sandy M.: Investigation of Technique for Conducting Landing-Impact Tests at Simulated Planetary Gravity. NASA TN D-6459, 1971.

TABLE I.- SCALE RELATIONSHIPS FOR SCALING MODEL RESULTS OBTAINED IN EARTH'S GRAVITY FIELD TO FULL-SCALE RESULTS IN MAR'S GRAVITY FIELD

[Gravitational* scale factor, $\beta = \frac{8}{3} = 2.66$; geometric scale factor, $\lambda = \frac{3}{8} = \frac{1}{2.66}$]

Quantity	3/8-scale experimental model	Scale factor	Full-scale Mars vehicle
Length**	l	$1/\lambda$	l/λ
Linear acceleration**	a	$1/\beta$	a/β
Force**	F	$1/\lambda^3$	F/λ^3
Area	A	$1/\lambda^2$	A/λ^2
Mass	m	β/λ^3	$m\beta/\lambda^3$
Moment of inertia	I	β/λ^5	$I\beta/\lambda^5$
Time	t	$1/\lambda$	t/λ
Speed	v	$\sqrt{\frac{1}{\beta} \times \frac{1}{\lambda}} = 1$	v
Stress	σ	$1/\lambda$	σ/λ
Spring constant	k	$1/\lambda^2$	k/λ^2

*The acceleration of gravity on Mars was assumed to be 3.69 m/sec^2 (12.1 ft/sec^2) and that on Earth to be 9.82 m/sec^2 (32.2 ft/sec^2) for this investigation.

**Scale factors which determine remaining scale relationships.

TABLE II.- PERTINENT MEASURED PARAMETERS OF 1/2.66-SCALE INVERTED TRIPOD MODEL

Parameter	1/2.66-scale model	Full scale
Mass, kg (slugs)	11.3 (0.772)	563 (38.6)
Moment of inertia, kg-m^2 (slug-ft^2):		
I_X roll	0.988 (0.729)	350 (258)
I_Y pitch	0.495 (0.365)	175 (129)
I_Z yaw	0.476 (0.351)	168 (124)
Body:		
Center-of-gravity height, m (in.)	0.248 (9.77)	0.660 (26.0)
Landing-gear radius, m (in.)	0.5685 (22.38)	1.51 (59.5)
Nominal unsprung mass of single landing gear, kg (slugs)	0.4466 (0.0306)	22.36 (1.532)
Nominal landing-gear strut stroke, m (in.):		
Primary, first stage	0.035 (1.39)*	0.094 (3.69)
Primary, second stage	0.013 (0.50)	0.034 (1.34)
Primary, third stage	0.013 (0.50)	0.034 (1.34)
Primary, fourth stage	0.072 (2.83)	0.192 (7.54)
Secondary, compression	0.082 (3.23)	0.218 (8.59)
Secondary, tension	0.014 (0.54)	0.036 (1.4)
Nominal honeycomb-cartridge dynamic crush force, N (lbf) ±10%:		
Primary, first stage	471 (106)	9000 (2000)
Primary, second stage	707 (159)	13 000 (3000)
Primary, third stage	943 (212)	18 000 (4000)
Primary, fourth stage	1890 (425)	36 000 (8000)
Secondary, compression	800 (180)	15 000 (3400)
Secondary, tension	632 (142)	11 900 (2670)

*Assumed to be 90 percent of honeycomb-cartridge length.

TABLE III.- PERTINENT MEASURED PARAMETERS OF 1/2.66-SCALE CANTILEVER MODEL

Parameter	1/2.66-scale model	Full scale
Mass, kg (slugs)	12.7 (0.871)	636 (43.6)
Moment of inertia, kg-m^2 (slug-ft^2):		
I_X roll	1.46 (1.08)	519 (383)
I_Y pitch	1.0 (0.76)	365 (269)
I_Z yaw	1.4 (0.75)	361 (266)
Body:		
Center-of-gravity height, m (in.)	0.3777 (14.87)	1.005 (39.55)
Landing-gear radius, m (in.)	0.6502 (25.76)	1.740 (68.52)
Nominal unsprung mass of single landing gear, kg (slugs)	0.482 (0.033)	24.1 (1.65)
Nominal landing-gear strut stroke, m (in.):		
Primary, first stage	0.074 (2.93)*	0.198 (7.79)
Primary, second stage	0.050 (1.98)	0.681 (5.27)
Secondary compression	0.036 (1.40)	0.094 (3.72)
Secondary tension, first stage	0.015 (0.61)	0.04 (1.6)
Secondary tension, second stage	0.051 (2.00)	0.135 (5.32)
Nominal honeycomb-cartridge dynamic crush force, N (lbf) ±10%:		
Primary, first stage	1000 (230)	19 000 (4300)
Primary, second stage	1700 (390)	32 000 (7300)
Secondary compression	710 (160)	13 000 (3000)
Secondary tension, first stage	180 (41)	3400 (770)
Secondary tension, second stage	710 (160)	13 000 (3000)

*Assumed to be 90 percent of honeycomb-cartridge length.

TABLE IV.- ACCELEROMETER LOCATIONS WITH RESPECT TO CENTER OF GRAVITY

[All values are full scale]

Accelerometer	No.	Measurement direction	Coordinates, cm (in.)		
			x	y	z
Normal	1	X-axis	0	0	0
Longitudinal	2	Parallel to Z-axis	-5.74 (-2.26)	0	0
Transverse	3	Parallel to Y-axis	-10.46 (-4.12)	0	0
Longitudinal	4	Parallel to Z-axis	28.85 (11.36)	0	0
Transverse	5	Parallel to Y-axis	24.13 (9.50)	0	0
Transverse	6	Parallel to Y-axis	24.13 (9.50)	0	87.83 (34.58)

TABLE V.- MAXIMUM ACCELERATIONS, STROKES AND FORCES FOR LANDINGS OF INVERTED TRIPOD MODEL

[All values are full scale (Mars prototype); R, right yaw (leg 2 down); L, left yaw (leg 3 down); C, compression; T, tension]

(a) SI Units

Run	Vertical velocity, m/s	Horizontal velocity, m/s	Landing attitude in –			Surface slope, deg	Friction coefficient, μ	Maximum acceleration at center of gravity, Earth g units			Stability
			Pitch, deg	Roll, deg	Yaw, deg			Normal	Longitudinal	Lateral	
1	7.074	0	0	0	0	0	0.4	-18	4, -4	-3, 2	Stable
2	7.084	2	10	180	.5L	-20	.4	-13	-4, 5	-5, 4	Stable
3	7.123	2	-2	180	1.0L	-20	.4	-10	-7, 4	-4, 3	Stable
4	6.849	2	-16	180	2.0R	-20	.4	-8	-7, 4	5, -4	Stable
5	6.849	2	-15	180	1.0R	-20	.8	-8	-9, 4	8, -2	Stable
6	7.074	2	2	30L	1.0R	-20	.4	-10	4, -6	-6, 5	Stable
7	6.910	2	-11.5	0	0	20	.4	-8	-8, 6	-5, 5	Stable
8	7.096	2	12	180	0	20	.4	-10	7, -4	-2, 2	Stable

Run	Vertical velocity, m/s	Horizontal velocity, m/s	Landing attitude in –			Surface slope, deg	Friction coefficient, μ	Maximum strut stroke, centimeters, for –													
								Gear 1					Gear 2					Gear 3				
			Pitch, deg	Roll, deg	Yaw, deg			Strut 1A	Strut 1B		Strut 1C		Strut 2A	Strut 2B		Strut 2C		Strut 3A	Strut 3B		Strut 3C	
								C	C	T	C	T	C	C	T	C	T	C	C	T	C	T
1	7.074	0	0	0	0	0	0.4	18	0	0	0	0	18	-0.3	0	0	0	17	-0.3	0	-0.5	0
2	7.084	2	10	180	.5L	-20	.4	11	0	0	0	0	19	0	.5	0	2.8	18	-.3	.8	-.3	.3
3	7.123	2	-2	180	1.0L	-20	.4	12	-.3	0	0	0	15	0	0	-.3	1.5	17	-.3	1.5	0	0
4	6.849	2	-16	180	2.0R	-20	.4	8.1	-3.3	0	-3.3	0	15	0	0	0	.5	16	0	1.8	-.8	0
5	6.849	2	-15	180	1.0R	-20	.4	12	-1	0	-1	0	13	.3	0	-.3	.8	15	0	.8	-1	0
6	7.074	2	2	30L	1.0R	-20	.4	17	0	0	0	.3	13	-3.0	0	-.3	.5	10	0	0	-.3	0
7	6.910	2	-11.5	0	0	20	.4	10	-14	0	-13	0	15	-2.8	0	-.3	.8	14	0	0	-.3	0
8	7.096	2	12	180	0	20	.4	6.6	0	0	0	.3	16	-7.9	0	0	3.3	15	0	2.3	-15	0

Run	Vertical velocity, m/s	Horizontal velocity, m/s	Landing attitude in –			Surface slope, deg	Friction coefficient, μ	Maximum strut forces, kN, for –													
								Gear 1					Gear 2					Gear 3				
			Pitch, deg	Roll, deg	Yaw, deg			Strut 1A	Strut 1B		Strut 1C		Strut 2A	Strut 2B		Strut 2C		Strut 3A	Strut 3B		Strut 3C	
								C	C	T	C	T	C	C	T	C	T	C	C	T	C	T
1	7.074	0	0	0	0	0	0.4	38	-11	11	-8.9	6.7	33	-15	6.7	-12.	11	39	-16	13	-11	6.2
2	7.084	2	10	180	.5L	-20	.4	16	-14	13	-5.3	6.7	38	-13	13	-12	13	36	-13	14	-13	14
3	7.123	2	-2	180	1.0L	-20	.4	18	-16	9.3	-18	6.7	27	-11	16	-12	18	36	-11	13	-12	16
4	6.849	2	-16	180	2.0R	-20	.4	17	-16	0	-16	0	20	-9	0	-10	12	31	-11	14	-14	0
5	6.849	2	-15	180	1.0R	-20	.4	18	-17	6.7	-17	1	18	-16	5.3	-13	13	32	-8.5	16	-13	9.3
6	7.074	2	2	30L	1.0R	-20	.4	40	-9.3	8.0	-2	18	19	-18	14	-6.7	13	18	-16	9.3	-17	12
7	6.910	2	-11.5	0	0	20	.4	22	-19	6.7	-19	0	32	-21	1	-17	12	18	-19	12	-14	13
8	7.096	2	12	180	0	20	.4	18	-4.9	8.4	-13	4	35	-22	0	0	15	26	-4.4	15	-19	0

TABLE V.- MAXIMUM ACCELERATIONS, STROKES AND FORCES FOR LANDINGS OF INVERTED TRIPOD MODEL – Concluded

[All values are full scale (Mars prototype); R, right yaw (leg 2 down); L, left yaw (leg 3 down); C, compression; T, tension]

(b) U.S. Customary Units

Run	Vertical velocity, ft/s	Horizontal velocity, ft/s	Landing attitude in –			Surface slope, deg	Friction coefficient, μ	Maximum acceleration at center of gravity, Earth g units			Stability
			Pitch, deg	Roll, deg	Yaw, deg			Normal	Longitudinal	Lateral	
1	23.21	0	0	0	0	0	0.4	-18	4, -4	-3, 2	Stable
2	23.24	6	10	180	.5L	-20	.4	-13	-4, 5	-5, 4	Stable
3	23.37	6	-2	180	1.0R	-20	.4	-10	-7, 4	-4, 3	Stable
4	22.47	6	-16	180	2.0R	-20	.4	-8	-7, 4	5, -4	Stable
5	22.47	6	-15	180	1.0R	-20	.8	-8	-9, 4	8, -2	Stable
6	23.21	6	2	30L	1.0R	-20	.4	-10	4, -6	-6, 5	Stable
7	22.67	6	-11.5	0	0	20	.4	-8	-8, 6	-5, 5	Stable
8	23.28	6	12	180	0	20	.4	-10	7, -4	-2, 2	Stable

Run	Vertical velocity, ft/s	Horizontal velocity, ft/s	Landing attitude in –			Surface slope, deg	Friction coefficient, μ	Maximum strut stroke, in., for –											
								Gear 1					Gear 2					Gear 3				
			Pitch, deg	Roll, deg	Yaw, deg			Strut 1A	Strut 1B		Strut 1C		Strut 2A	Strut 2B		Strut 2C		Strut 3A	Strut 3B		Strut 3C	
								C	C	T	C	T	C	C	T	C	T	C	C	T	C	T
1	23.21	0	0	0	0	0	0.4	7.0	0	0	0	0	7.0	-0.1	0	0	0	6.7	-0.1	0	-0.2	0
2	23.24	6	10	180	.5L	-20	.4	4.2	0	0	0	0	7.5	0	.2	0	1.1	7.0	-.1	.3	-.1	.1
3	23.37	6	-2	180	1.0R	-20	.4	4.9	-.1	0	0	0	5.9	0	0	-.1	.6	6.5	-.1	.6	0	0
4	22.47	6	-16	180	2.0R	-20	.4	3.2	-1.3	0	-1.3	0	5.8	0	0	0	.2	6.3	0	.7	-.3	0
5	22.47	6	-15	180	1.0R	-20	.8	4.6	-.5	0	-.4	0	5.3	-.1	0	-.1	.3	6.0	0	.3	-.5	0
6	23.21	6	2	30L	1.0R	-20	.4	6.6	0	0	0	.1	5.0	-1.2	0	-.1	.2	4.1	0	0	-.1	0
7	22.67	6	-11.5	0	0	20	.4	4.1	-5.6	0	-5.2	0	6.0	-1.1	0	-.1	.3	5.5	0	0	-.1	0
8	23.38	6	12	180	0	20	.4	2.6	0	0	0	.1	6.2	-3.1	0	0	1.3	5.8	0	9.0	-5.8	0

Run	Vertical velocity, ft/s	Horizontal velocity, ft/s	Landing attitude in –			Surface slope, deg	Friction coefficient, μ	Maximum strut forces, thousand pounds, for –														
								Gear 1					Gear 2					Gear 3				
			Pitch, deg	Roll, deg	Yaw, deg			Strut 1A	Strut 1B		Strut 1C		Strut 2A	Strut 2B		Strut 2C		Strut 3A	Strut 3B		Strut 3C	
								C	C	T	C	T	C	C	T	C	T	C	C	T	C	T
1	23.21	0	0	0	0	0	0.4	8.5	-2.4	2.5	-2.0	1.5	7.5	-3.4	1.5	-2.8	2.5	8.8	-3.5	3.0	-2.5	1.4
2	23.24	6	10	180	.5L	-20	.4	3.6	-3.2	2.9	-1.2	1.5	8.5	-3.0	3.0	-2.8	3.0	8.0	-3.0	3.2	-3.0	3.1
3	23.37	6	-2	180	1.0R	-20	.4	4.0	-3.5	2.1	-4.0	1.5	6.0	-2.5	3.5	-2.7	4.0	8.0	-2.5	3.0	-2.8	3.5
4	22.47	6	-16	180	2.0R	-20	.4	3.8	-3.5	0	-3.5	0	4.6	-2.0	0	-2.3	2.6	7.0	-2.5	3.2	-3.2	0
5	22.47	6	-15	180	1.0R	-20	.8	4.0	-3.9	1.5	-3.9	.3	4.1	-3.5	1.2	-3.0	2.9	7.3	-1.9	3.5	-3.0	2.1
6	23.21	6	2	30L	1.0R	-20	.4	9.0	-2.1	1.8	-.4	4.0	4.2	-4.0	3.2	-1.5	3.0	4.0	-3.5	2.1	-3.8	2.8
7	22.67	6	-11.5	0	0	20	.4	5.0	-4.2	1.5	-4.2	0	7.2	-4.8	.3	-3.9	2.8	4.0	-4.2	2.7	-3.1	3.0
8	23.38	6	12	180	0	20	.4	4.0	-1.1	1.9	-3.0	.9	7.8	-5.0	0	0	3.3	5.8	-1.0	3.3	-4.3	0

TABLE VI.- MAXIMUM ACCELERATIONS, STROKES AND FORCES FOR LANDINGS OF CANTILEVERED MODEL

[All values are full scale (Mars prototype); R, right yaw (leg 2 down); L, left yaw (leg 3 down); C, compression; T, tension]

(a) SI Units

Run	Vertical velocity, m/s	Horizontal velocity, m/s	Landing attitude in –			Surface slope, deg	Friction coefficient, μ	Maximum acceleration at center of gravity, Earth g units			Stability
			Pitch, deg	Roll, deg	Yaw, deg			Normal	Longitudinal	Lateral	
1	7.04	0	5	0	0	0	0.4	-20	-7, 6	1, -1	Stable
2	7.10	2	15	180	1.0R	-20	.4	-14	-4, 5	4, -5	Stable
3	7.01	2	-2.5	180	0	-20	.4	-11	-2, 7	4, -4	Stable
4	6.83	2	-14	180	.5R	-20	.4	-9	-5, 3	5, -6	Stable
5	6.83	2	-15	180	1.0R	-20	.8	-11	-5, 5	-7, 5	Turned over
6	7.07	2	-1	30L	0	-20	.4	-11	-6, 5	4, -3	Stable
7	6.98	2	-8	0	0	20	.4	-9	-5, 4	6, -8	Stable
8	7.10	2	9	180	2.0L	20	.4	-10	4, -6	-5, 3	Stable

Run	Vertical velocity, m/s	Horizontal velocity, m/s	Landing attitude in –			Surface slope, deg	Friction coefficient, μ	Maximum strut stroke, centimeters, for –													
								Gear 1					Gear 2					Gear 3				
			Pitch, deg	Roll, deg	Yaw, deg			Strut 1A	Strut 1B		Strut 1C		Strut 2A	Strut 2B		Strut 2C		Strut 3A	Strut 3B		Strut 3C	
								C	C	T	C	T	C	C	T	C	T	C	C	T	C	T
1	7.04	0	5	0	0	0	0.4	10	0	5.3	0	4.8	19	0	2	0	3.8	19	0	5.1	0	1.5
2	7.10	2	15	180	1.0R	-20	.4	11	0	3.8	0	4.3	16	-.5	3.8	0	3.8	17	0	5.1	-.5	3.8
3	7.01	2	-2.5	180	0	-20	.4	8.9	0	4.8	0	4.3	17	-.8	2.8	0	4.1	18	0	4.3	-.8	3.8
4	6.83	2	-14	180	.5R	-20	.4	14	-.8	.5	-1	.5	17	-.5	2.5	-.5	4.1	17	-.5	3.8	-2	1.5
5	6.83	2	-15	180	1.0R	-20	.8	14	-.8	1	-2	2	17	-1	4.8	0	4.3	8.4	0	5.1	-2	3.3
6	7.07	2	-1	30L	0	-20	.4	16	0	3.8	0	5.1	12	0	4.3	0	4.6	7.6	0	3.8	0	4.1
7	6.98	2	-8	0	0	20	.4	16	-8.0	3.8	-7.4	3.8	14	0	3.3	0	2.8	13	0	3.8	0	3.3
8	7.10	2	9	180	2.0L	20	.4	6.4	0	2.8	0	3.8	18	-5.1	2	0	8.1	17	0	7.6	-7.9	1.5

Run	Vertical velocity, m/s	Horizontal velocity, m/s	Landing attitude in –			Surface slope, deg	Friction coefficient, μ	Maximum strut forces, kN, for –													
								Gear 1					Gear 2					Gear 2				
			Pitch, deg	Roll, deg	Yaw, deg			Strut 1A	Strut 1B		Strut 1C		Strut 2A	Strut 2B		Strut 2C		Strut 3A	Strut 3B		Strut 3C	
								C	C	T	C	T	C	C	T	C	T	C	C	T	C	T
1	7.04	0	5	0	0	0	0.4	45.4	0	16	0	16	33	-3	4.9	-1	12	37	-3	13	-3	4.9
2	7.10	2	15	180	1.0R	-20	.4	32	-3	15	-4	14	25	-11	14	-6.7	15	36	-6.7	13	-14	11
3	7.01	2	-2.5	180	0	-20	.4	27			0	11	32			-3	14	30	-4.9	14	-11	6.7
4	6.83	2	-14	180	.5R	-20	.4	46.7	-14	4.4	-14	4	39	-13	8.9	-6.7	16	33	-6.7	13	-15	5.8
5	6.83	2	-15	180	1.0R	-20	.8	31	-14	4.4	-14	3	39	-15	11	-11	14	35	-4.4	16	-15	7.6
6	7.07	2	-1	30L	0	-20	.4	44.5	-4.4	8.9	-4	16	29	-6.7	15	-9.3	11	27	-4.9	13	-1	14
7	6.98	2	-8	0	0	20	.4	37	-16	12	-15	8.4	31	-8.4	16	-8.4	4.4	31	-4.4	8.4	-8.9	7.1
8	7.10	2	9	180	2.0L	20	.4	36	-6.2	8.9	-4	9.8	33	-15	3	0	16	35	-2	14	-13	4

TABLE VI.- MAXIMUM ACCELERATIONS, STROKES AND FORCES FOR LANDINGS OF CANTILEVERED MODEL – Concluded

[All values are full scale (Mars prototype); R, right yaw (leg 2 down); L, left yaw (leg 3 down); C, compression; T, tension]

(b) U.S. Customary Units

Run	Vertical velocity, ft/s	Horizontal velocity, ft/s	Landing attitude in –			Surface slope, deg	Friction coefficient, μ	Maximum acceleration at center of gravity, Earth g units			Stability
			Pitch, deg	Roll, deg	Yaw, deg			Normal	Longitudinal	Lateral	
1	23.1	0	5	0	0	0	0.4	-20	-7, 6	1, -1	Stable
2	23.3	6	15	180	1.0R	-20	.4	-14	-4, 5	4, -5	Stable
3	23.0	6	-2.5	180	0	-20	.4	-11	-2, 7	4, -4	Stable
4	22.4	6	-14	180	.5R	-20	.4	-9	-5, 3	5, -6	Stable
5	22.4	6	-15	180	1.0R	-20	.8	-11	-5, 5	-7, 5	Turned over
6	23.2	6	-1	30L	0	-20	.4	-11	-6, 5	4, -3	Stable
7	22.9	6	-8	0	0	20	.4	-9	-5, 4	6, -8	Stable
8	23.3	6	9	180	2.0L	20	.4	-10	4, -6	-5, 3	Stable

Run	Vertical velocity, ft/s	Horizontal velocity, ft/s	Landing attitude in –			Surface slope, deg	Friction coefficient, μ	Maximum strut stroke, in., for –													
								Gear 1					Gear 2					Gear 3				
			Pitch, deg	Roll, deg	Yaw, deg			Strut 1A	Strut 1B		Strut 1C		Strut 2A	Strut 2B		Strut 2C		Strut 3A	Strut 3B		Strut 3C	
								C	C	T	C	T	C	C	T	C	T	C	C	T	C	T
1	23.1	0	5	0	0	0	0.4	4.0	0	2.1	0	1.9	7.5	0	0.7	0	1.5	7.5	0	2.0	0	0.6
2	23.3	6	15	180	1.0R	-20	.4	4.4	0	1.5	0	1.7	6.2	-.2	1.5	0	1.5	6.6	0	2.0	-.2	1.5
3	23.0	6	-2.5	180	0	-20	.4	3.5	0	1.9	0	1.7	6.8	-.3	1.1	0	1.6	7.1	0	1.7	-.3	1.5
4	22.4	6	-14	180	.5R	-20	.4	5.5	-.3	.2	-.5	.2	6.6	-.2	1.0	-.2	1.6	6.7	-.2	1.5	-.8	.6
5	22.4	6	-15	180	1.0R	-20	.8	5.7	-.3	.5	-.6	.7	6.6	-.4	1.9	0	1.7	3.3	0	2.0	-.8	1.3
6	23.2	6	-1	30L	0	-20	.4	6.1	0	1.5	0	2.0	4.8	0	1.7	0	1.8	3.0	0	1.5	0	1.6
7	22.9	6	-8	0	0	20	.4	6.5	-3.0	1.5	-2.9	1.5	5.6	0	1.3	0	1.1	5.2	0	1.5	0	1.3
8	23.3	6	9	180	2.0L	20	.4	2.5	0	1.1	0	1.5	7.0	-2.0	.8	0	3.2	6.8	0	3.0	-3.1	.6

Run	Vertical velocity, ft/s	Horizontal velocity, ft/s	Landing attitude in –			Surface slope, deg	Friction coefficient, μ	Maximum strut forces, thousand pounds, for –													
								Gear 1					Gear 2					Gear 3				
			Pitch, deg	Roll, deg	Yaw, deg			Strut 1A	Strut 1B		Strut 1C		Strut 2A	Strut 2B		Strut 2C		Strut 3A	Strut 3B		Strut 3C	
								C	C	T	C	T	C	C	T	C	T	C	C	T	C	T
1	23.1	0	5	0	0	0	0.4	10.2	0	3.5	0	3.5	7.5	-0.7	1.1	-0.3	2.7	8.4	-0.6	3.0	-0.6	1.1
2	23.3	6	15	180	1.0R	-20	.4	7.2	-.7	3.4	-.9	3.1	5.5	-2.5	3.1	-1.5	3.3	8.2	-1.5	3.0	-3.1	2.5
3	23.0	6	-2.5	180	0	-20	.4	6.0			0	2.5	7.2			-.7	3.2	6.8	-1.1	3.2	-2.5	1.5
4	22.4	6	-14	180	.5R	-20	.4	10.5	-3.2	1.0	-3.1	.9	8.7	-3.0	2.0	-1.5	3.5	7.5	-1.5	3.0	-3.4	1.3
5	22.4	6	-15	180	1.0R	-20	.8	7.0	-3.1	1.0	-3.1	.7	8.7	-3.4	2.4	-2.5	3.1	8.0	-1.0	3.5	-3.4	1.7
6	23.2	6	-1	30L	0	-20	.4	10.0	-1.0	2.0	-.8	3.6	6.5	-1.5	3.4	-2.1	2.5	6.0	-1.1	3.0	-.3	3.1
7	22.9	6	-8	0	0	20	.4	8.3	-3.6	2.6	-3.4	1.9	7.0	-1.9	3.5	-1.9	1.0	7.0	-1.0	1.9	-2.0	1.6
8	23.3	6	9	180	2.0L	20	.4	8.2	-1.4	2.0	-.9	2.2	7.5	-3.4	.7	0	3.6	7.8	-.5	3.1	-3.0	.9

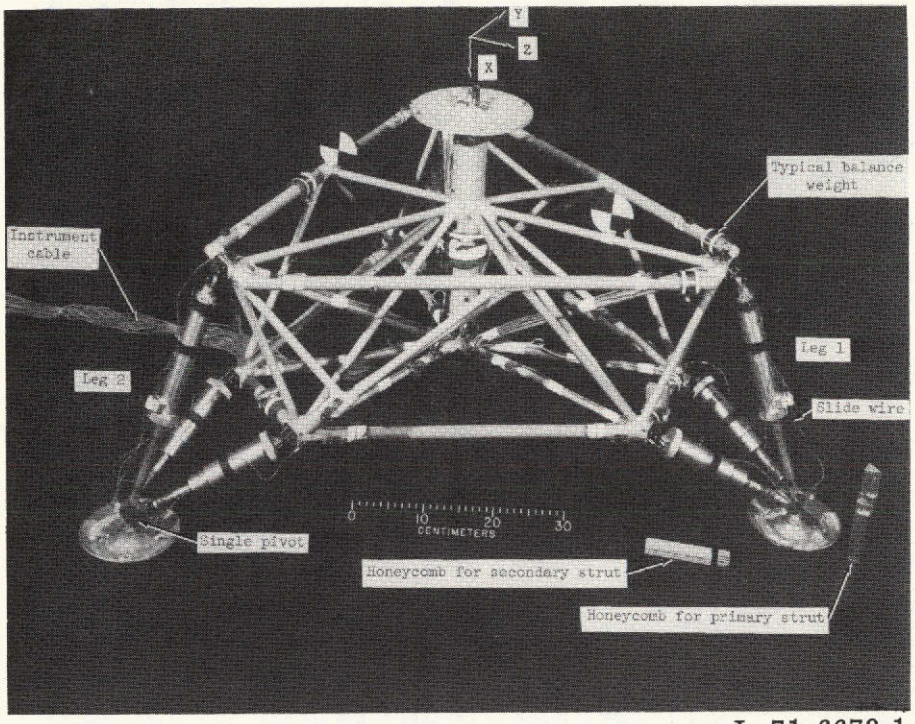

L-71-6678.1

(a) Inverted tripod model.

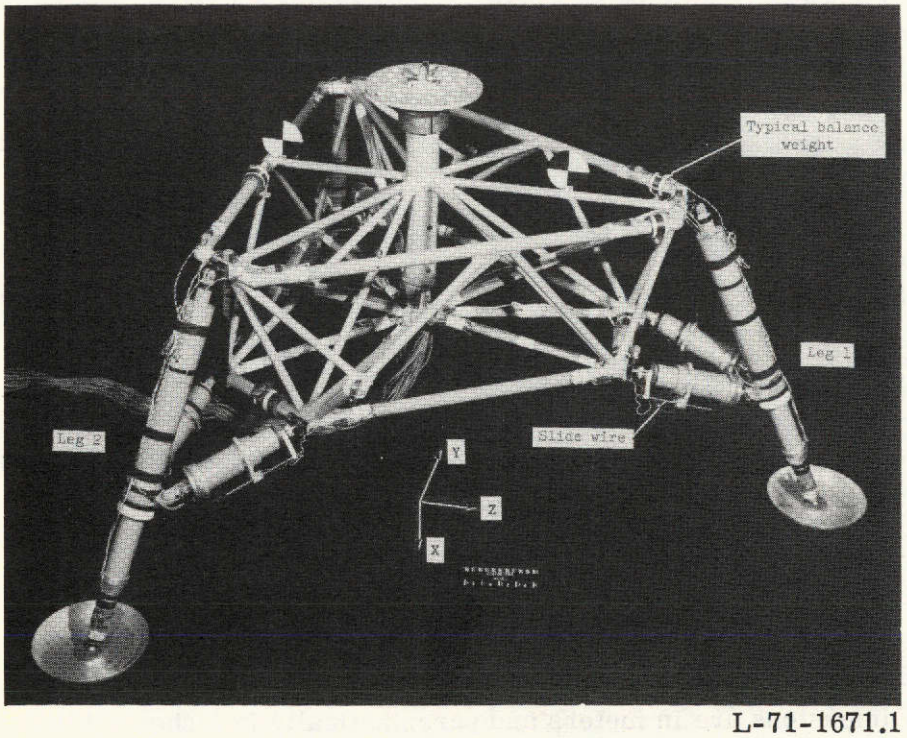

L-71-1671.1

(b) Cantilever model.

Figure 1.- Photographs of 3/8-scale models.

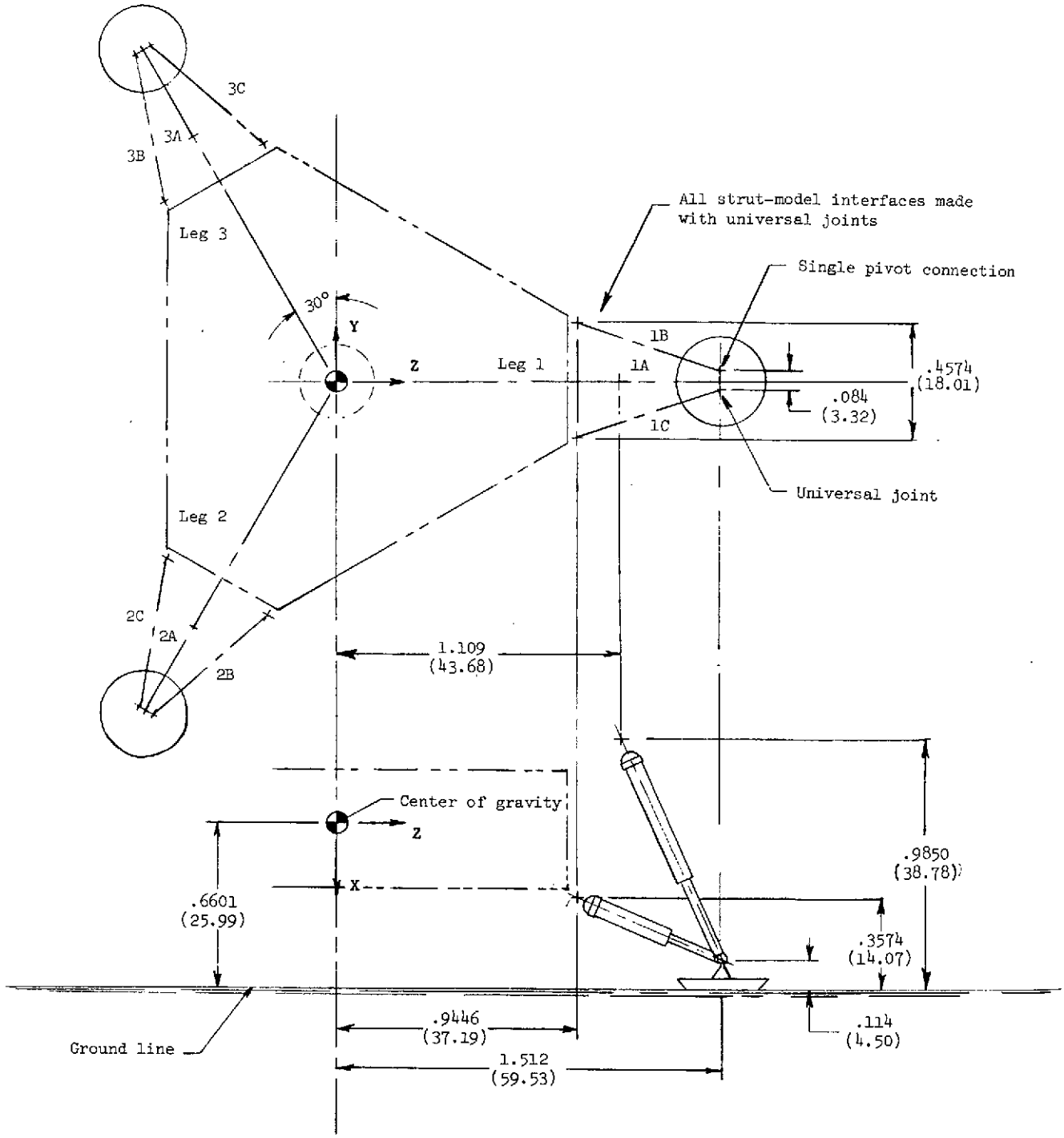

Figure 2.- General arrangement of 3/8-scale inverted tripod model. Dimensions are in meters and parenthetically in inches. All values are full scale.

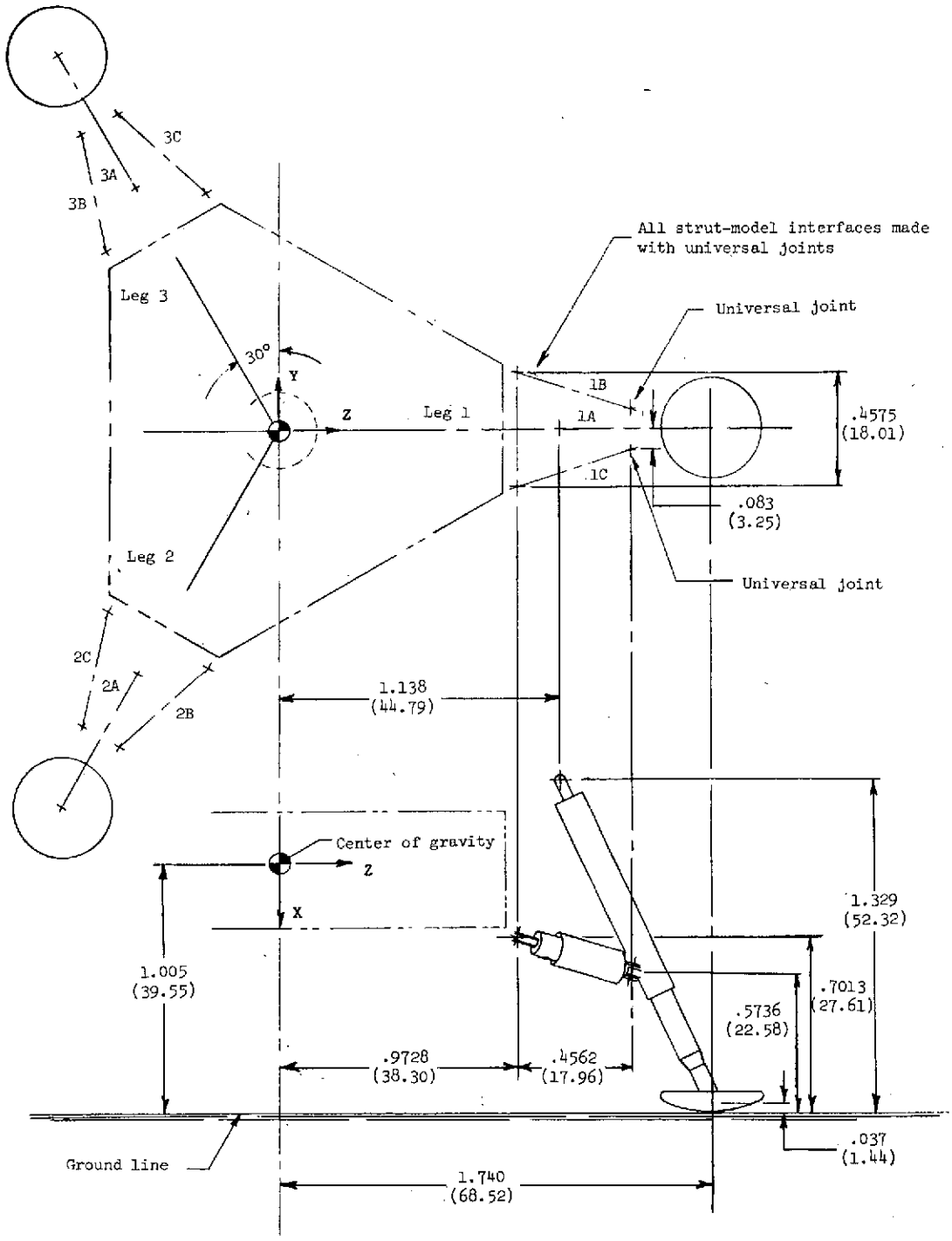

Figure 3.- General arrangement of 3/8-scale cantilever model. Dimensions are in meters and parenthetically in inches. All values are full scale.

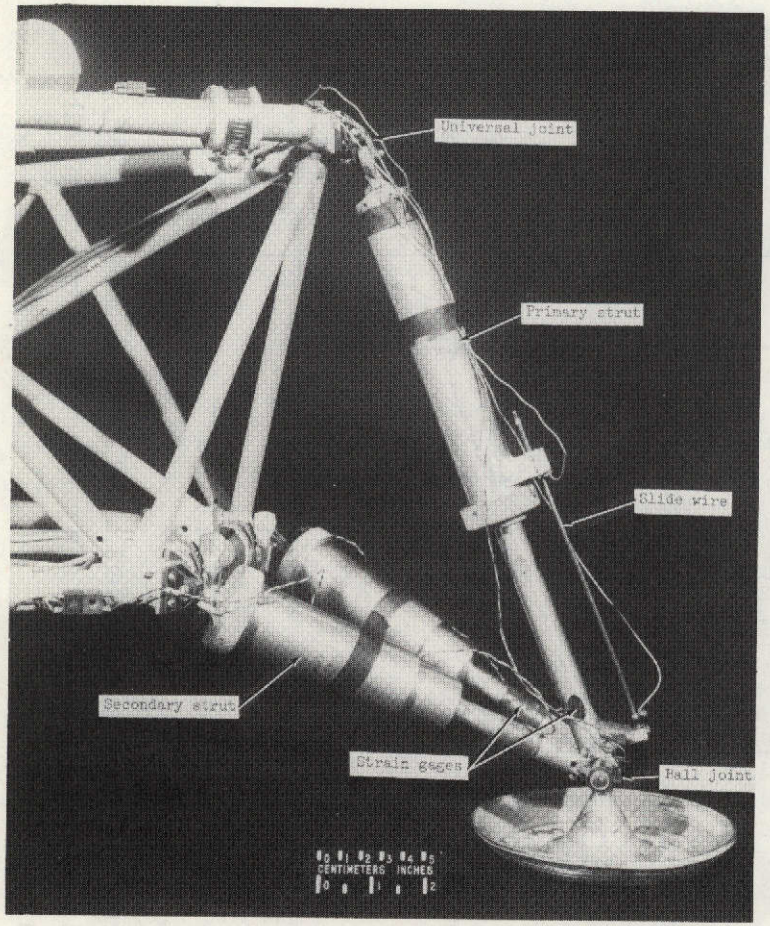

L-71-6681.1

(a) Inverted tripod model.

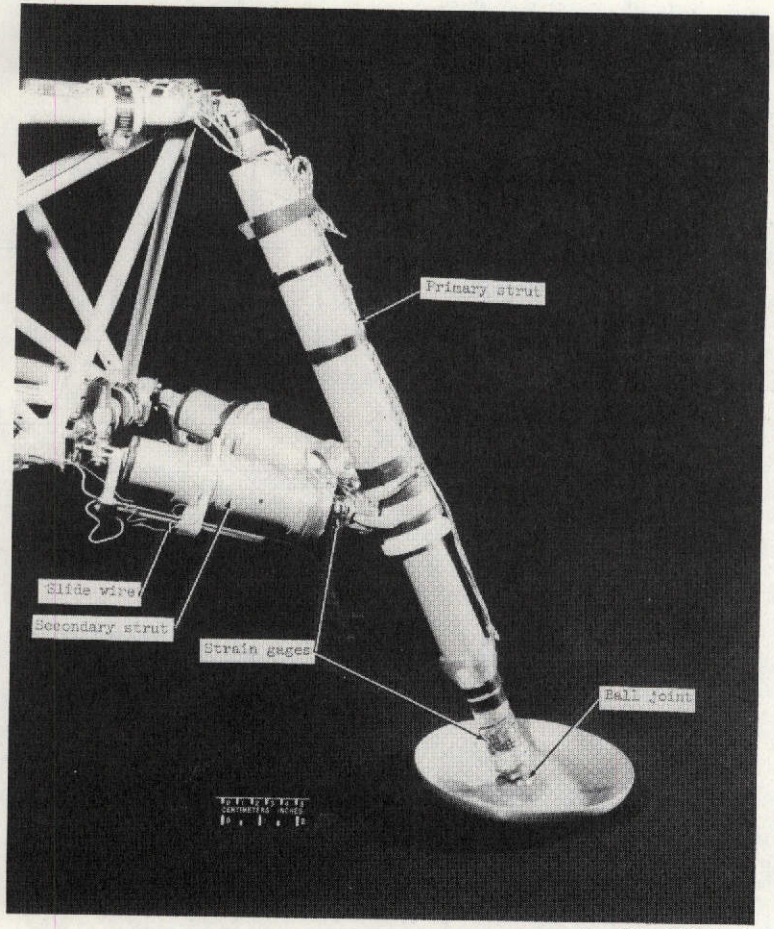

L-71-1670.1

(b) Cantilever model.

Figure 4.- Photographs of landing-gear details.

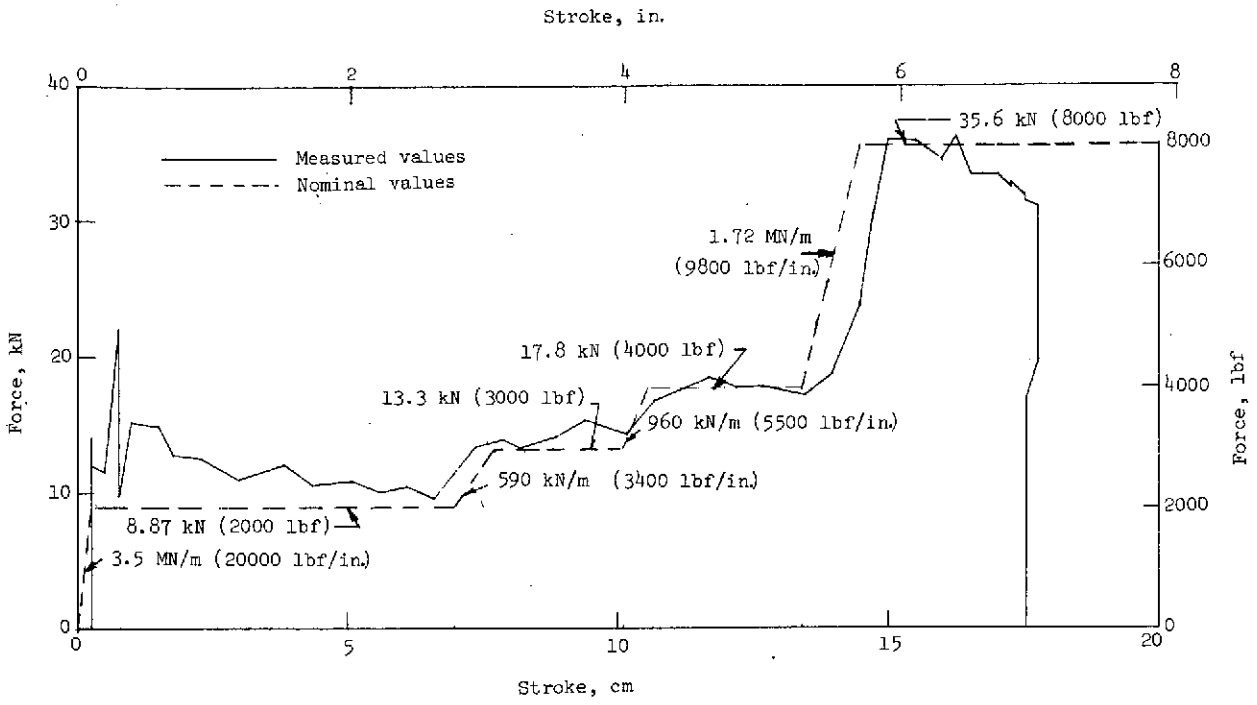

(a) Force-stroke history.

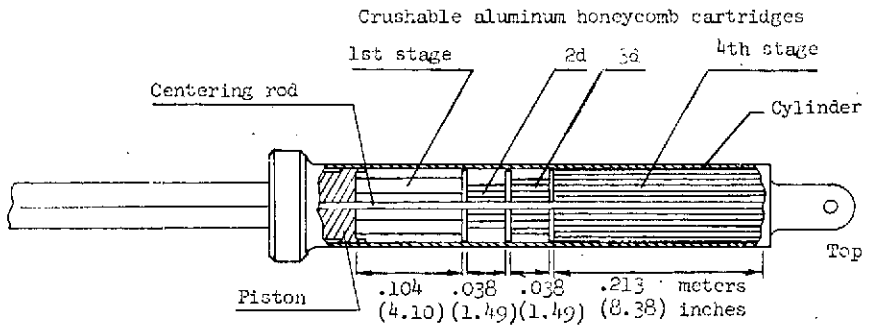

(b) Primary strut shock absorber.

Figure 5.- Details of primary strut shock absorber for inverted tripod model. All values are full scale.

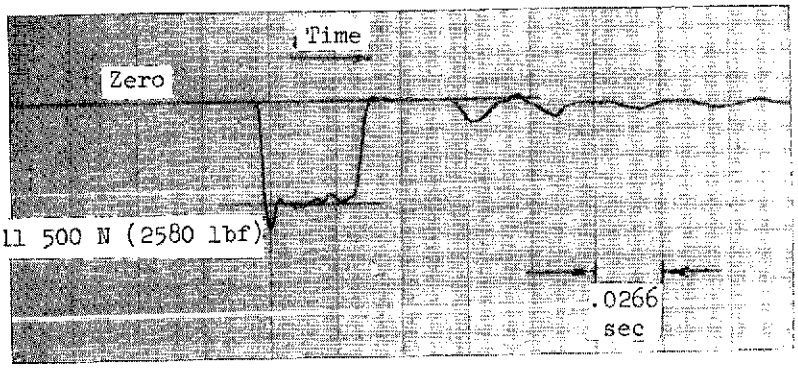

(a) Dynamic tension force time history.

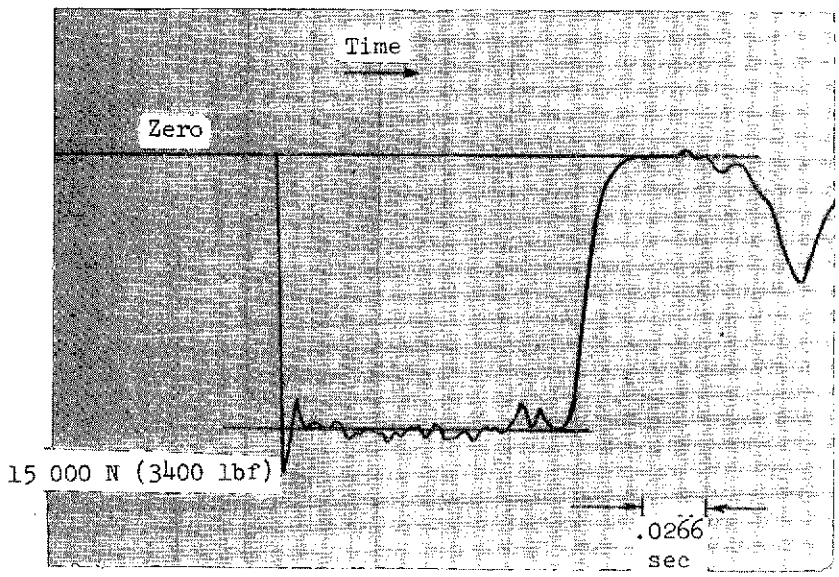

(b) Dynamic compression force time history.

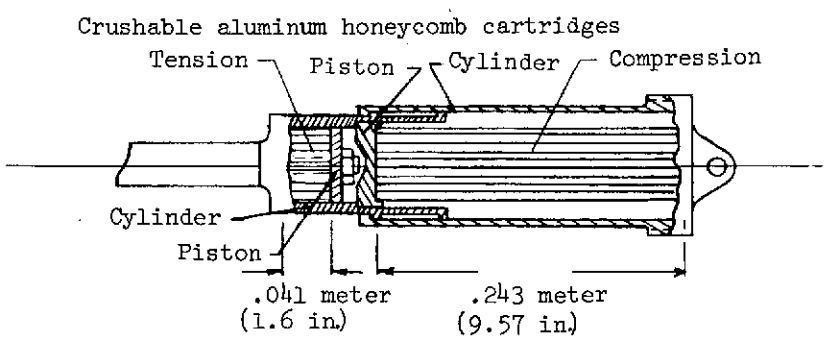

(c) Strut details.

Figure 6.- Secondary strut shock absorber details for inverted tripod model. All values are full scale.

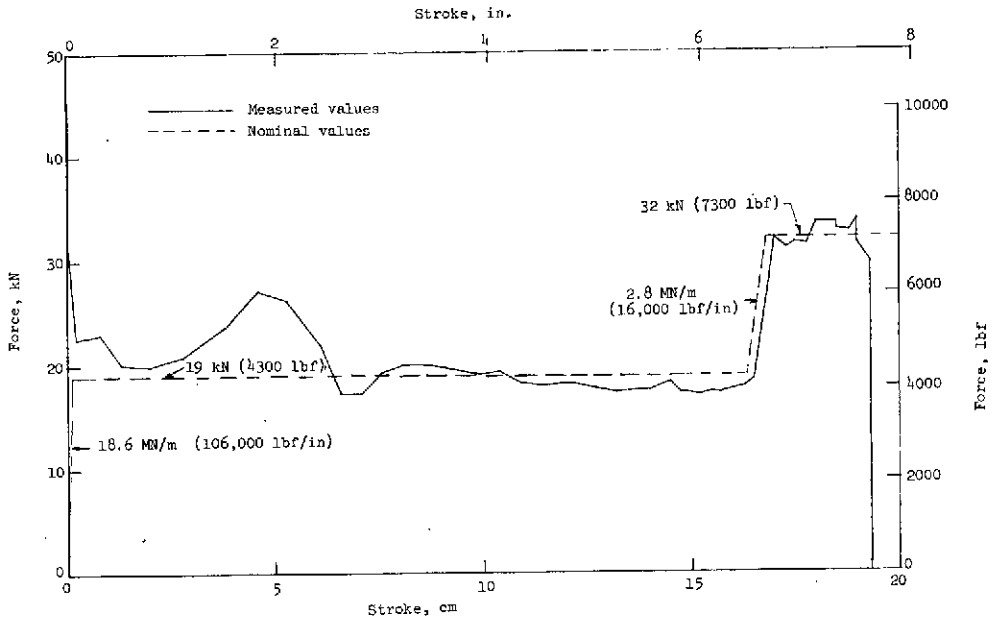

(a) Primary strut.

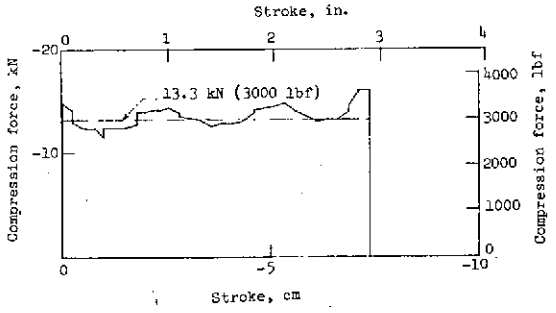

(b) Secondary strut, compression.

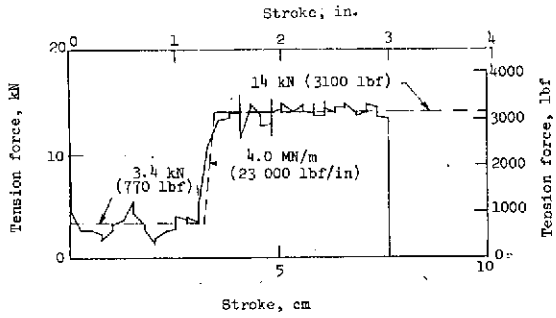

(c) Secondary strut, tension.

Figure 7.- Typical dynamic force stroke curves for cantilever model. All values are full scale.

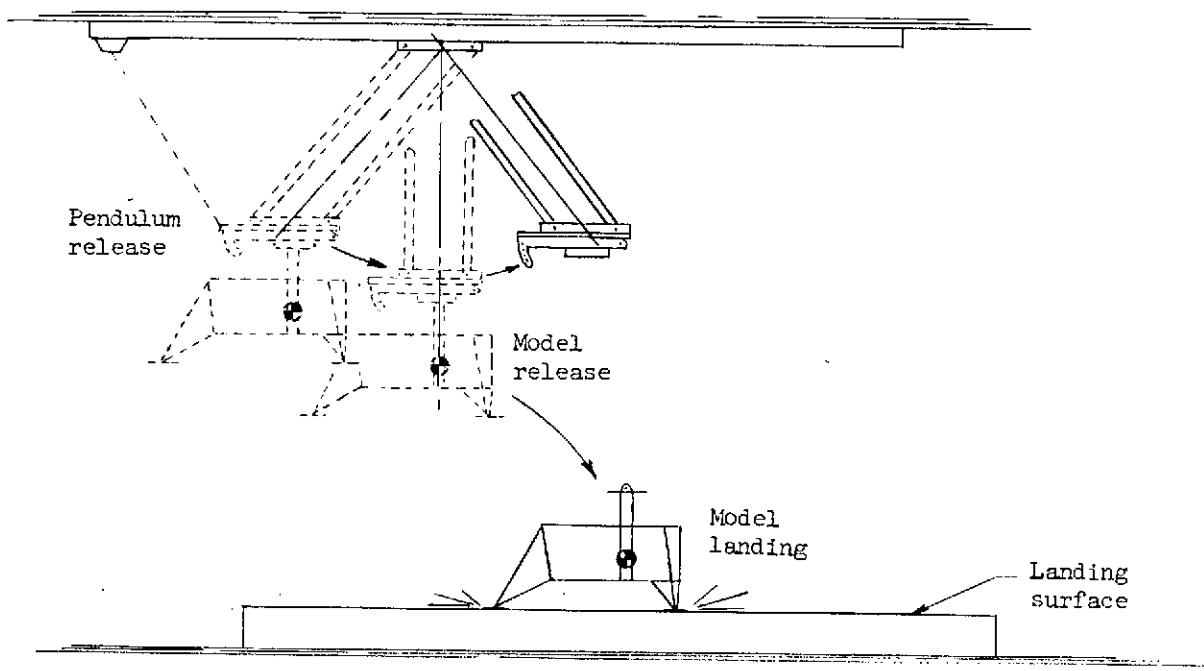

Figure 8.- Pendulum operation during typical model launch and landing.

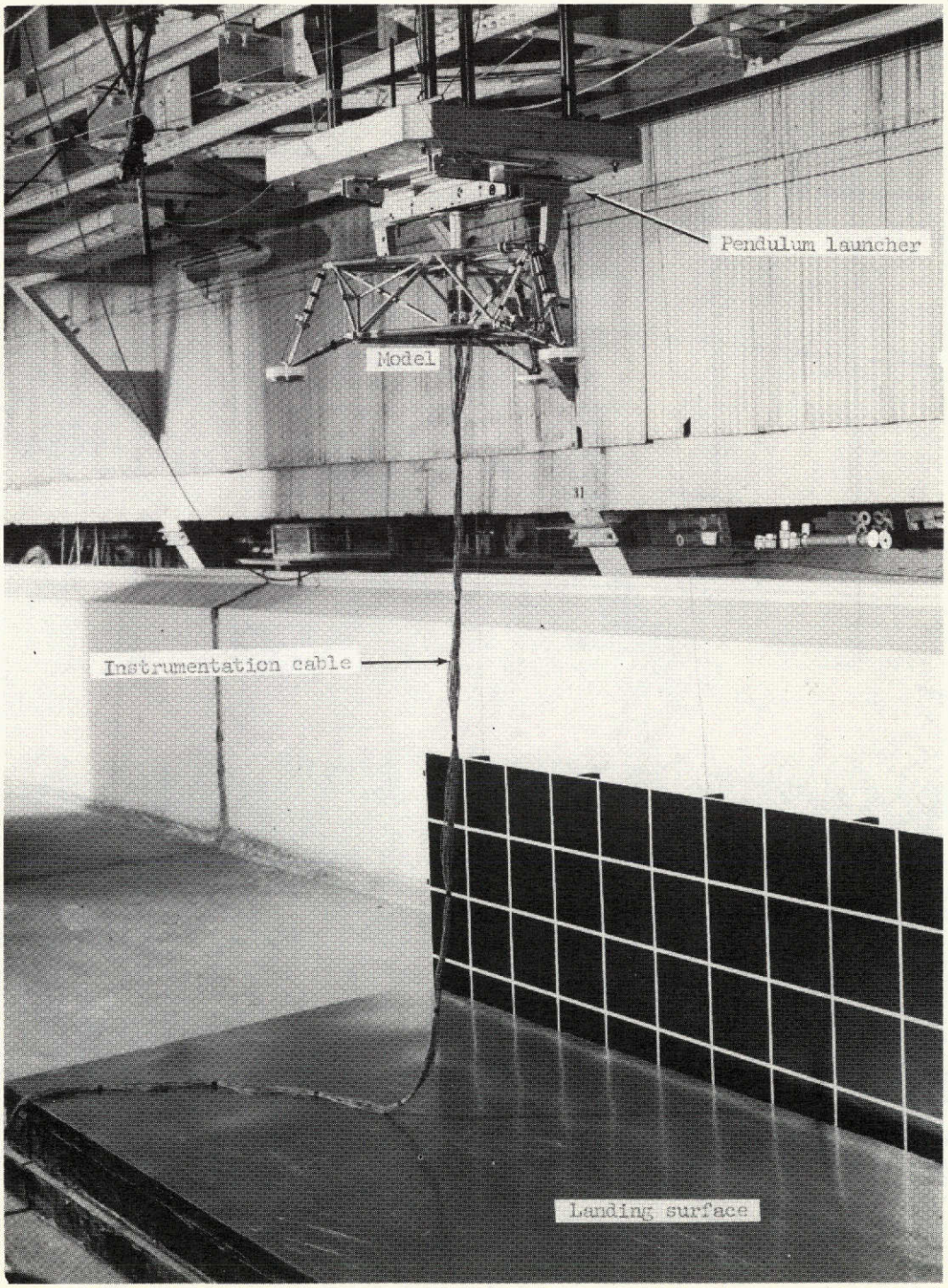

L-70-2294.1

Figure 9.- Photograph of test apparatus.

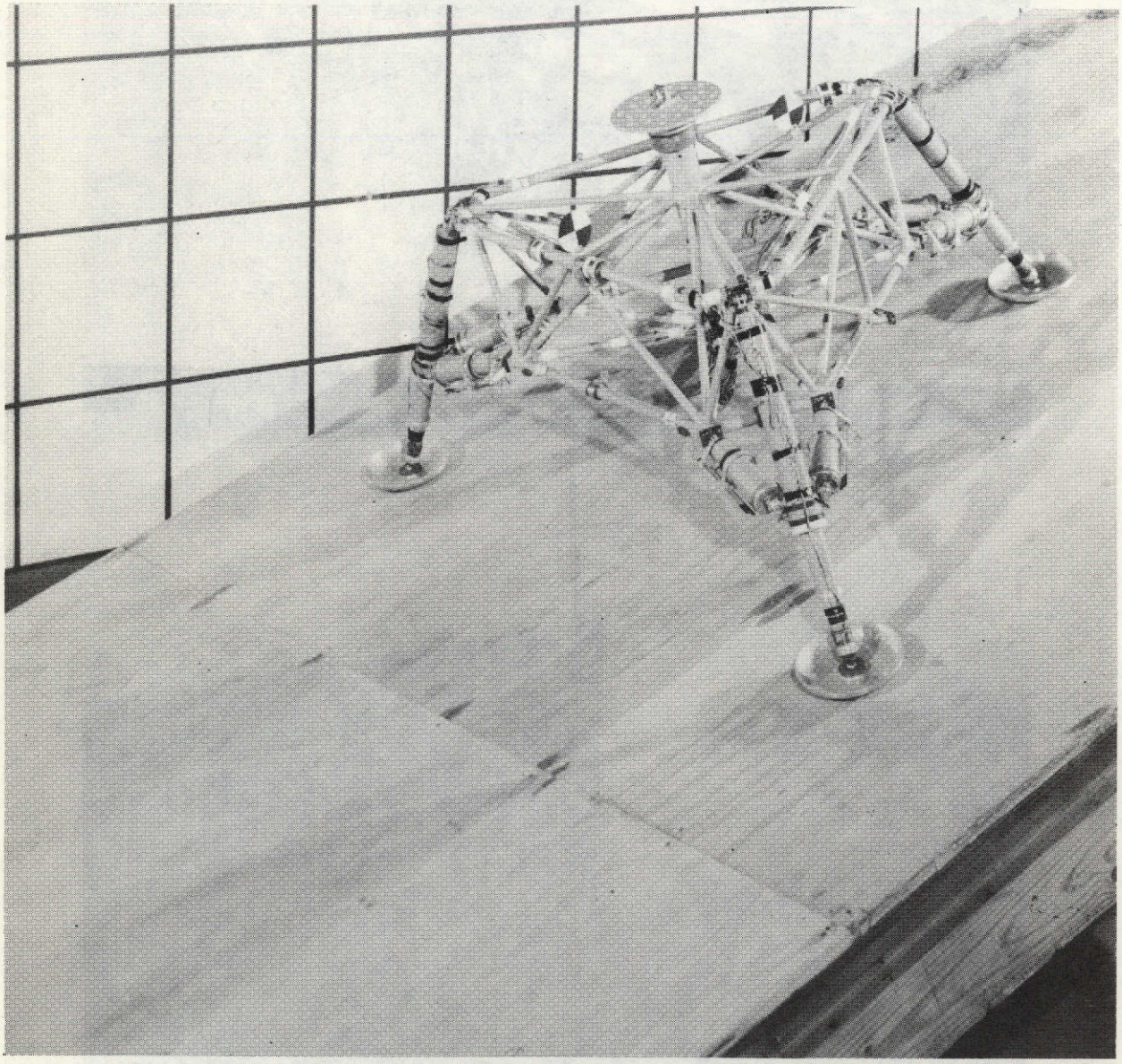

L-71-3217

Figure 10.- Photograph of cantilever model on 20^{o} slope.

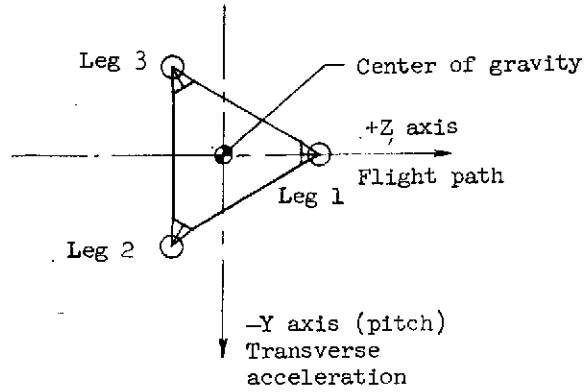

(a) Top view.

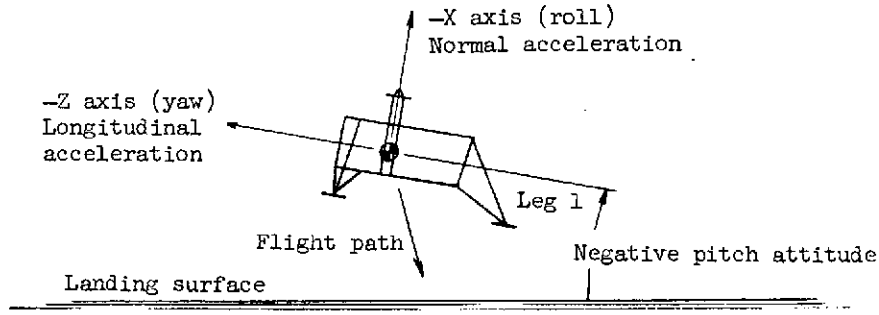

Roll attitude, 0°

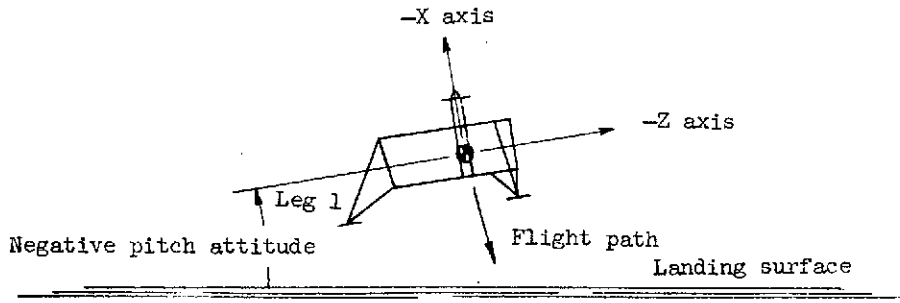

Roll attitude, 180°

(b) Side views.

Figure 11.- Sketches identifying vehicle axes, acceleration directions, attitudes, and flight path.

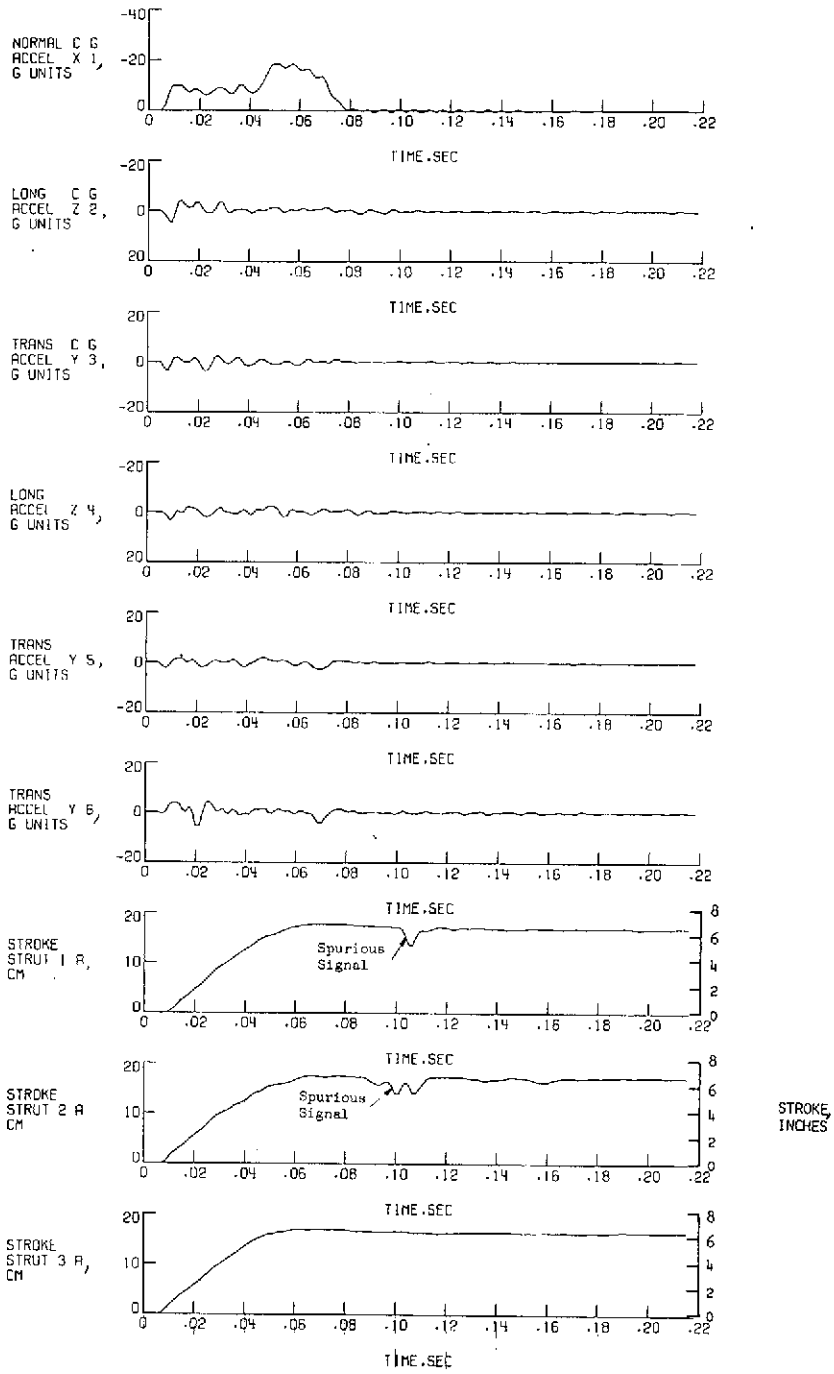

(a) Accelerations and primary strut strokes (run 1).

Figure 12.- Acceleration, stroke, and force time histories for inverted tripod model landing at run 1 conditions. All values are full scale. See table IV for accelerometer locations.

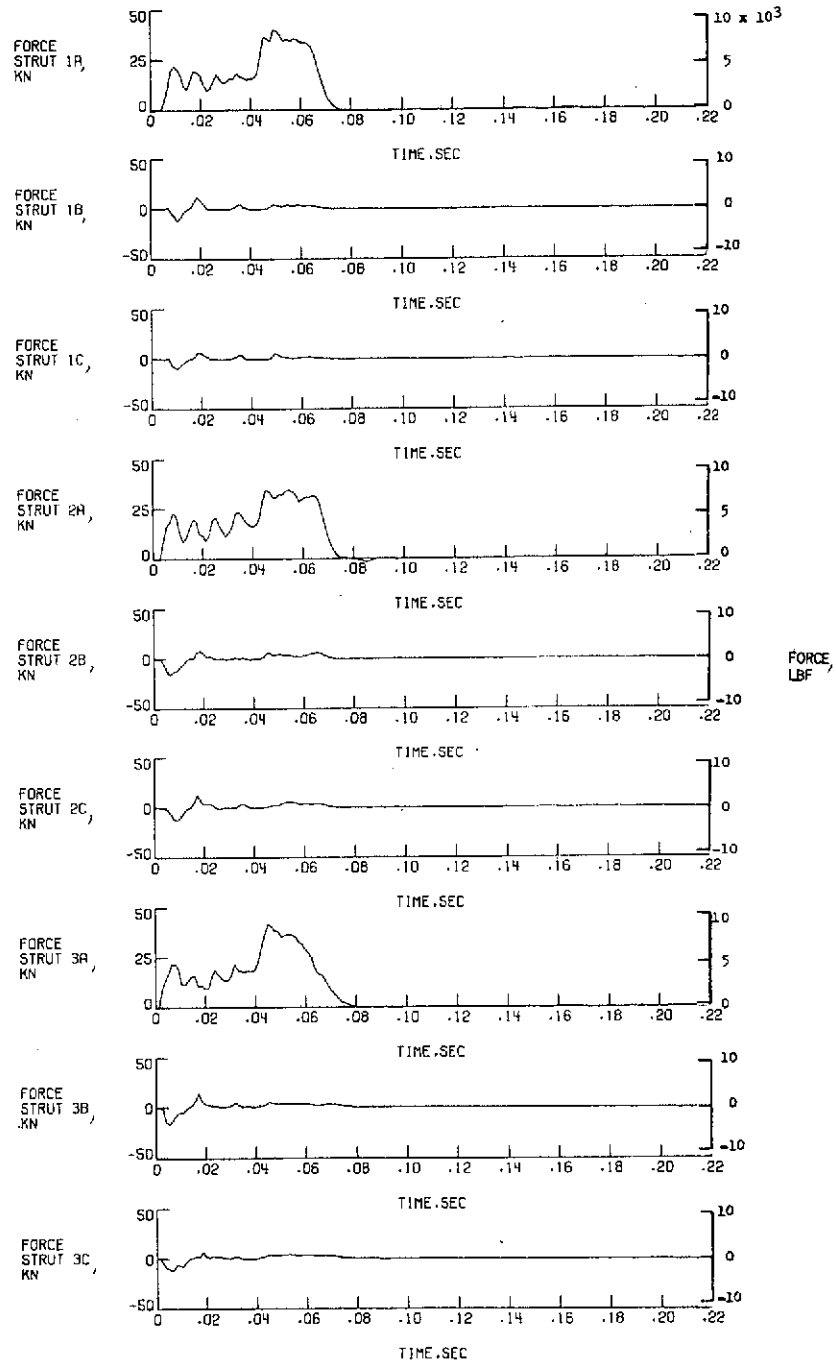

(b) Strut forces (run 1).

Figure 12.- Concluded.

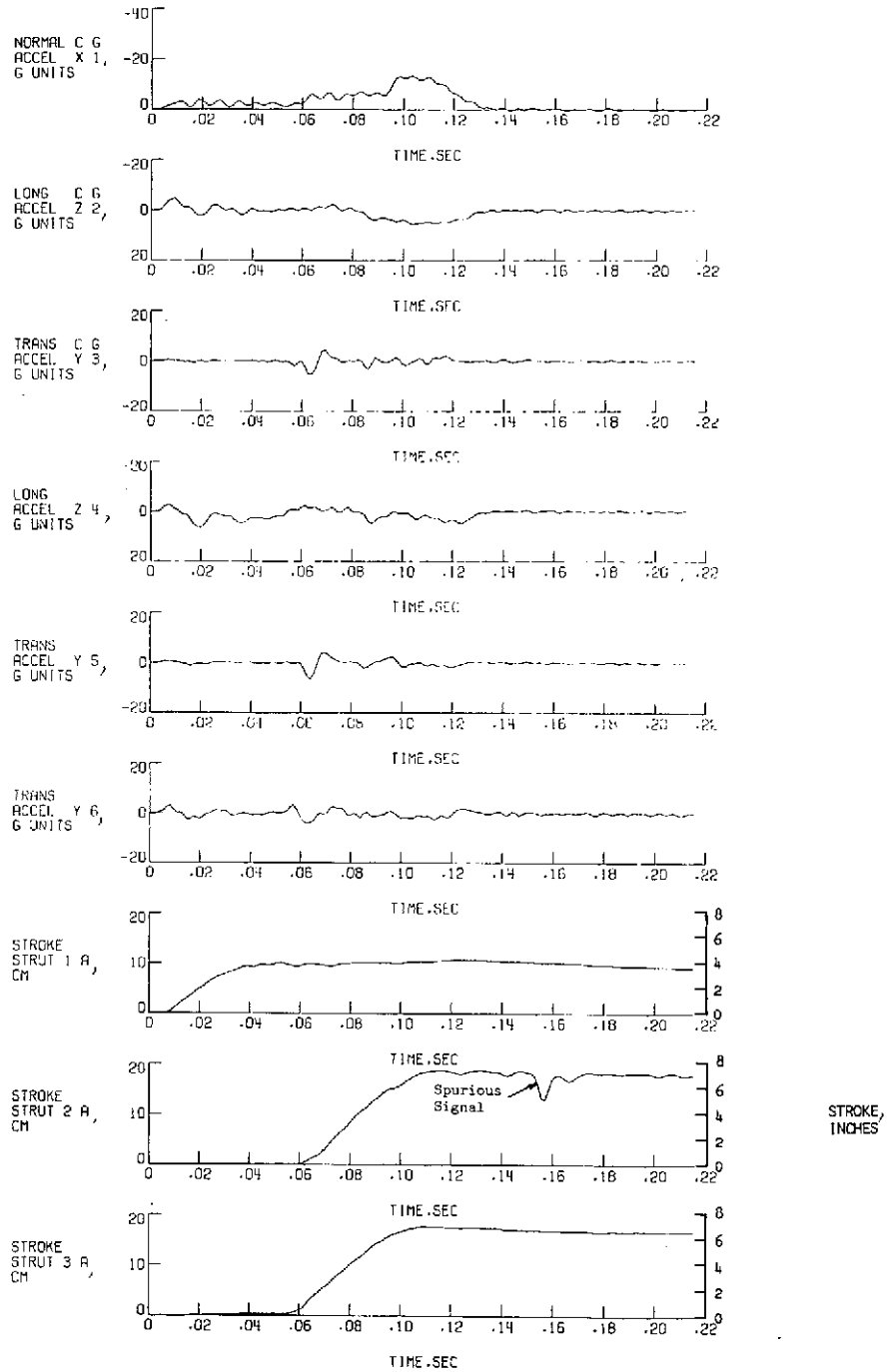

(a) Accelerations and primary strut strokes (run 2).

Figure 13.- Acceleration, stroke, and force time histories for inverted tripod model landing at run 2 conditions. All values are full scale. See table IV for accelerometer locations.

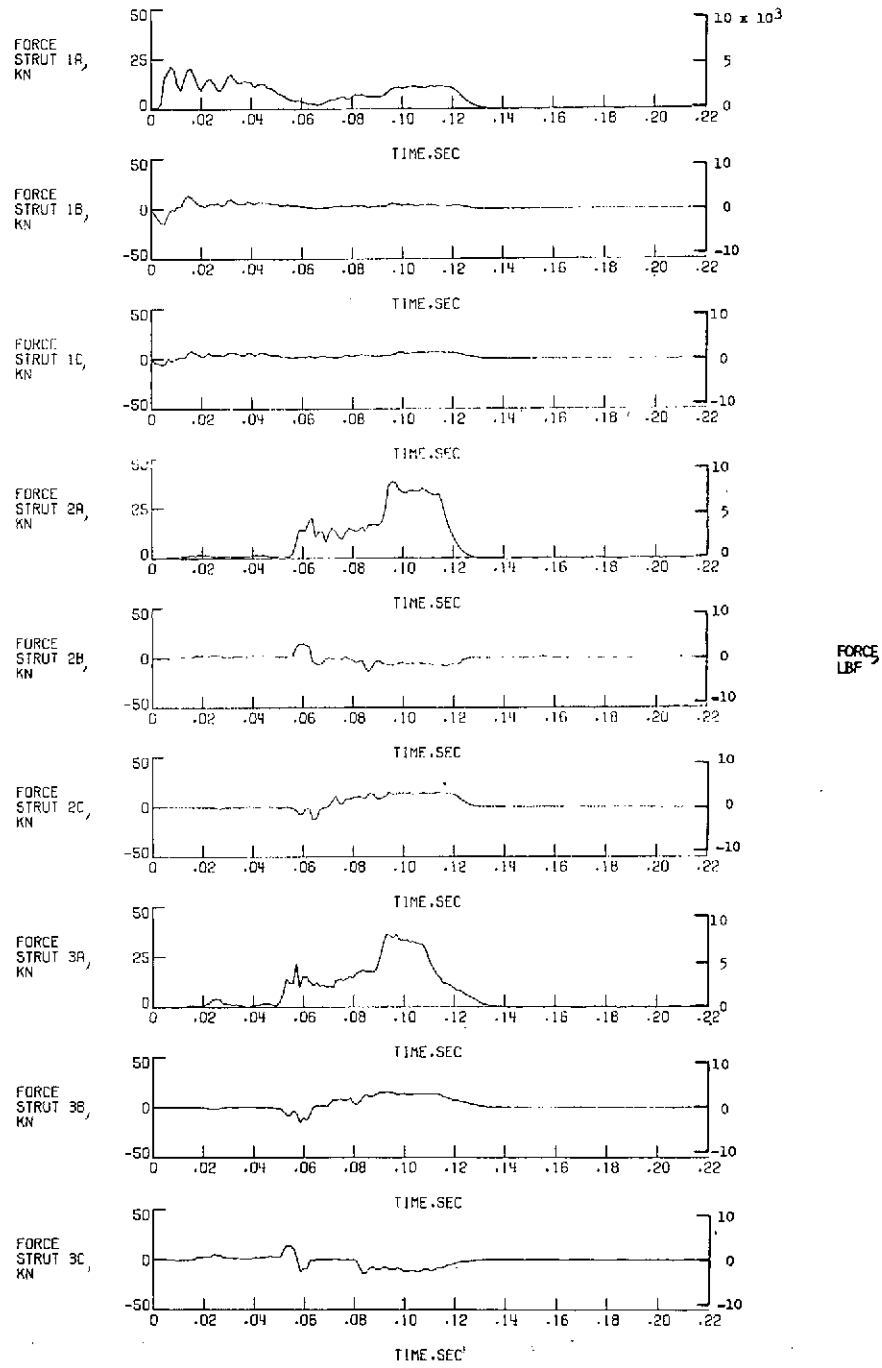

(b) Strut forces (run 2).

Figure 13.- Concluded.

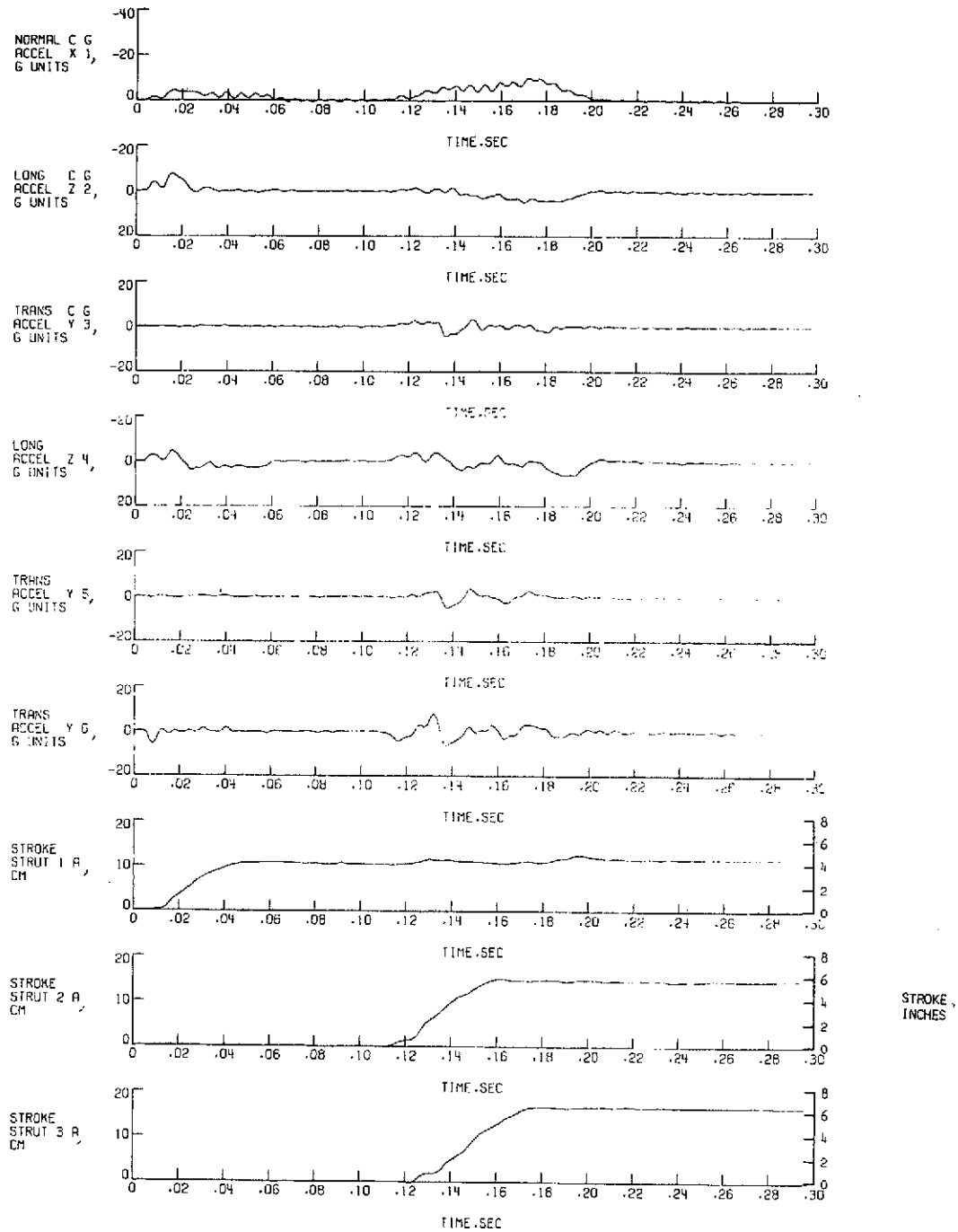

(a) Accelerations and primary strut strokes (run 3).

Figure 14.- Acceleration, stroke, and force time histories for inverted tripod model landing at run 3 conditions. All values are full scale. See table IV for accelerometer locations.

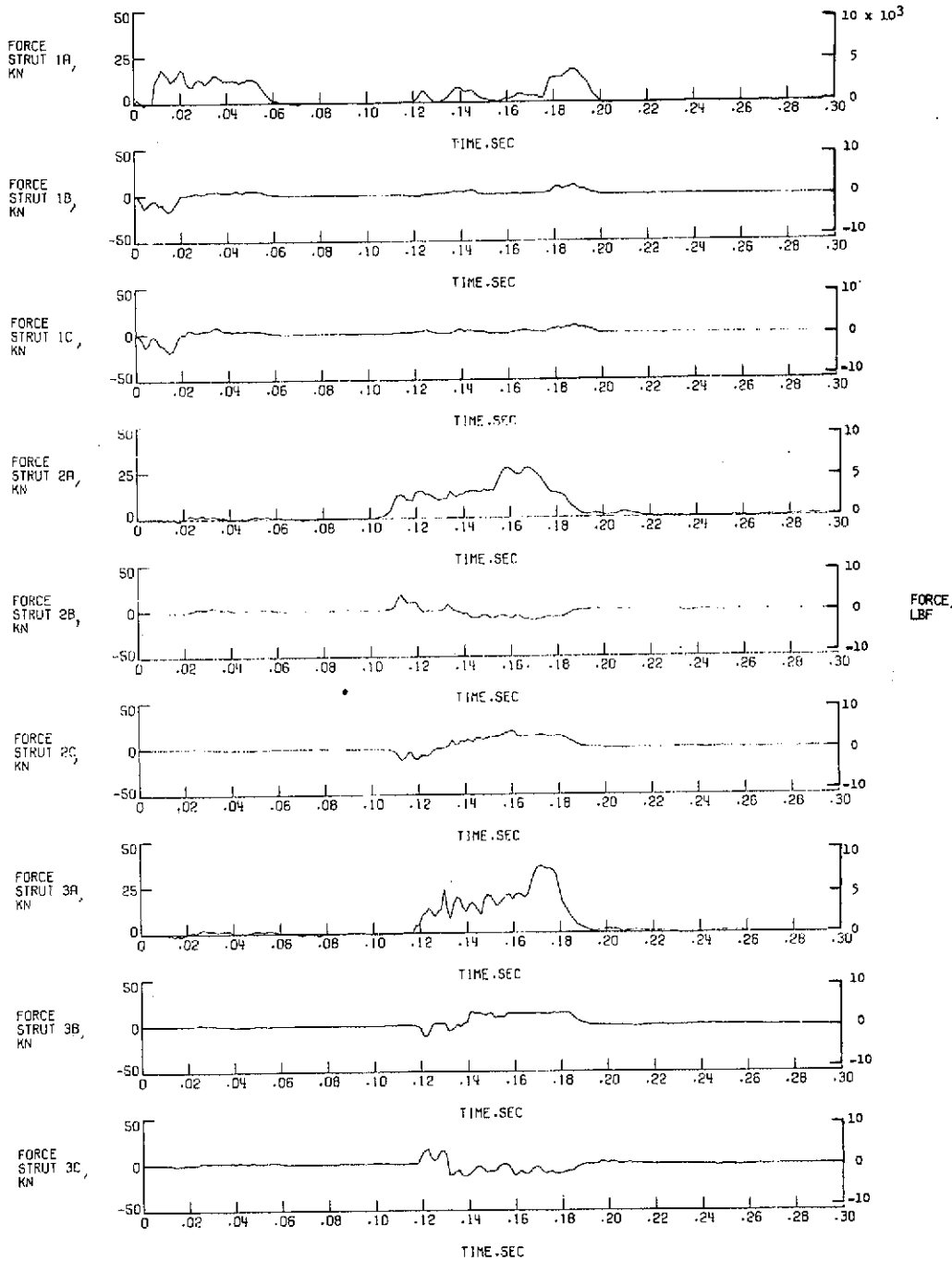

(b) Strut forces (run 3).

Figure 14.- Concluded.

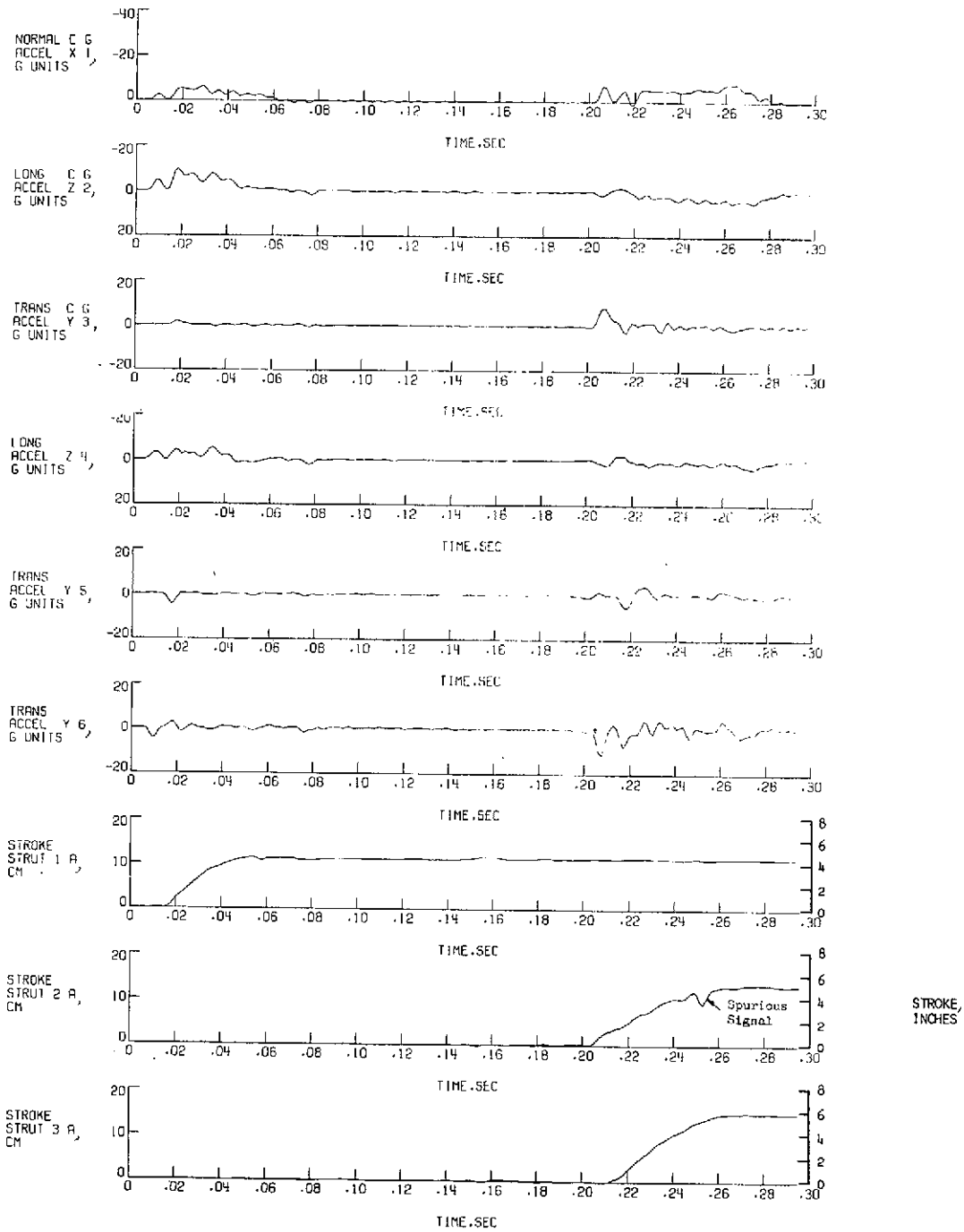

(a) Accelerations and primary strut strokes (run 5).

Figure 15.- Acceleration, stroke, and force time histories for inverted tripod model landing at run 5 conditions. All values are full scale. See table IV for accelerometer locations.

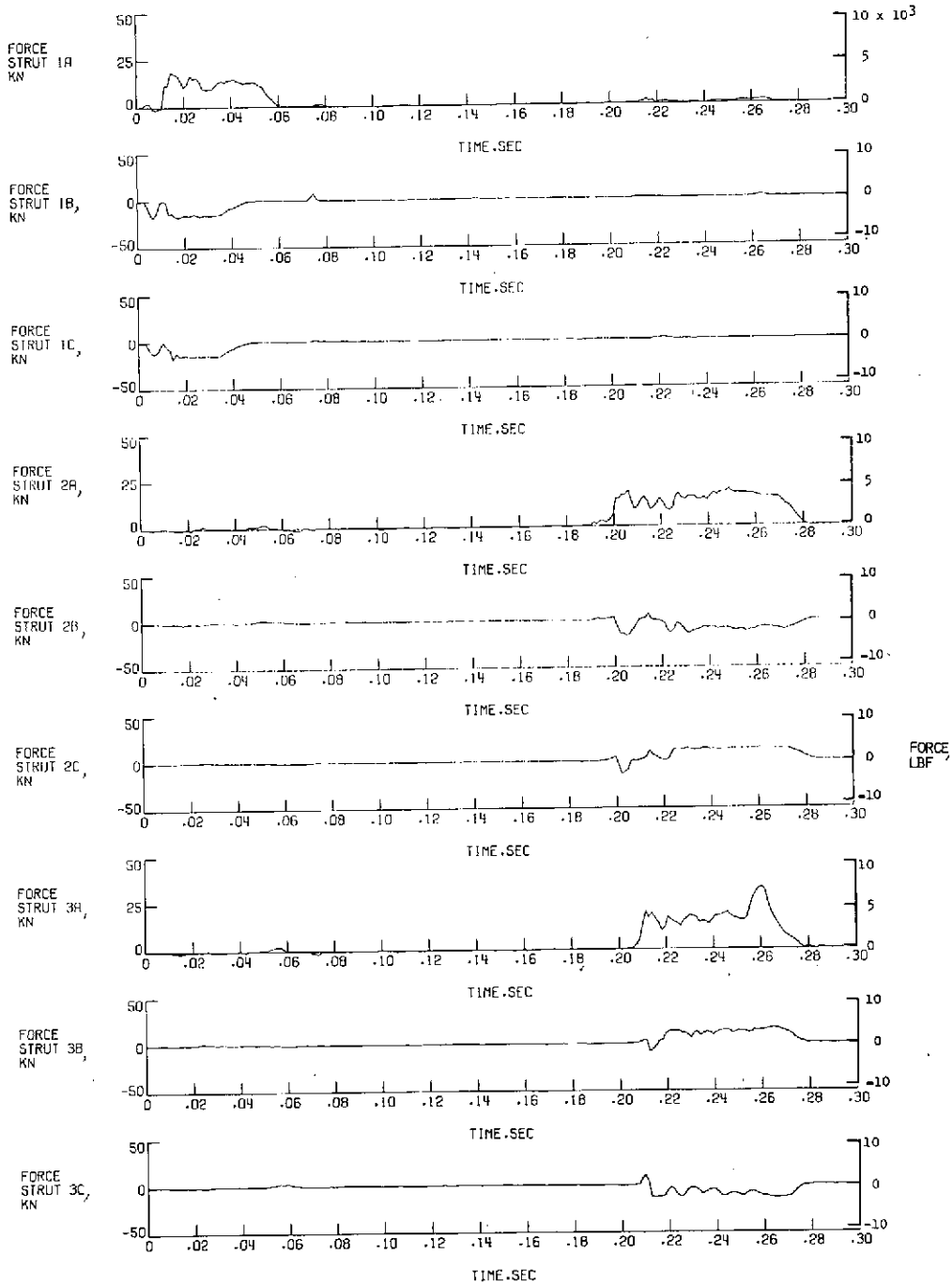

(b) Strut forces (run 5).

Figure 15.- Concluded.

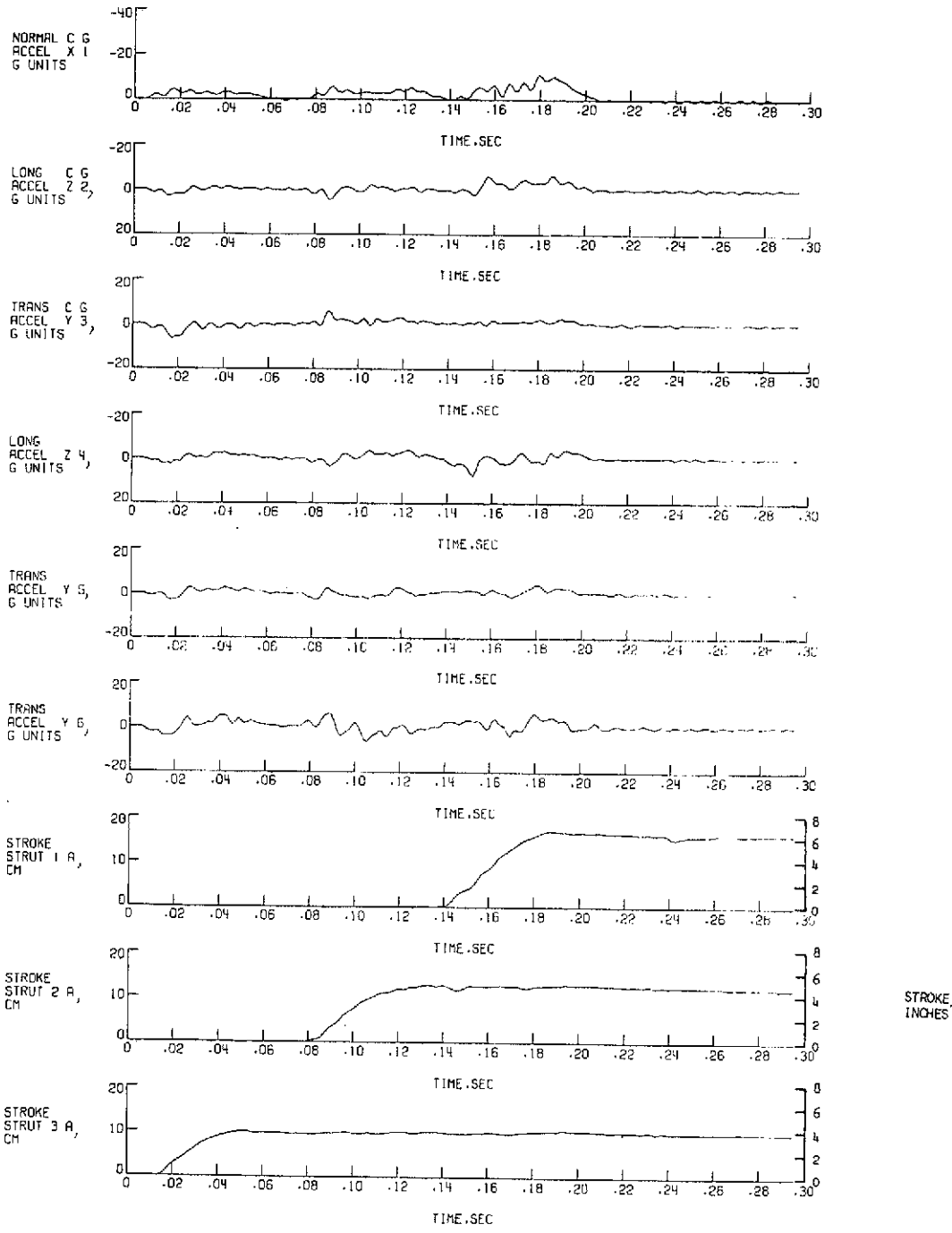

(a) Accelerations and primary strut strokes (run 6).

Figure 16.- Acceleration, stroke, and force time histories for inverted tripod model landing at run 6 conditions. All values are full scale. See table IV for accelerometer locations.

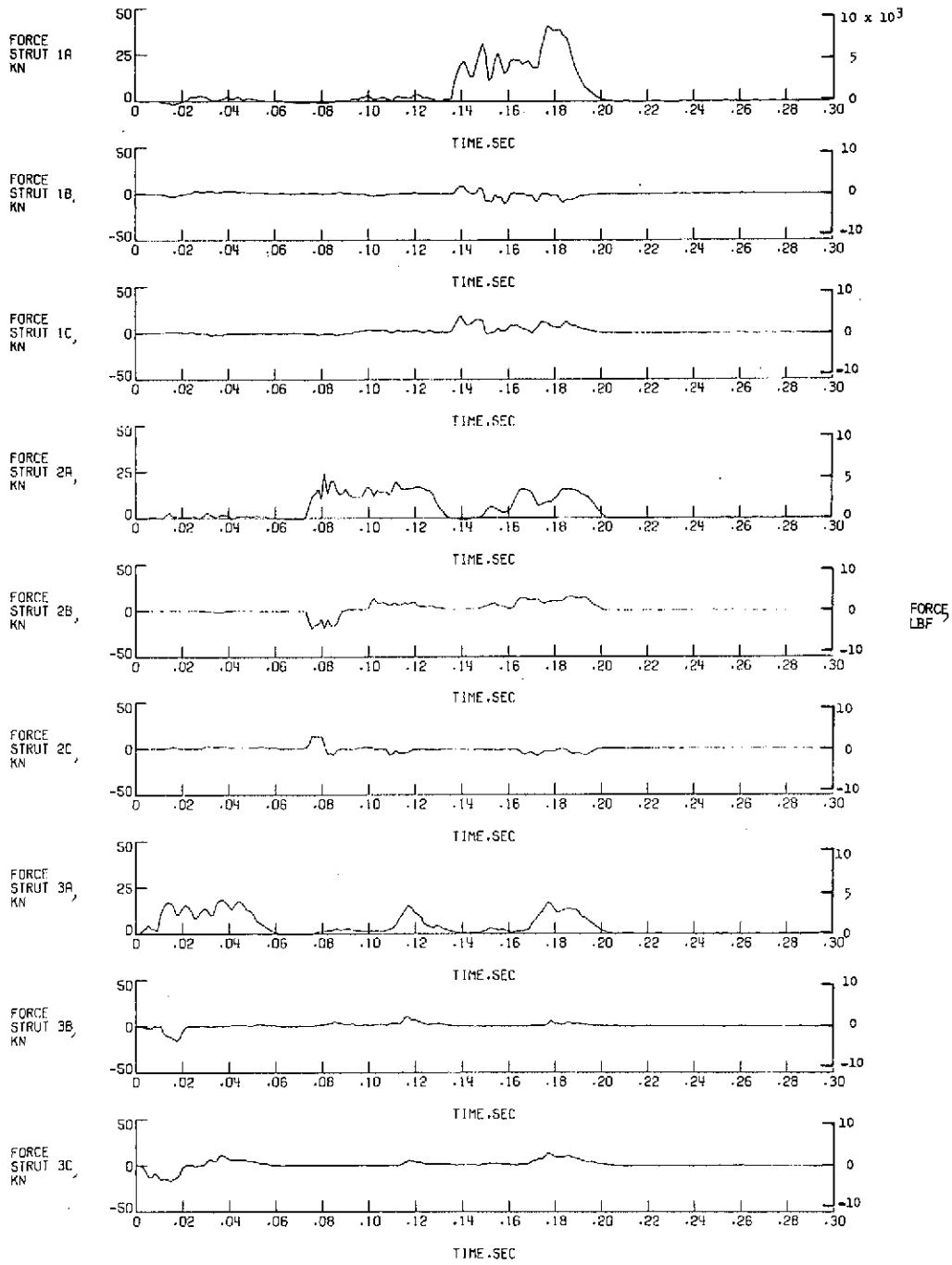

(b) Strut forces (run 6).

Figure 16.- Concluded.

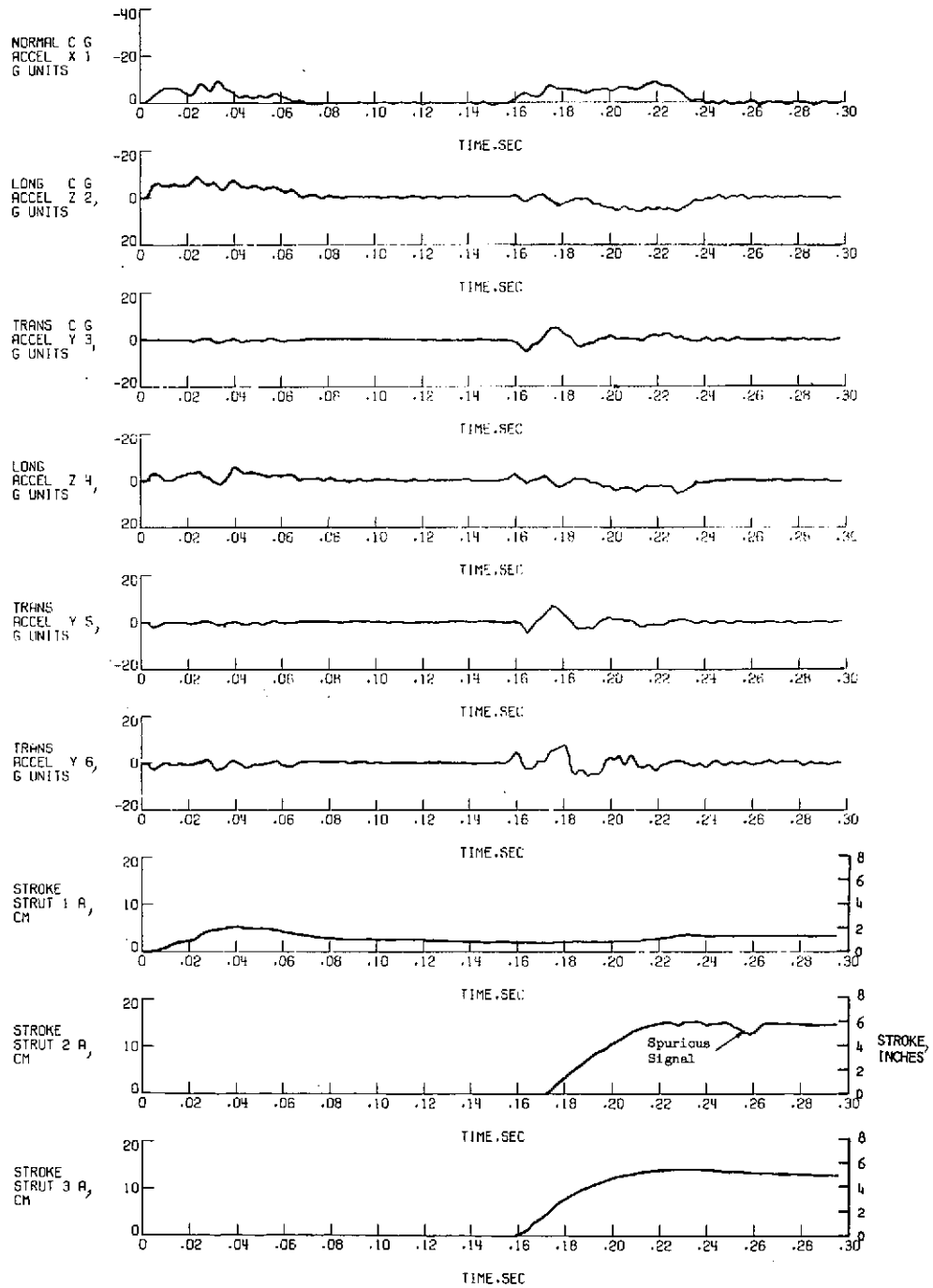

(a) Accelerations and primary strut strokes (run 7).

Figure 17.- Acceleration, stroke, and force time histories for inverted tripod model landing at run 7 conditions. All values are full scale. See table IV for accelerometer locations.

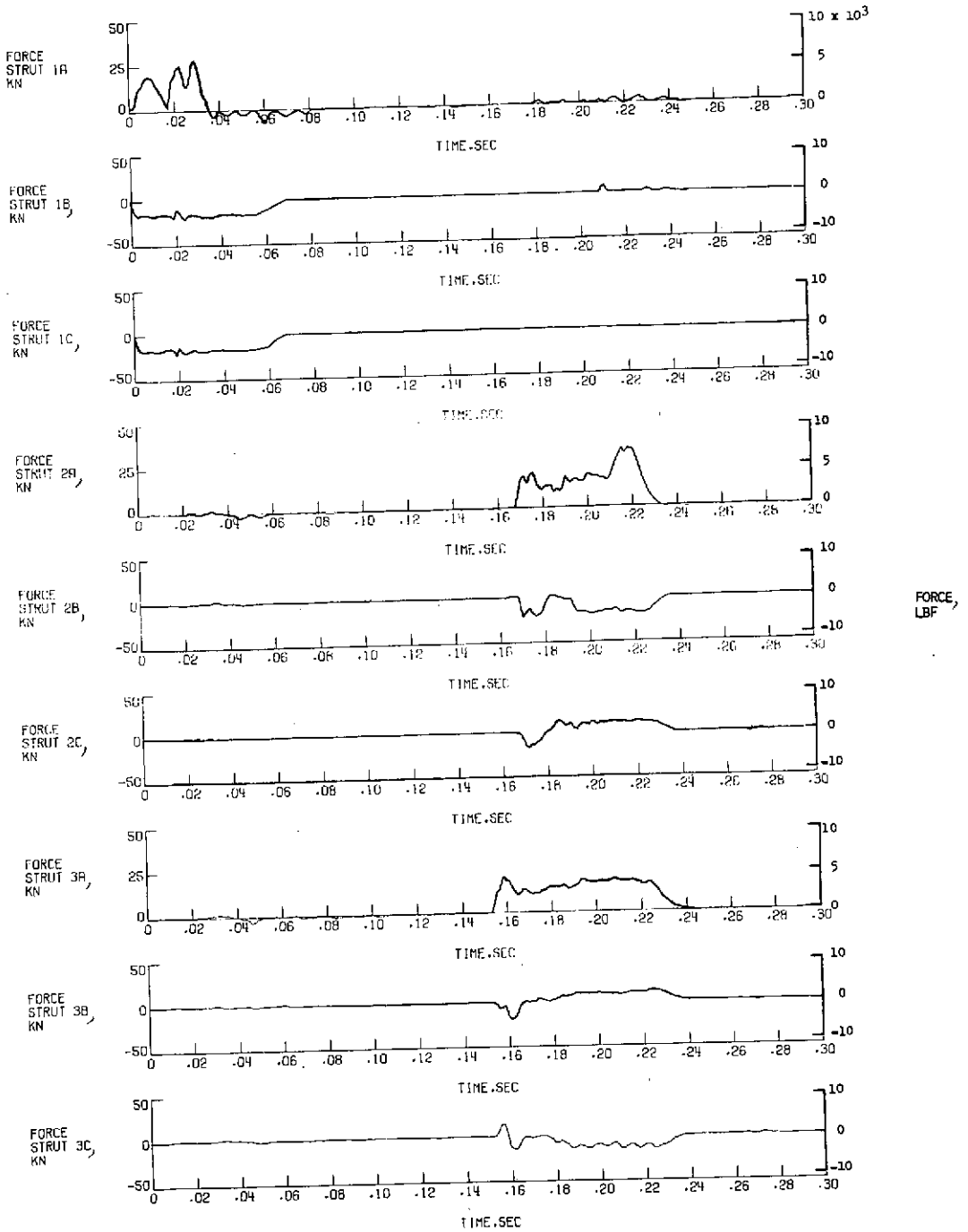

(b) Strut forces (run 7).

Figure 17.- Concluded.

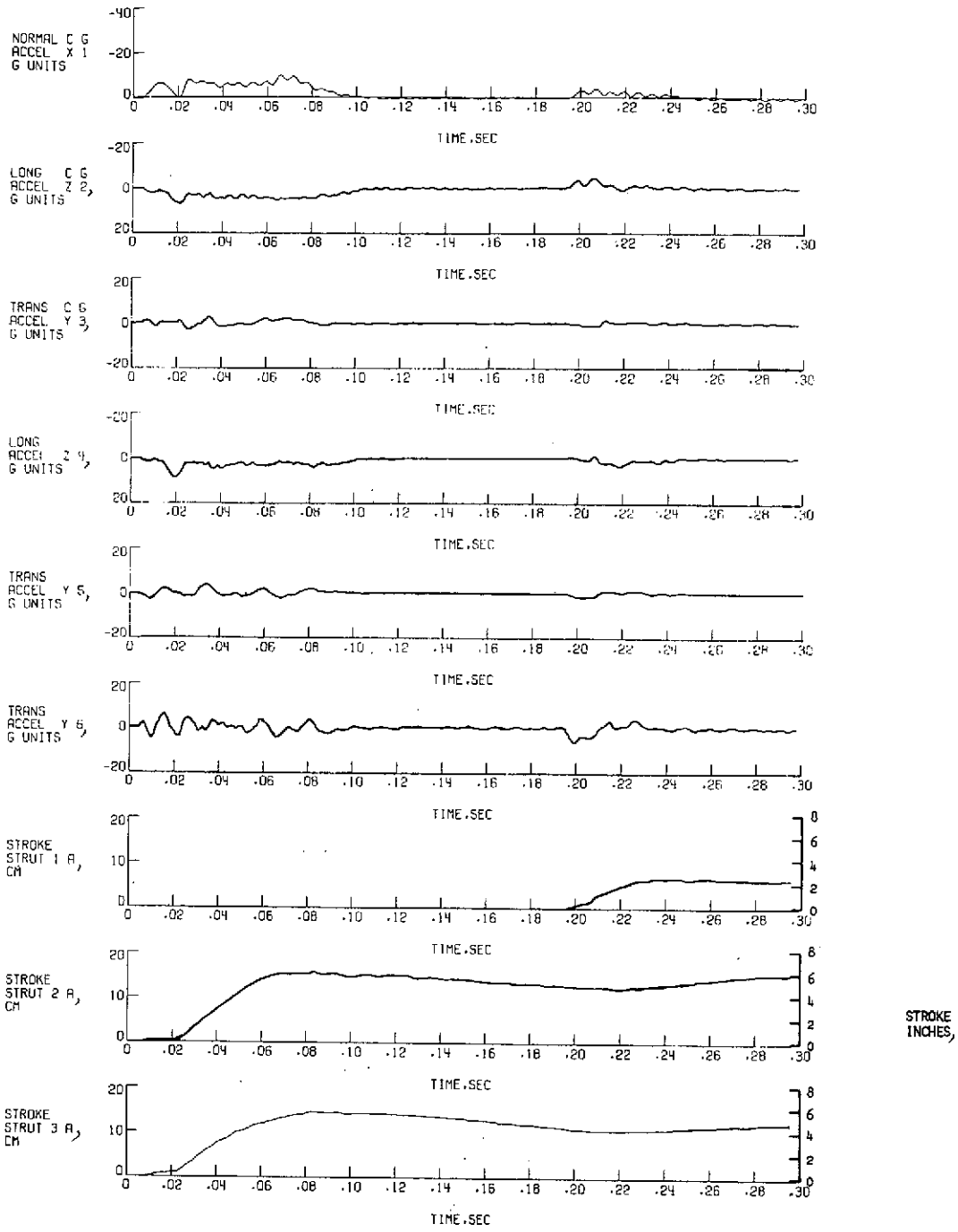

(a) Accelerations and primary strut strokes (run 8).

Figure 18.- Acceleration, stroke, and force time histories for inverted tripod model landing at run 8 conditions. All values are full scale. See table IV for accelerometer locations.

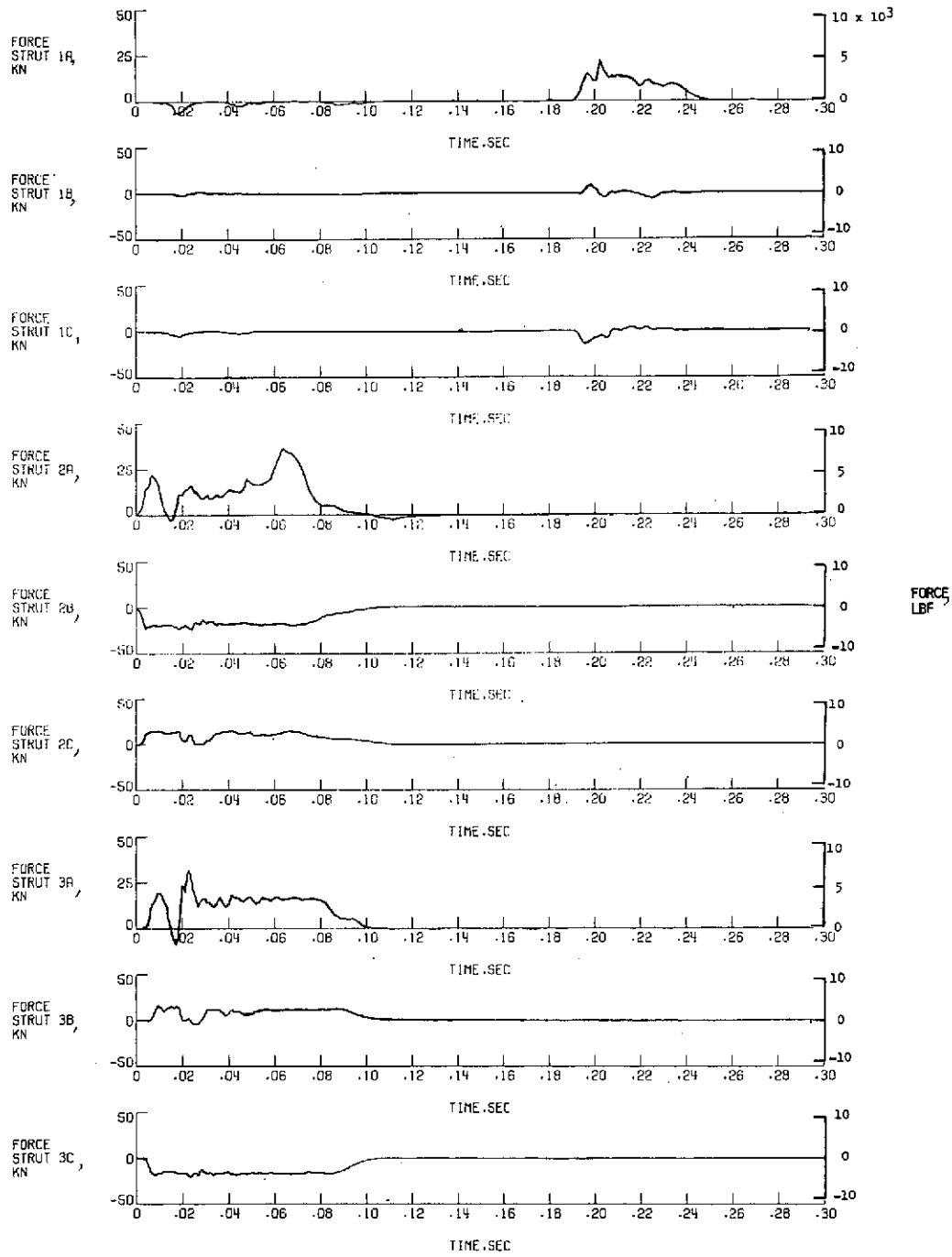

(b) Strut forces (run 8).

Figure 18.- Concluded.

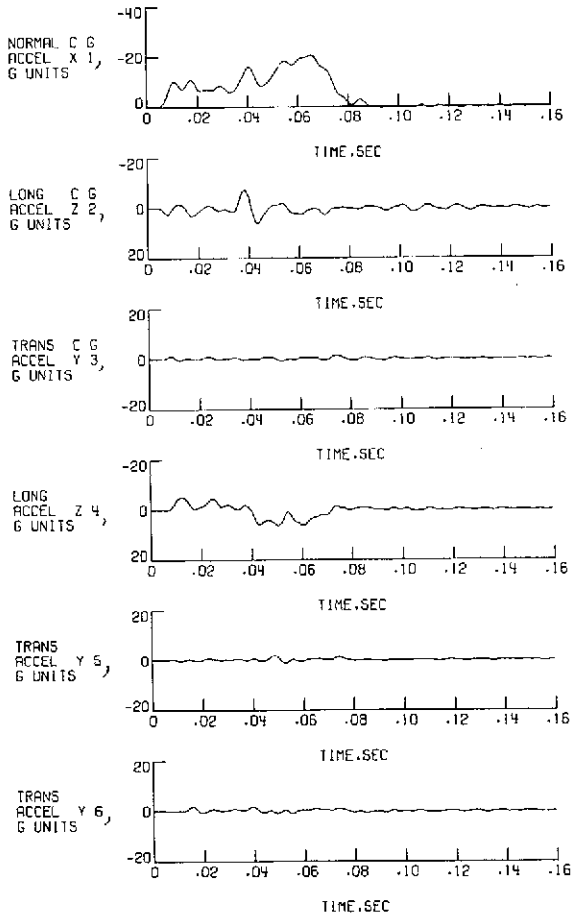

(a) Accelerations (run 1).

Figure 19.- Acceleration, stroke, and force time histories for cantilever model landing at run 1 conditions. All values are full scale. See table IV for accelerometer locations.

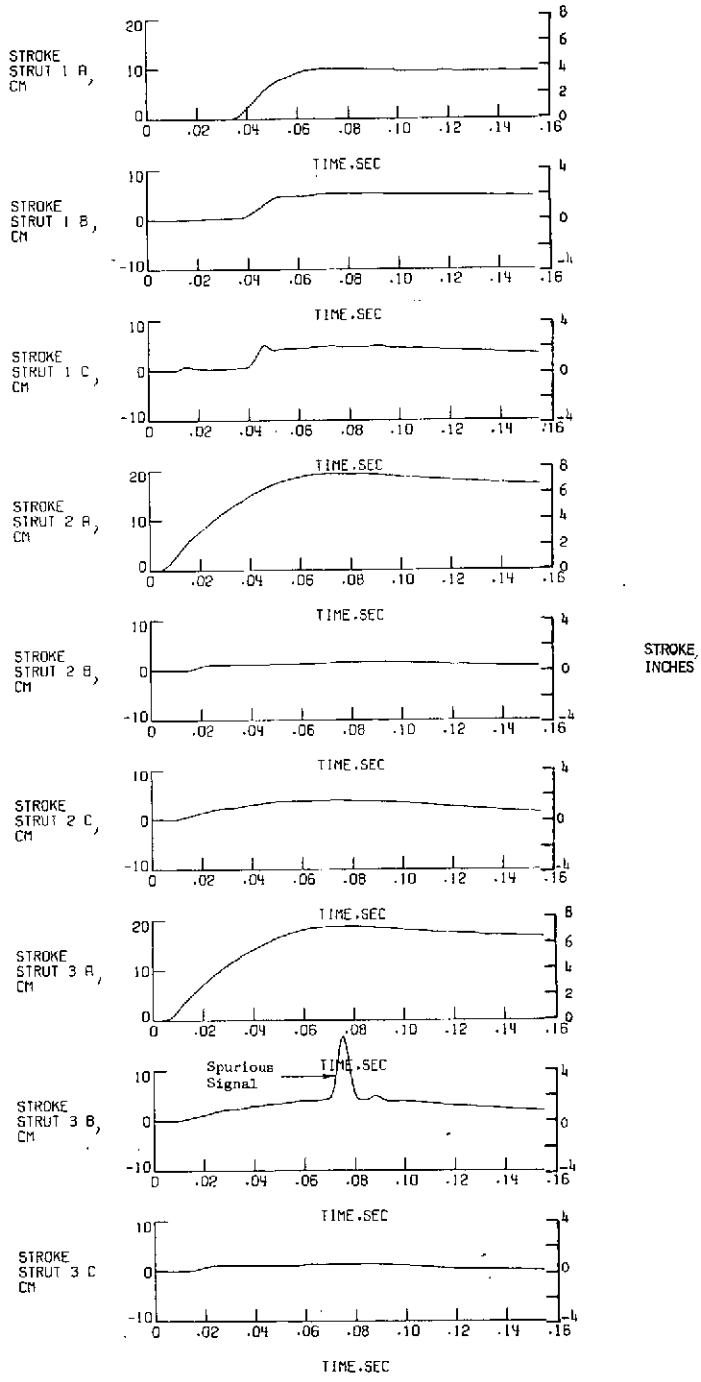

(b) Strut strokes (run 1).

Figure 19.- Continued.

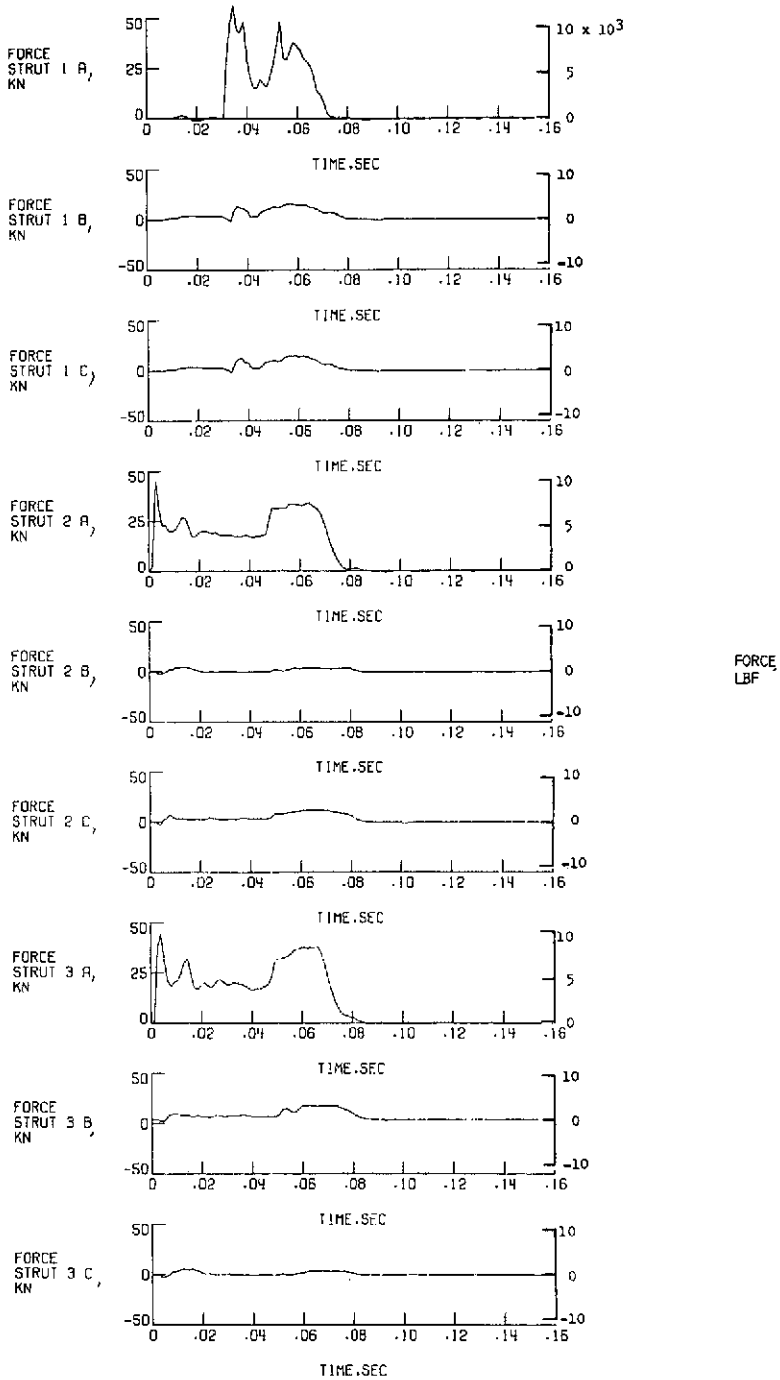

(c) Strut forces (run 1).

Figure 19.- Concluded.

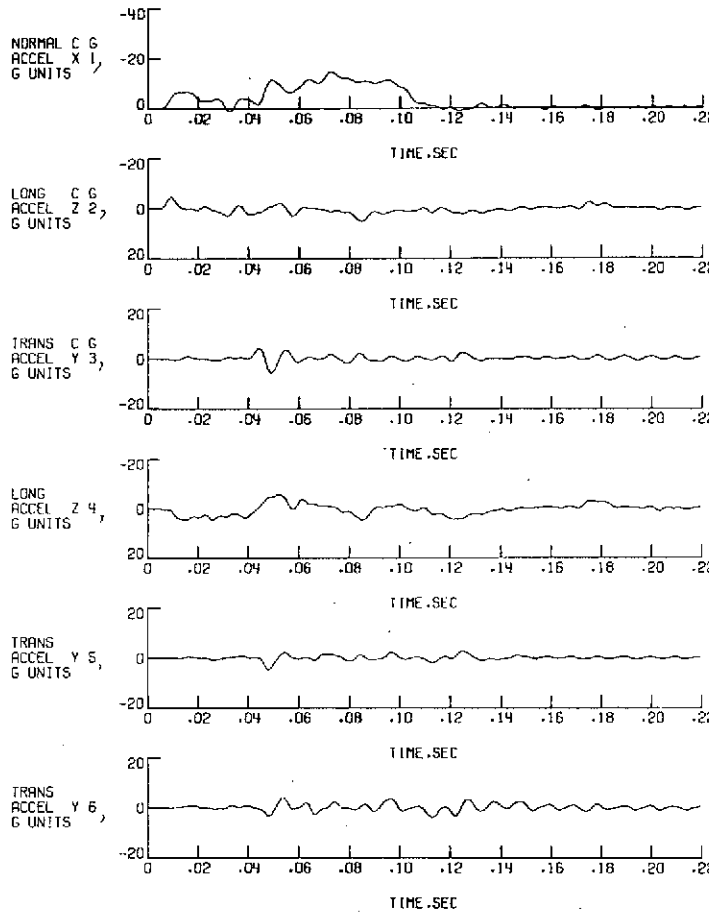

(a) Accelerations (run 2).

Figure 20.- Acceleration, stroke, and force time histories for cantilever model landing at run 2 conditions. All values are full scale. See table IV for accelerometer locations.

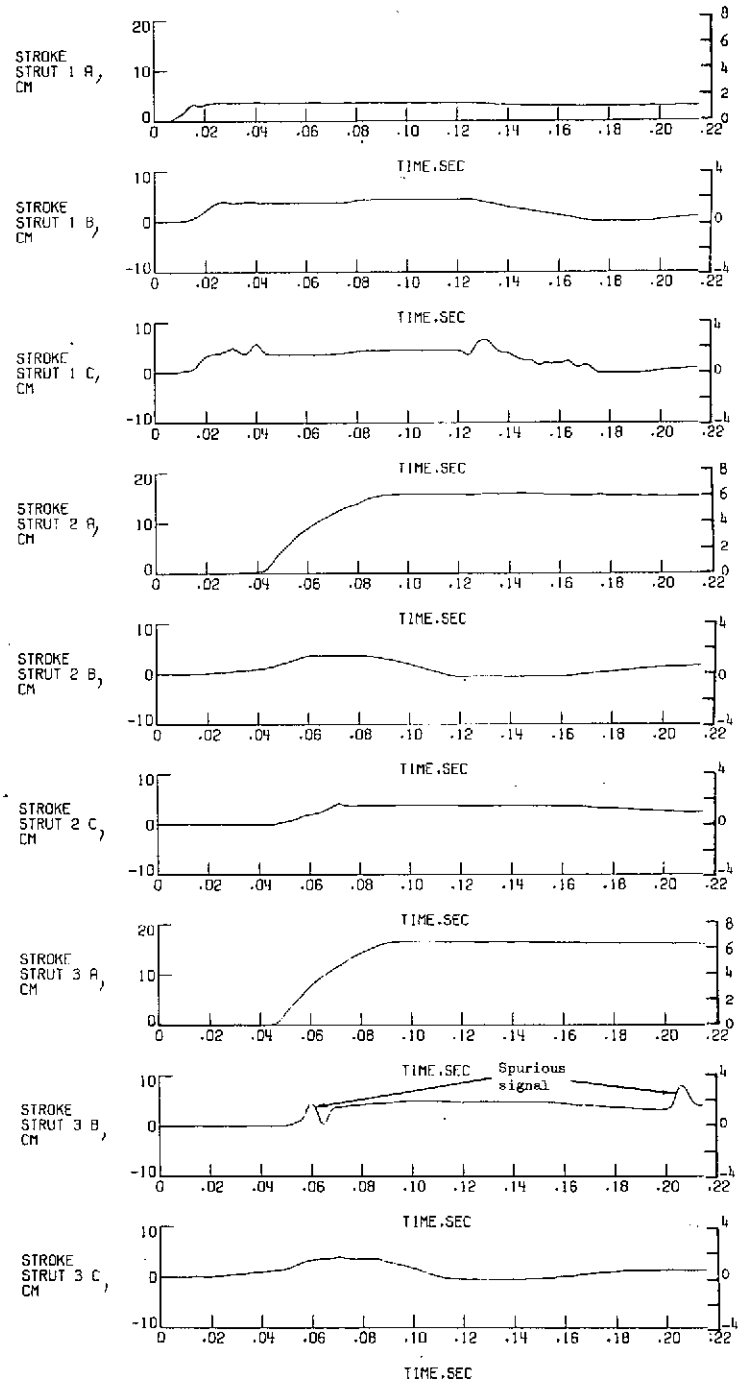

(b) Strut strokes (run 2).

Figure 20.- Continued.

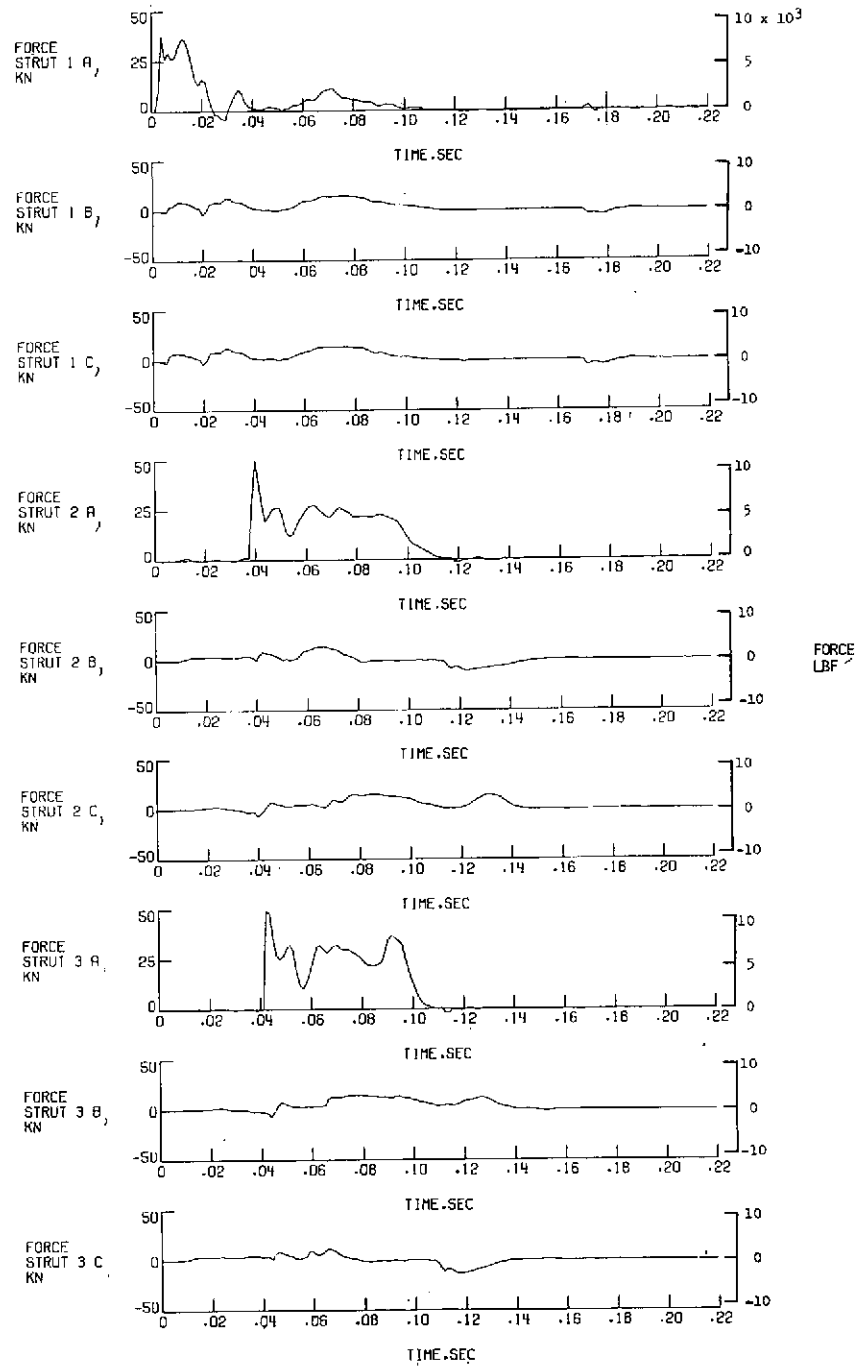

(c) Strut forces (run 2).

Figure 20.- Concluded.

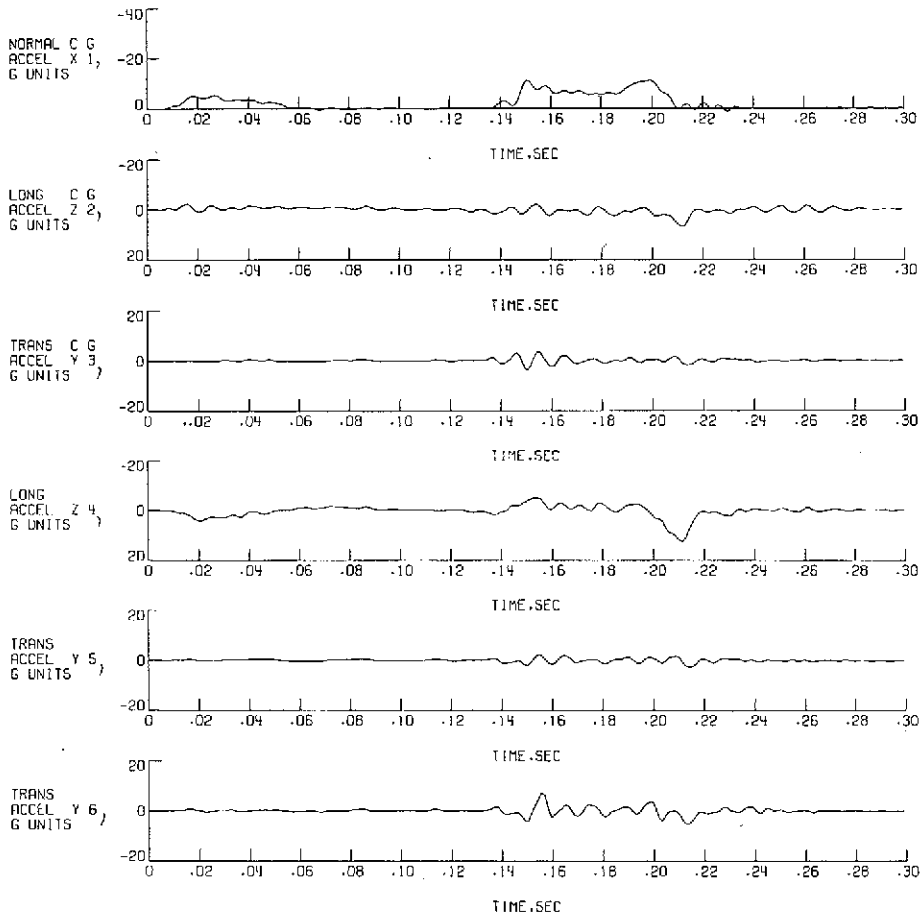

(a) Accelerations (run 3).

Figure 21.- Acceleration, stroke, and force time histories for cantilever model landing at run 3 conditions. All values are full scale. See table IV for accelerometer locations.

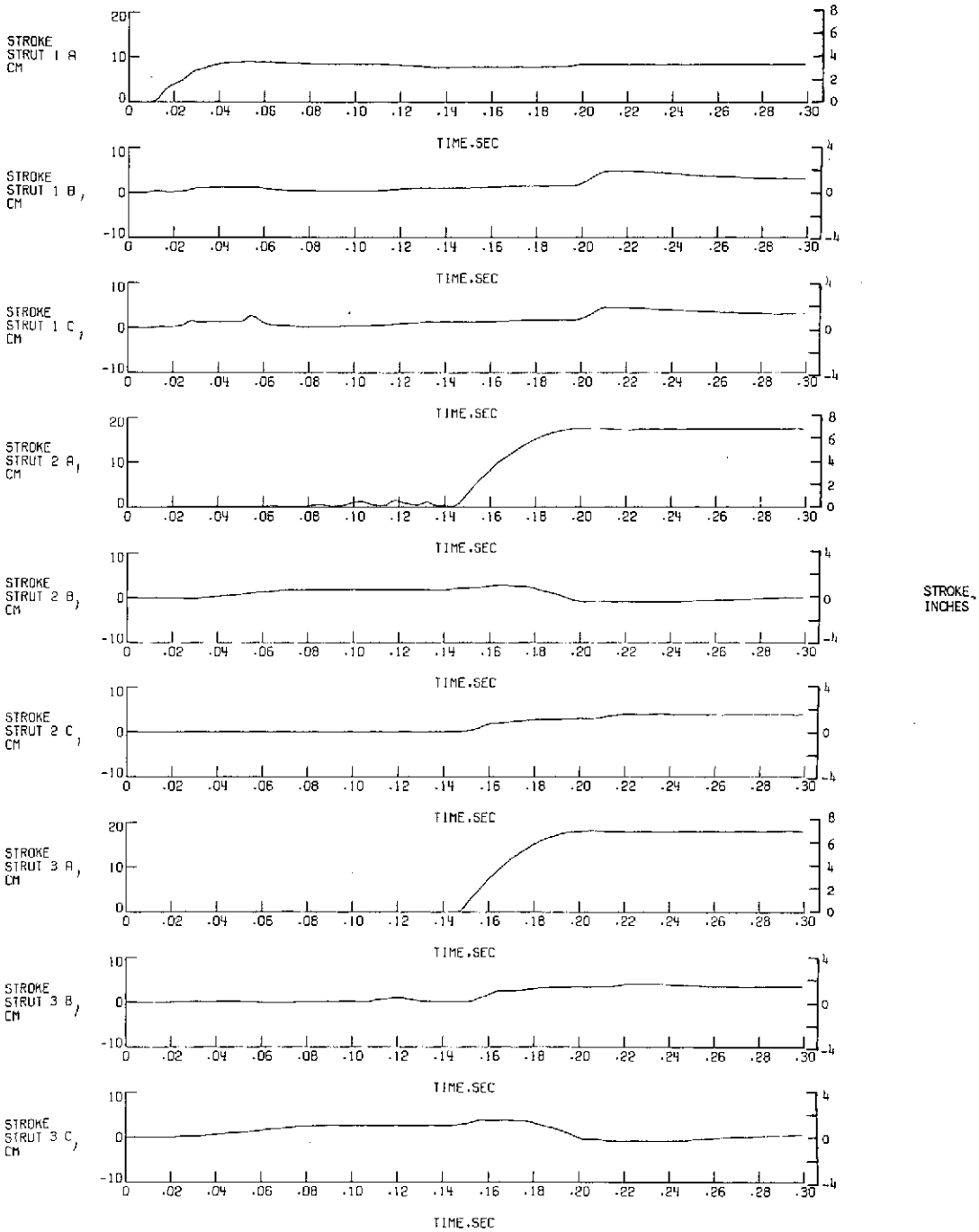

(b) Strut strokes (run 3).

Figure 21.- Continued.

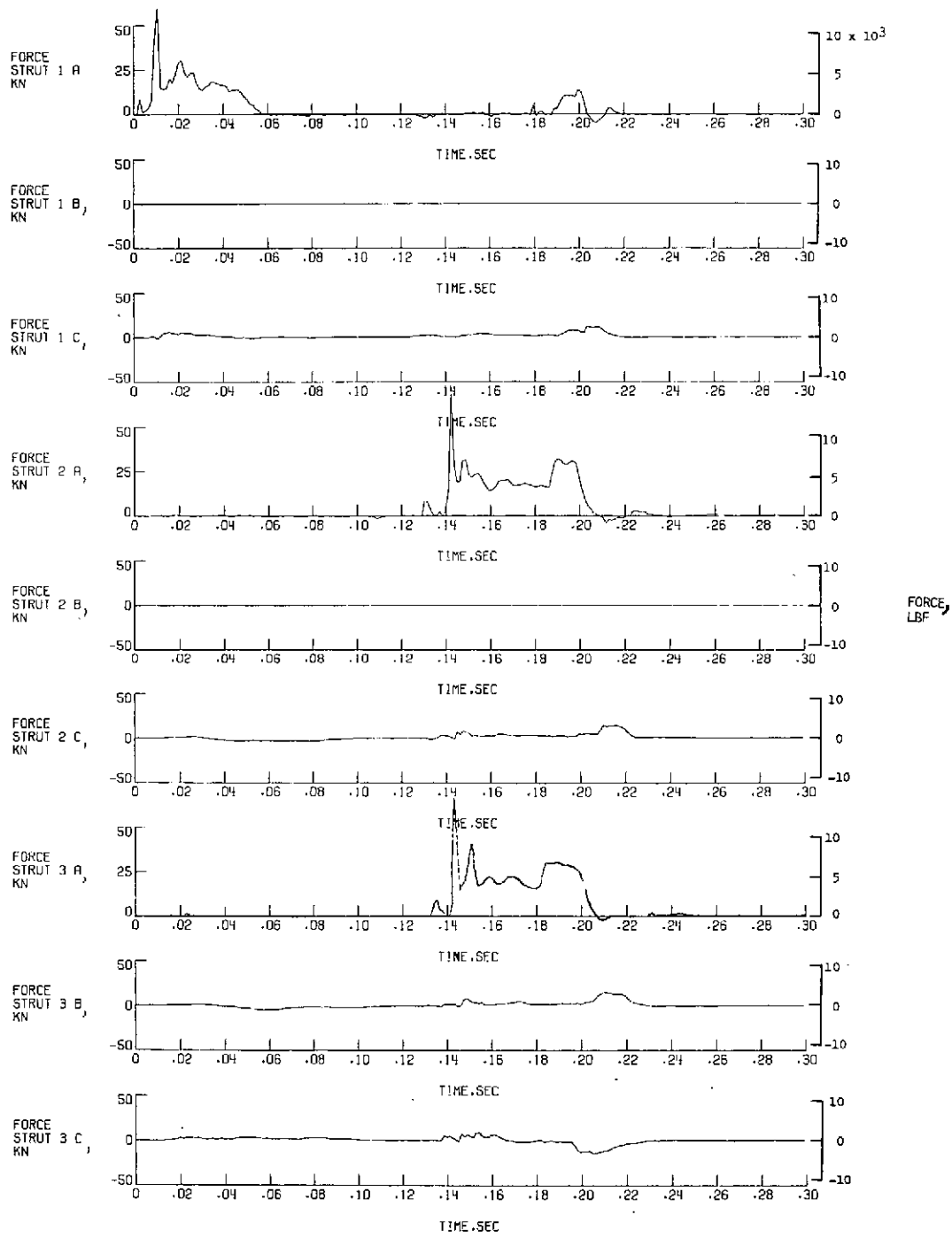

(c) Strut forces (run 3).

Figure 21.- Concluded.

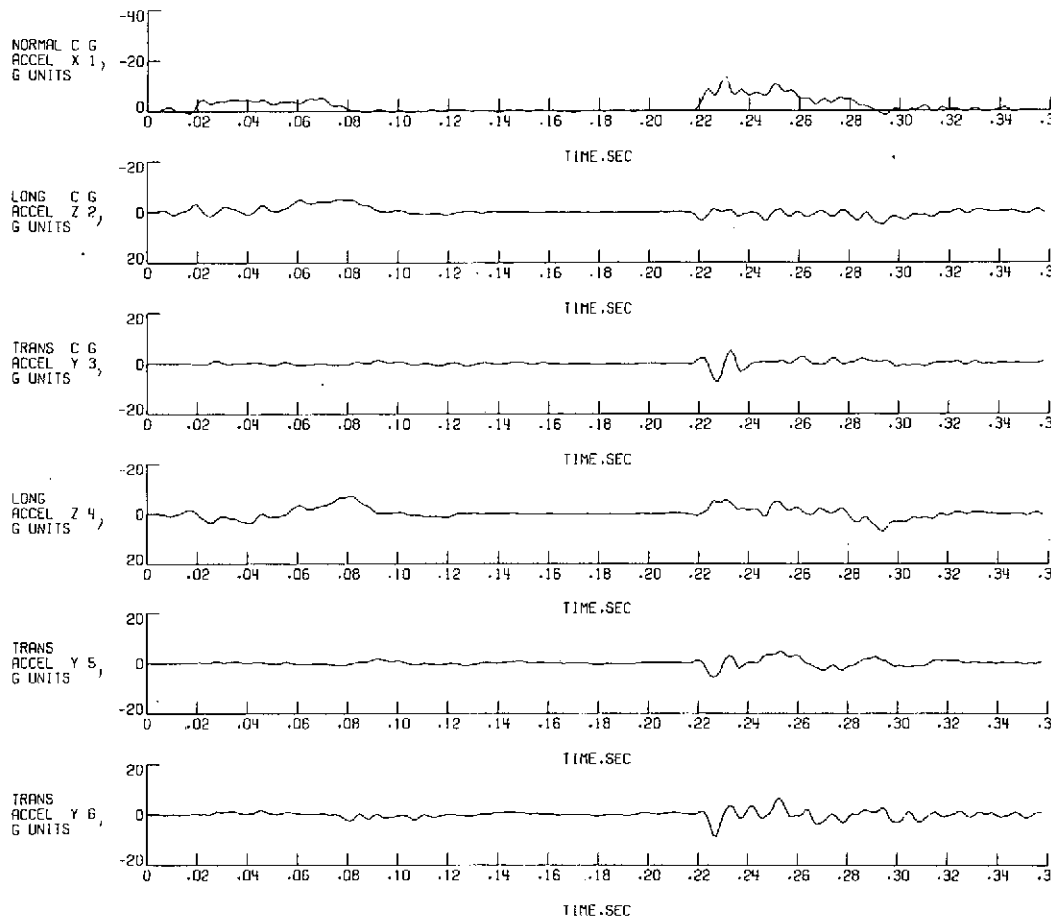

(a) Accelerations (run 5).

Figure 22.- Acceleration, stroke, and force time histories for cantilever model landing at run 5 conditions. All values are full scale. See table IV for accelerometer locations.

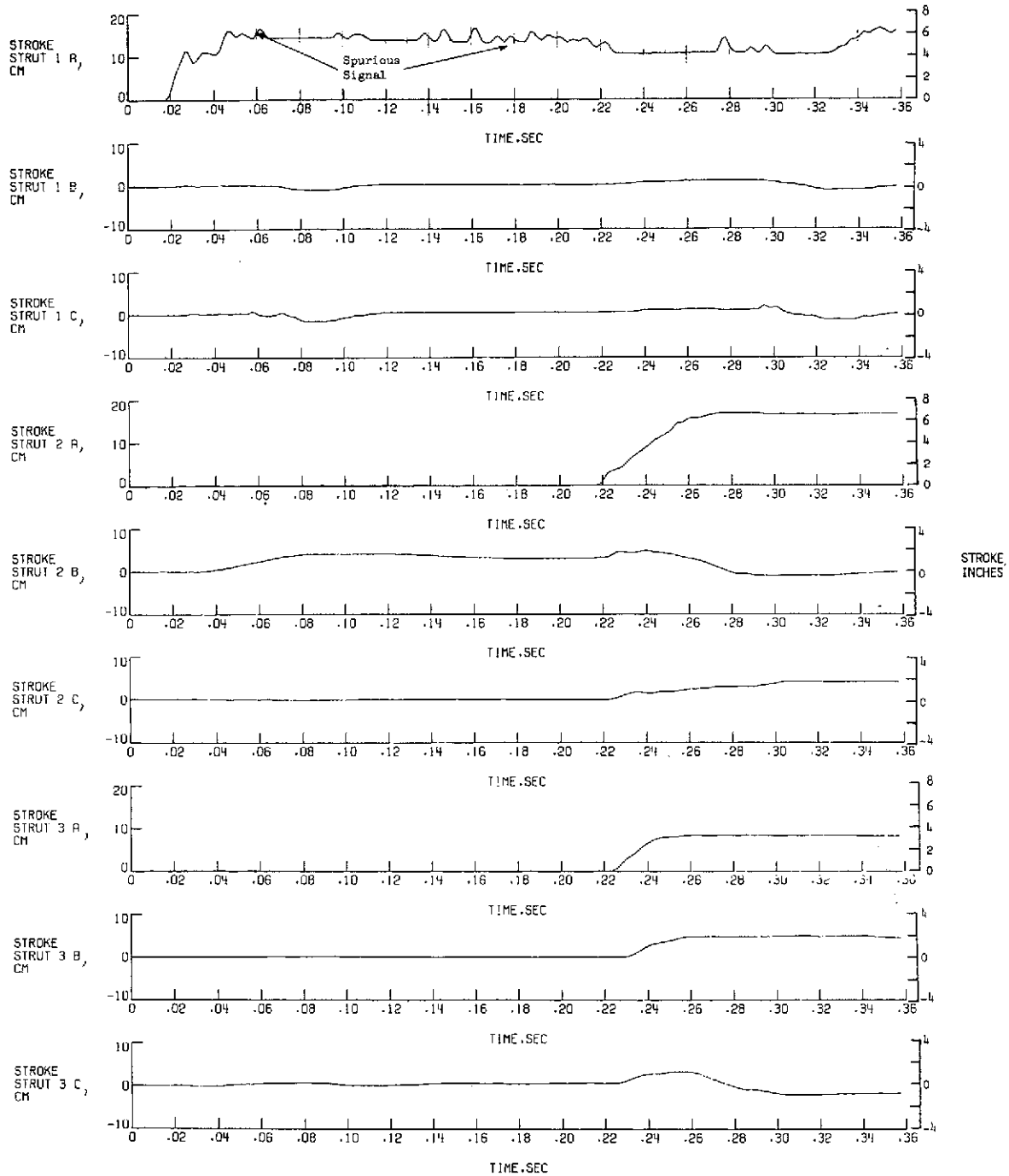

(b) Strut strokes (run 5).

Figure 22.- Continued.

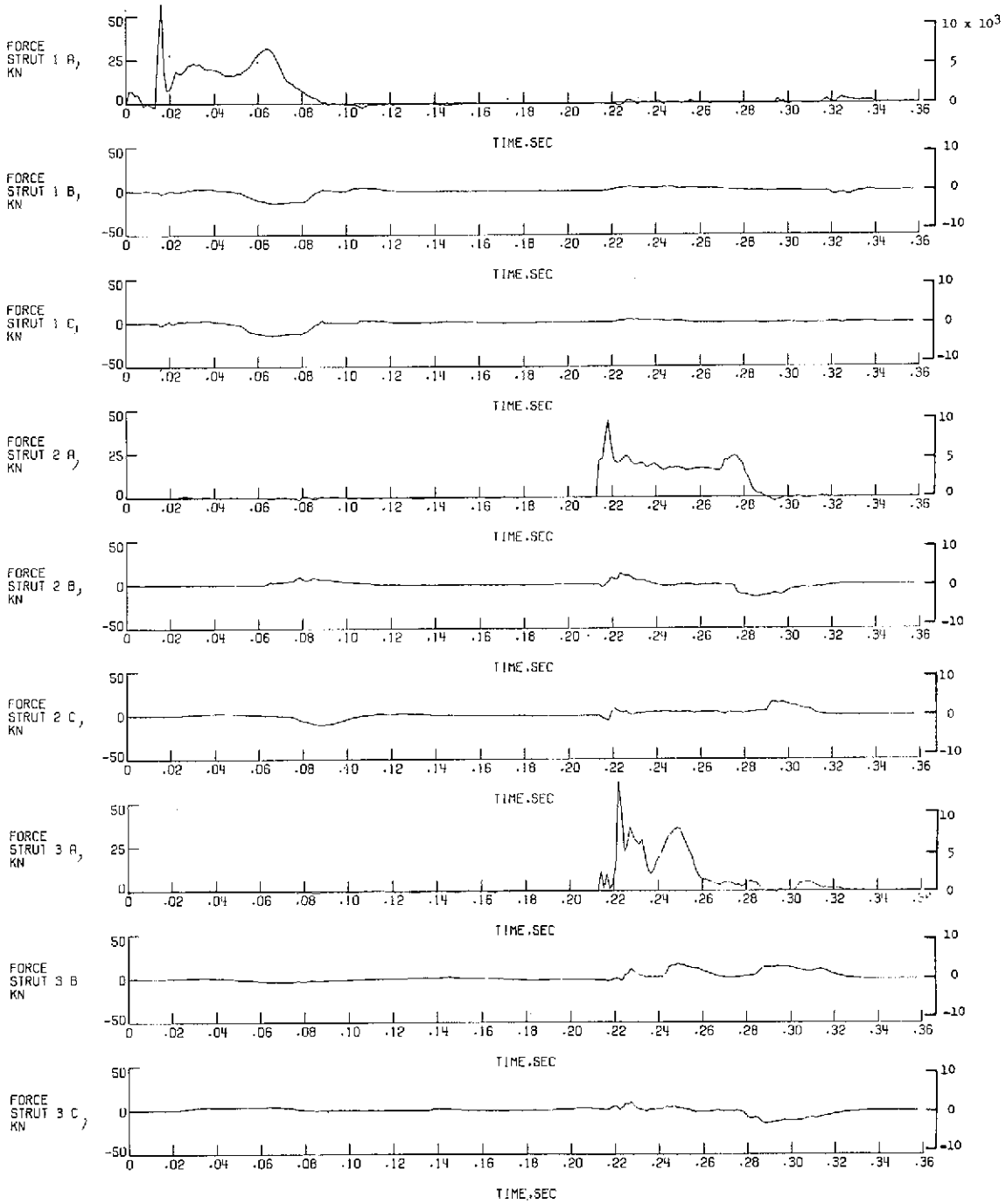

(c) Strut forces (run 5).

Figure 22.- Concluded.

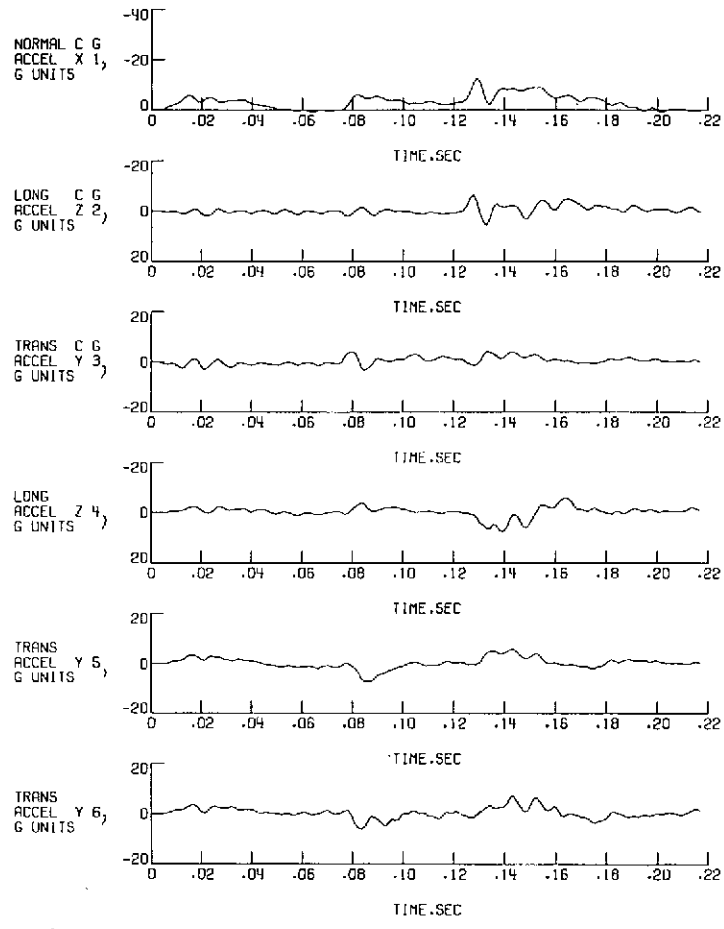

(a) Accelerations (run 6).

Figure 23.- Acceleration, stroke, and force time histories for cantilever model landing at run 6 conditions. All values are full scale. See table IV for accelerometer locations.

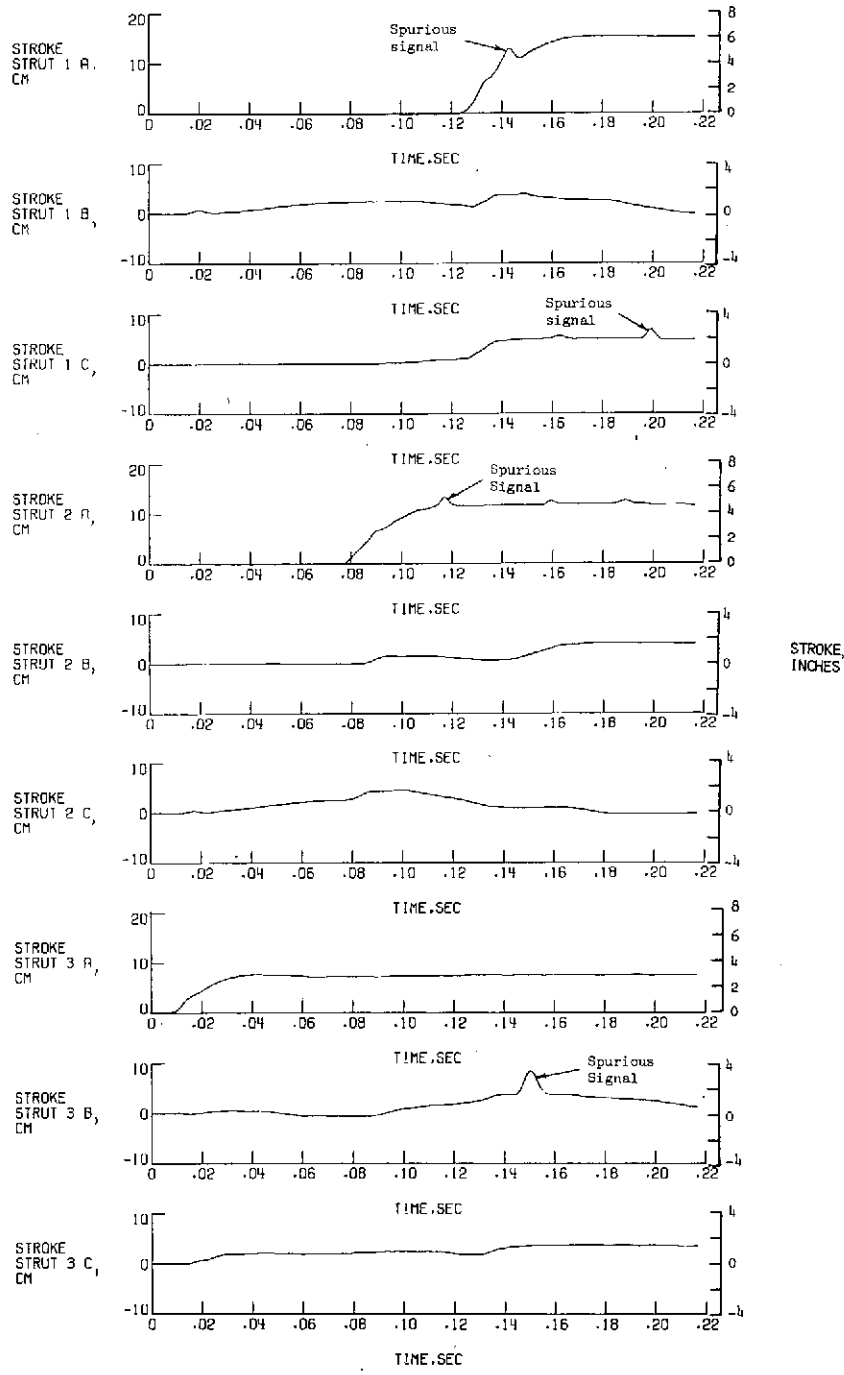

(b) Strut strokes (run 6).

Figure 23.- Continued.

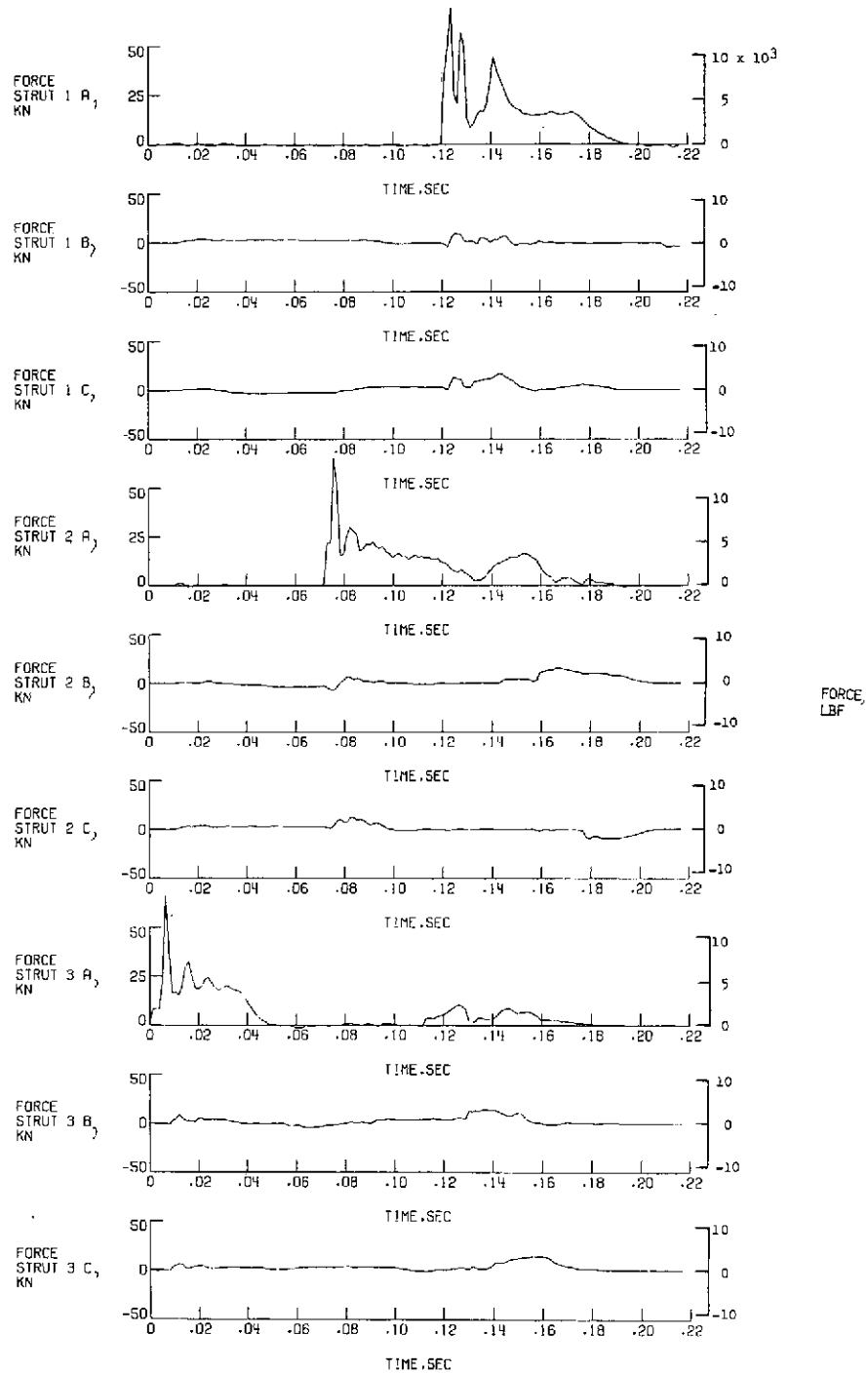

(c) Strut forces (run 6).

Figure 23.- Concluded.

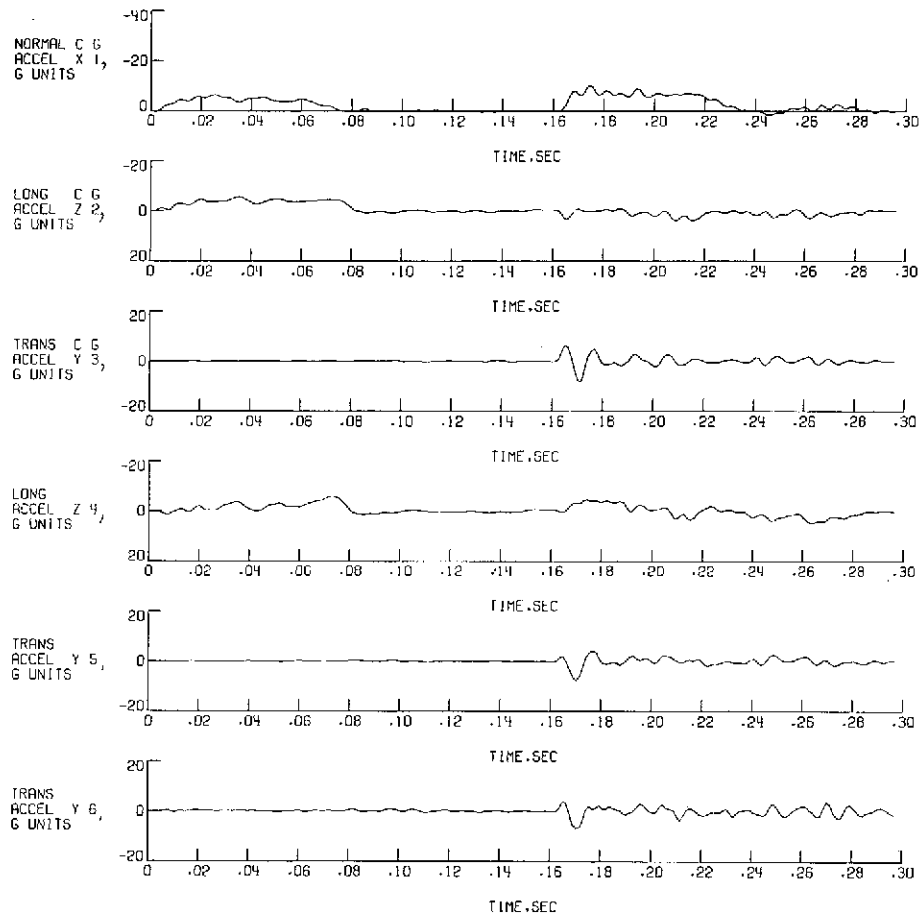

(a) Accelerations (run 7).

Figure 24.- Acceleration, stroke, and force time histories for cantilever model landing at run 7 conditions. All values are full scale. See table IV for accelerometer locations.

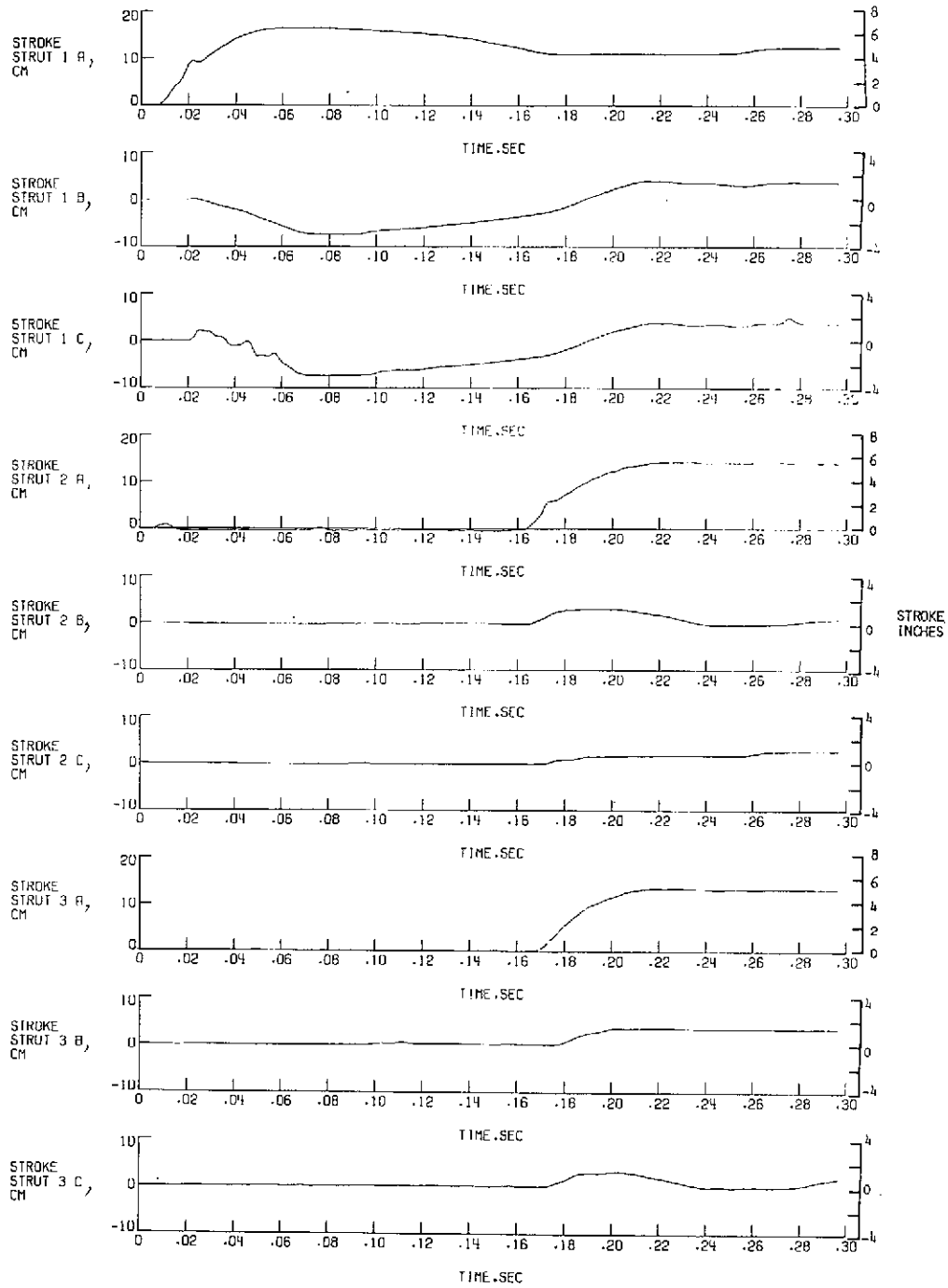

(b) Strut strokes (run 7).

Figure 24.- Continued.

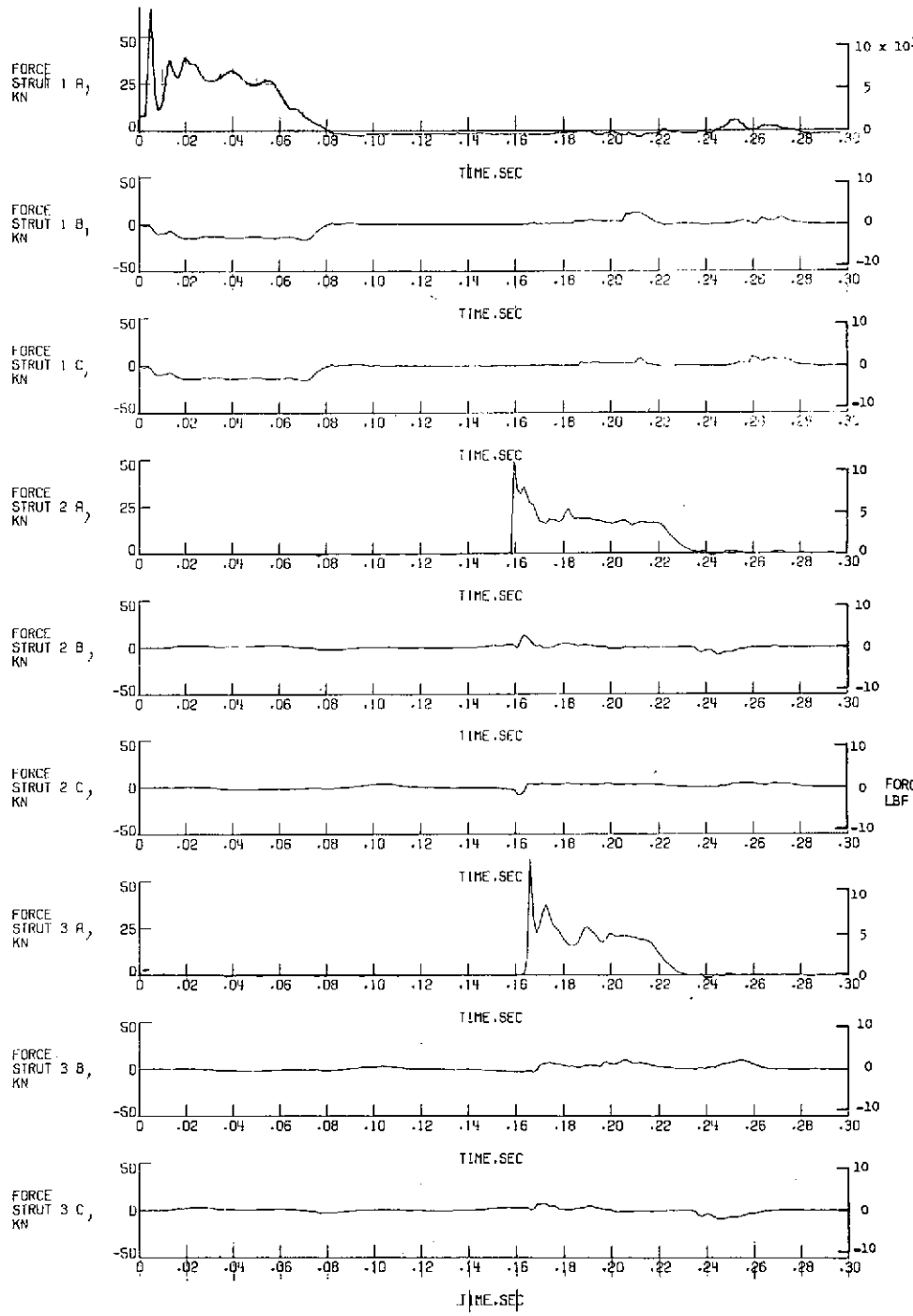

(c) Strut forces (run 7).

Figure 24.- Concluded.

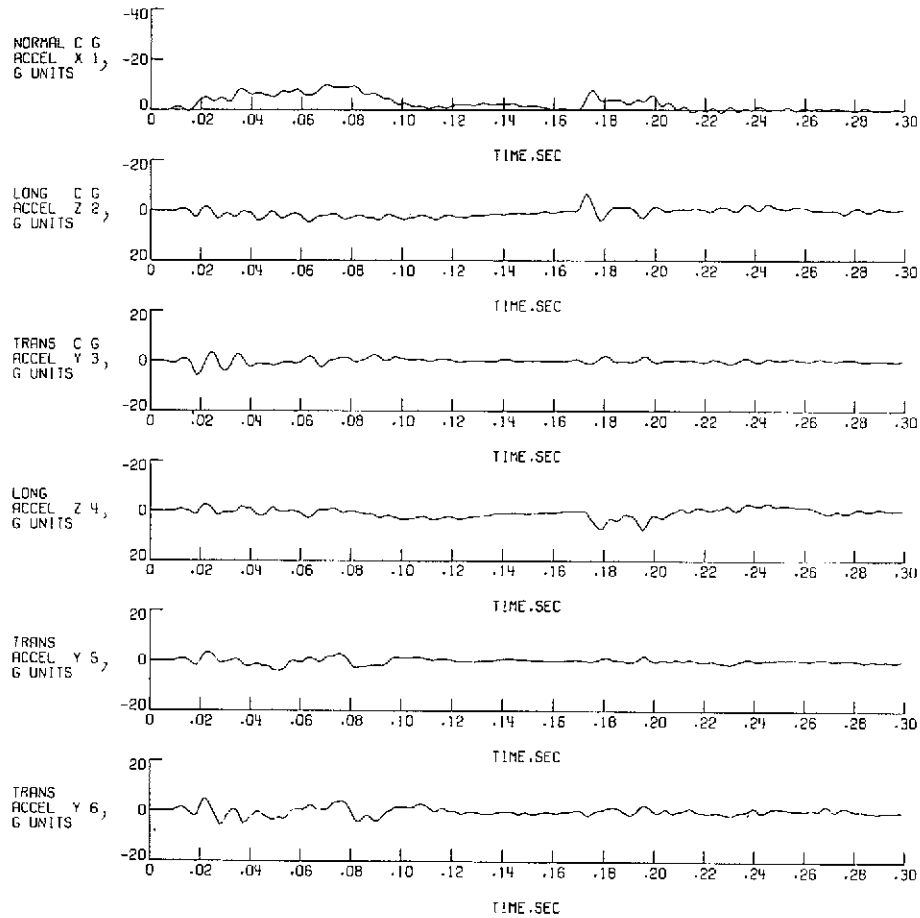

(a) Accelerations (run 8).

Figure 25.- Acceleration, stroke, and force time histories for cantilever model landing at run 8 conditions. All values are full scale. See table IV for accelerometer locations.

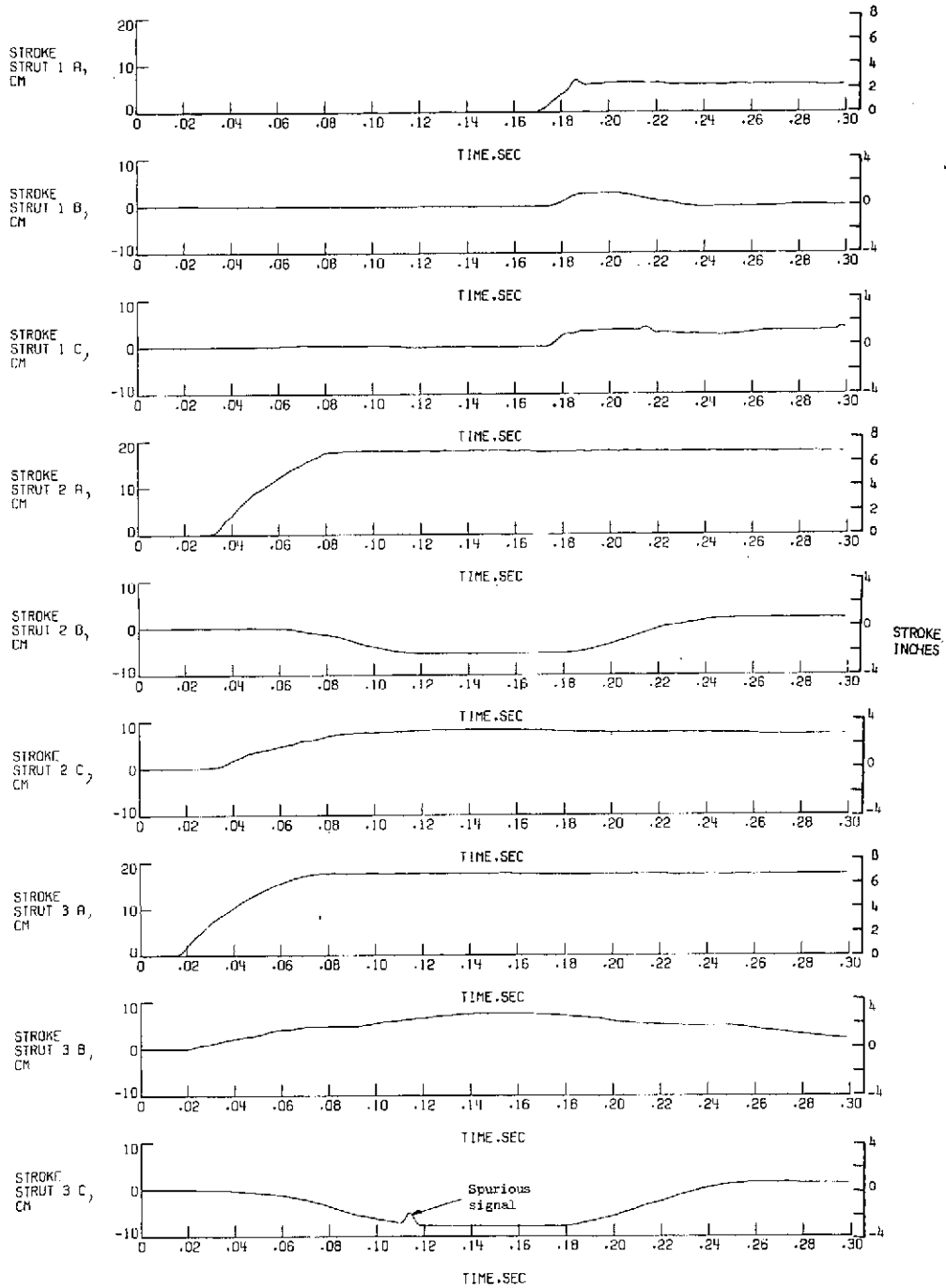

(b) Strut strokes (run 8).

Figure 25.- Continued.

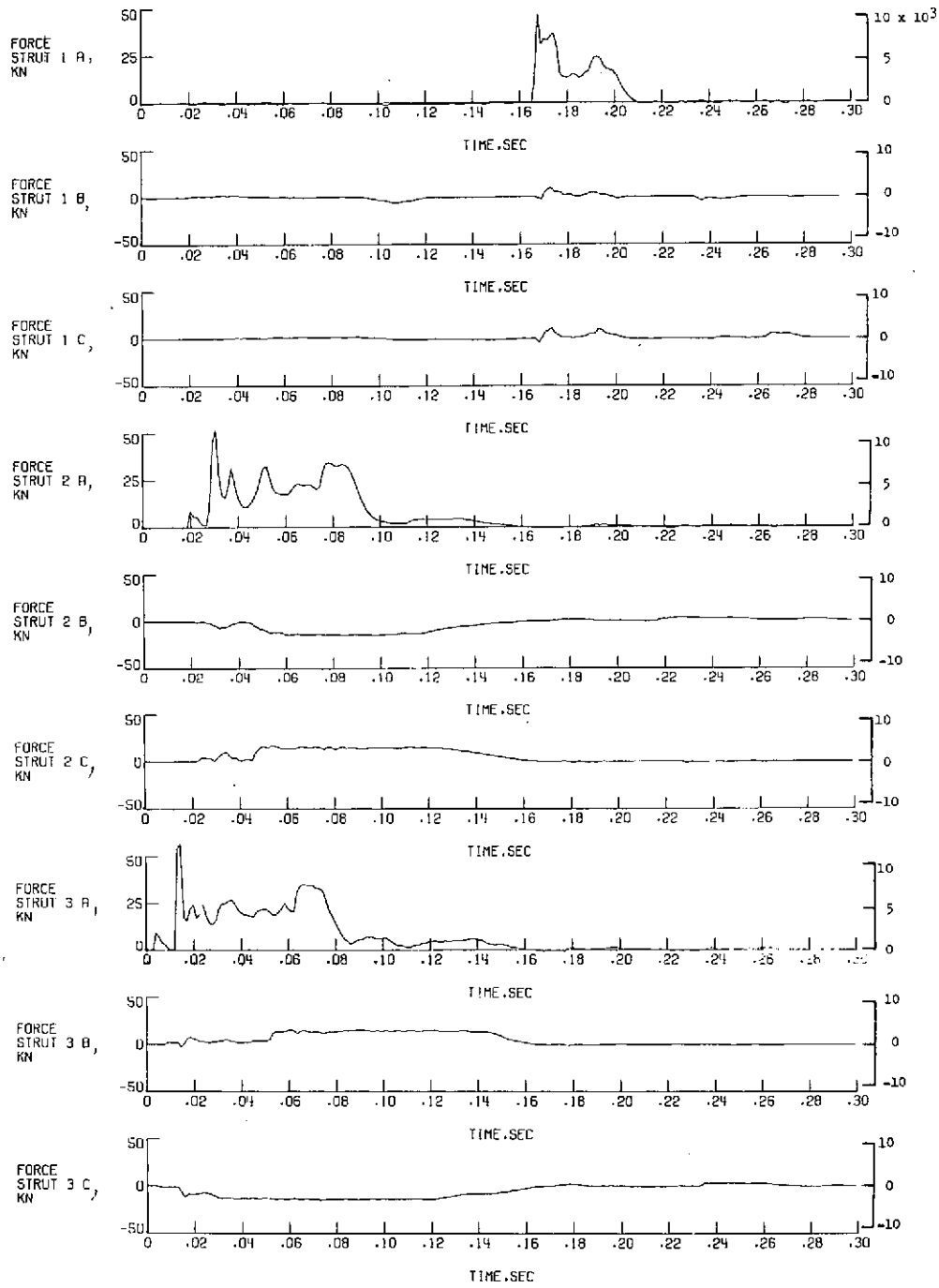

(c) Strut forces (run 8).

Figure 25.- Concluded.

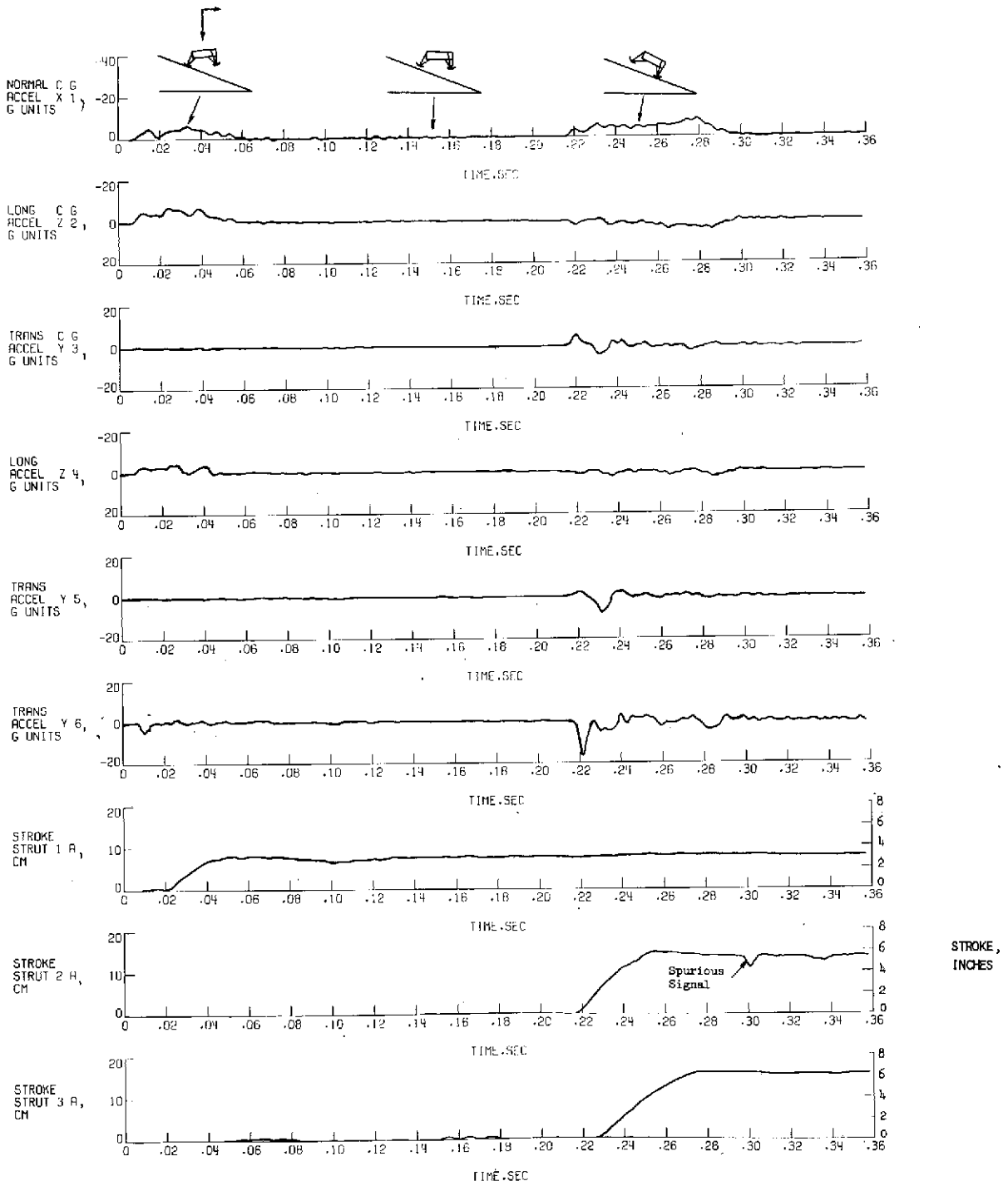

(a) Accelerations and primary strut strokes.

Figure 26.- Typical time histories for the inverted tripod model landing at run 4 conditions. V_v = 6.85 m/sec (22.5 ft/sec); V_h = 2 m/sec (6 ft/sec); pitch, -16°; roll, 180°; yaw, 2° right; μ = 0.4; slope, -20°. All values are full scale. See table IV for accelerometer locations.

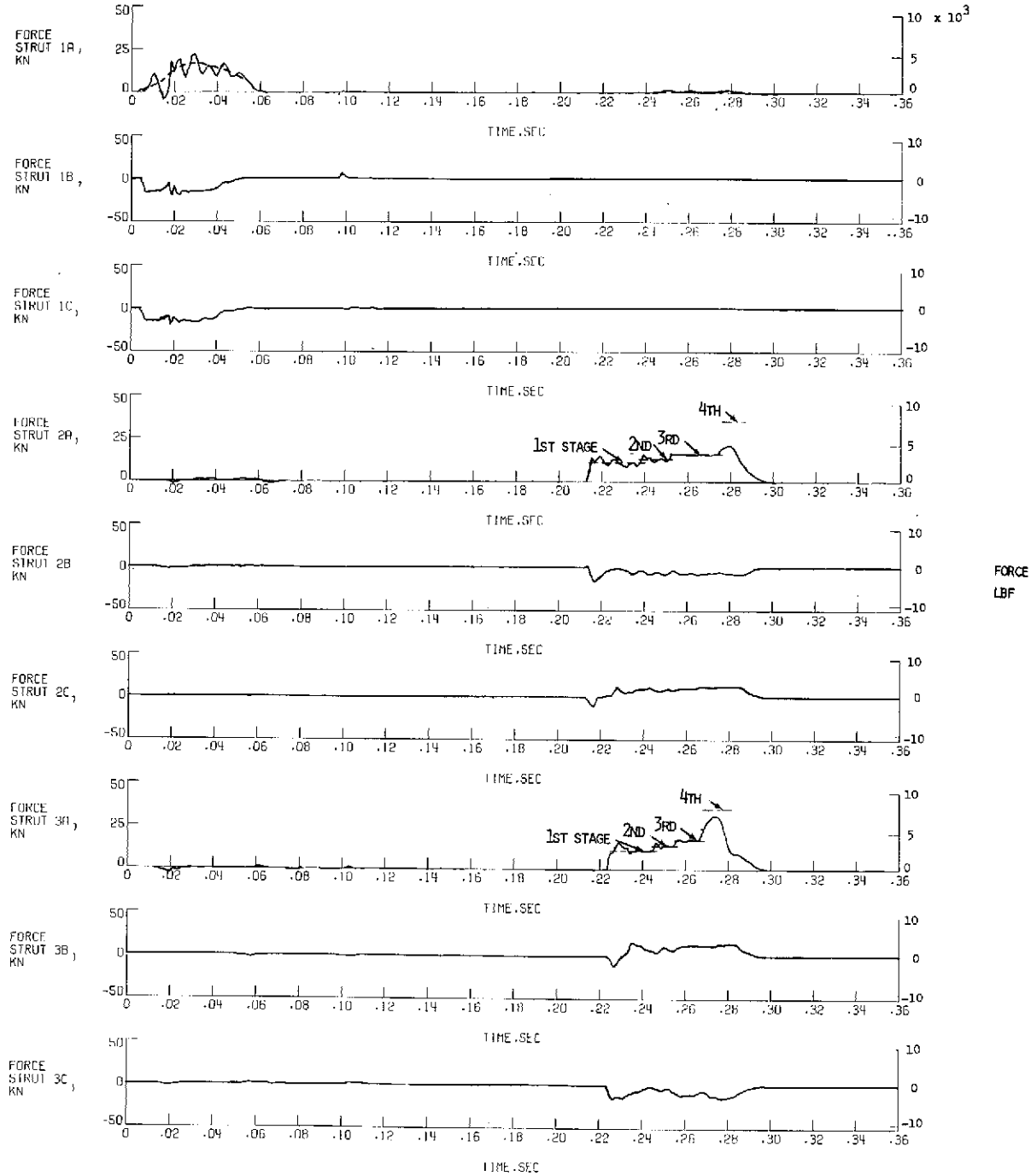

(b) Strut forces (run 4).

Figure 26.- Concluded.

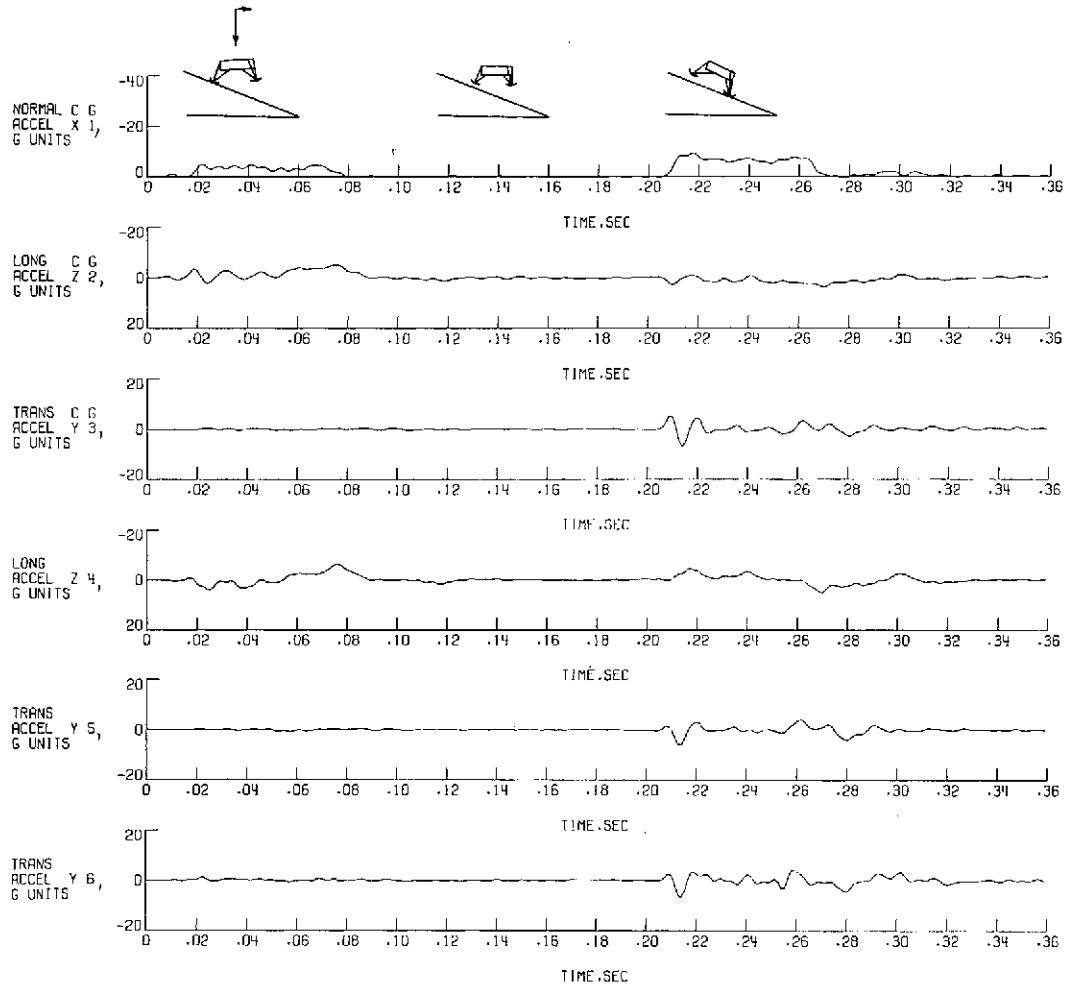

(a) Accelerations (run 4).

Figure 27.- Typical time histories for the cantilever model landing at run 4 conditions. V_v = 6.83 m/sec (22.4 ft/sec); V_h = 2 m/sec (6 ft/sec); pitch, -14°; roll, 180°; yaw, 0.5° right; μ = 0.4; slope, -20°. All values are full scale. See table IV for accelerometer locations.

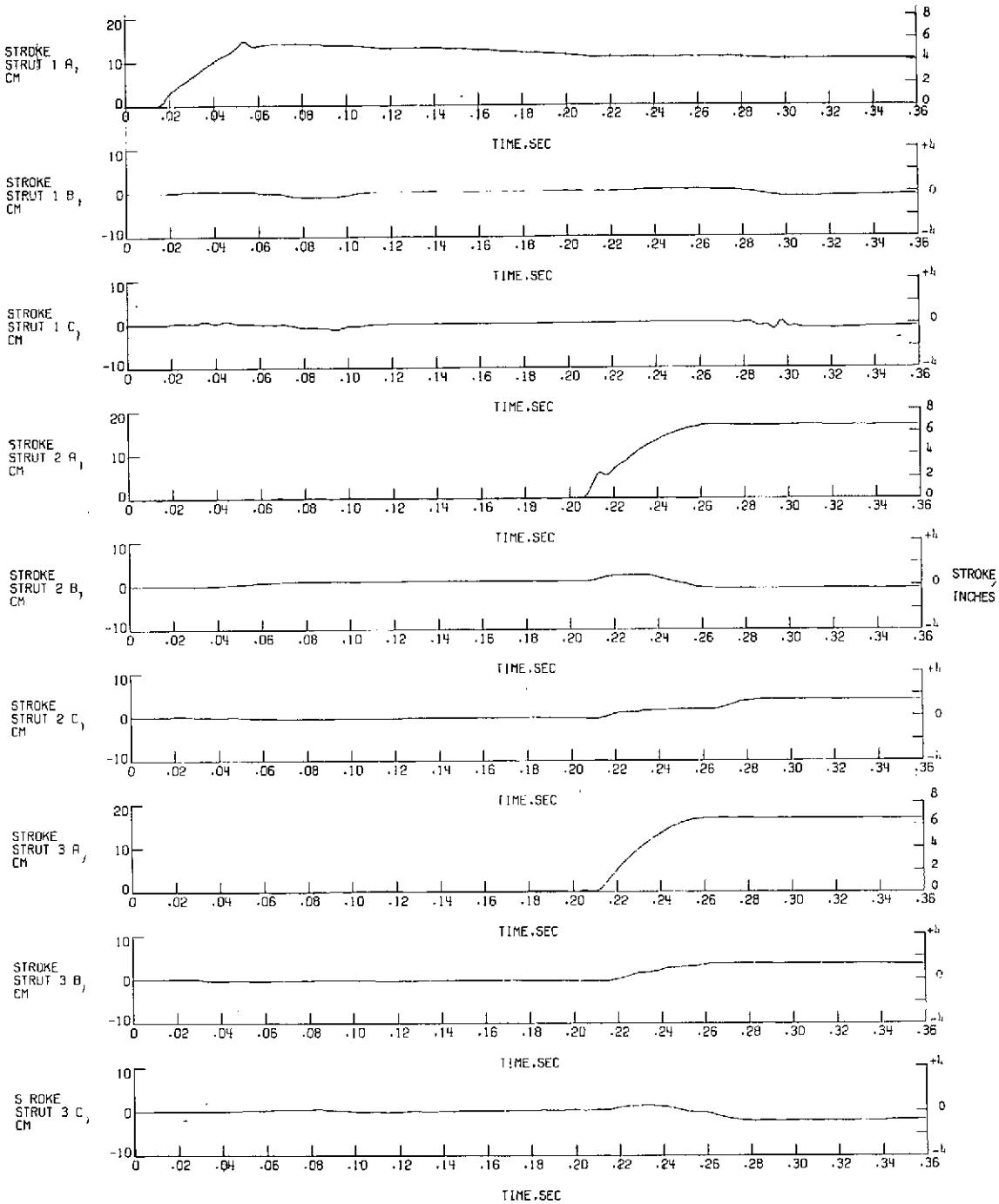

(b) Strut strokes (run 4).

Figure 27.- Continued.

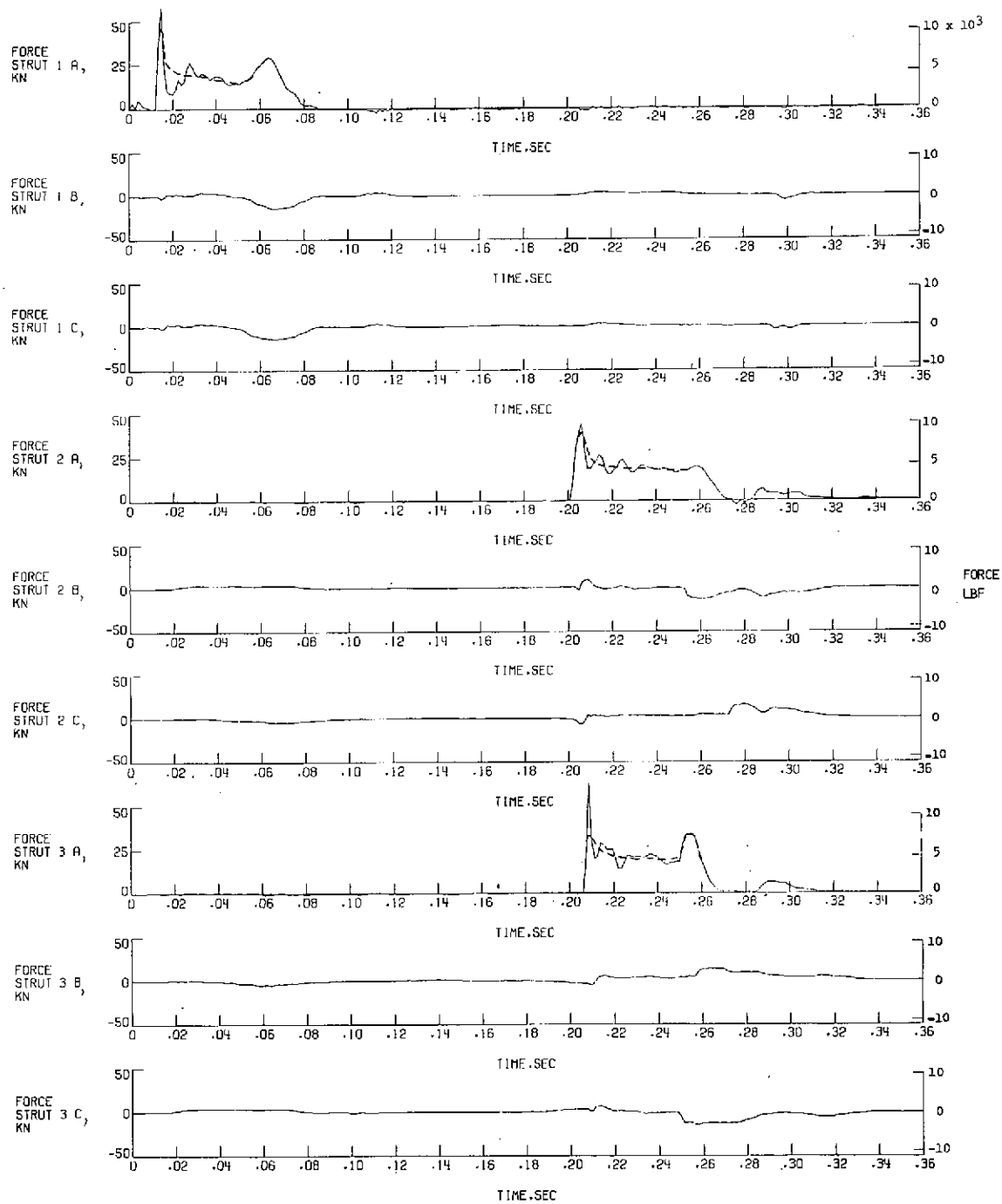

(c) Strut forces (run 4).

Figure 27.- Concluded.

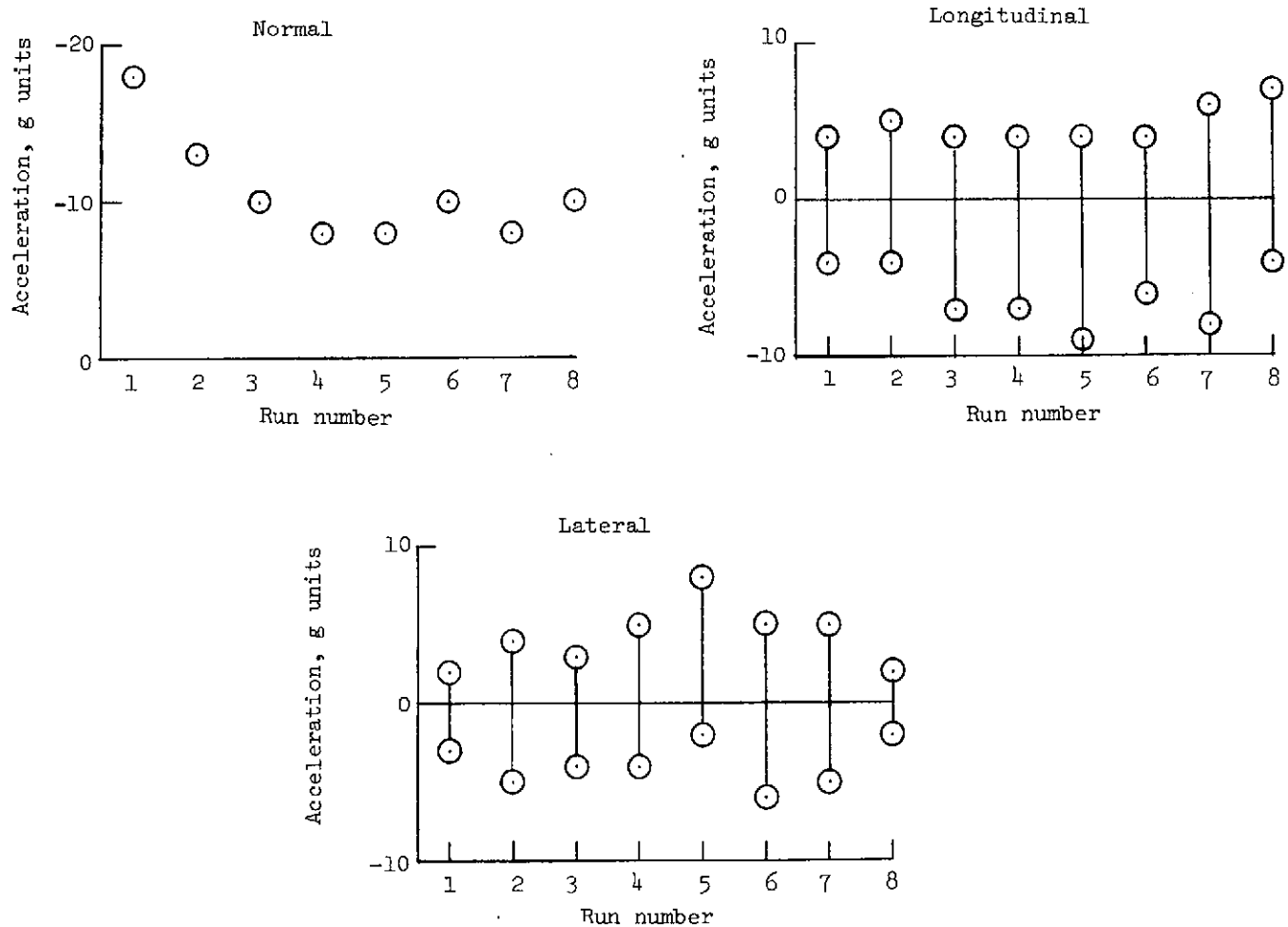

Figure 28.- Maximum acceleration values for inverted tripod model. All values are full scale.

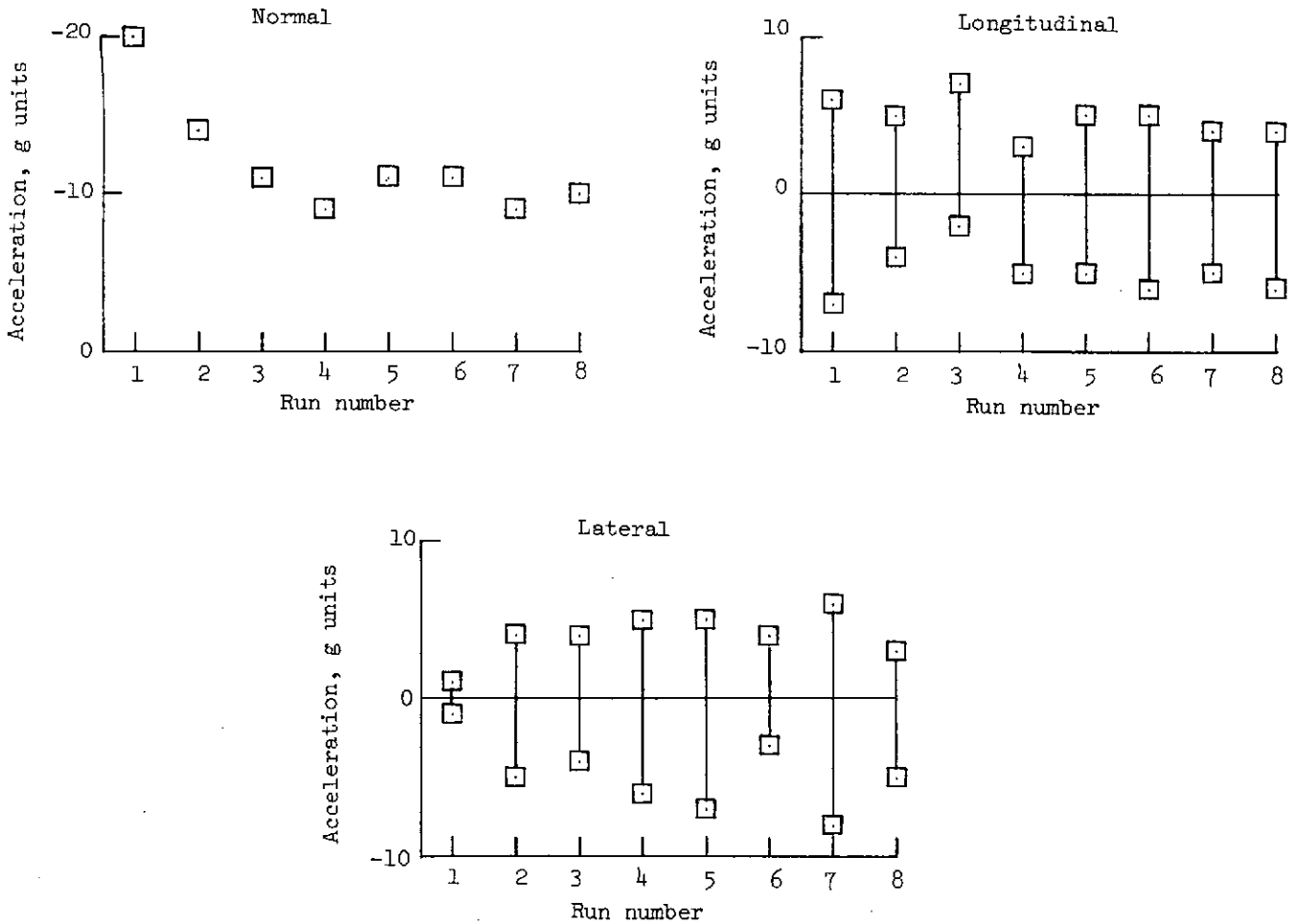

Figure 29.- Maximum acceleration values for cantilever model. All values are full scale.

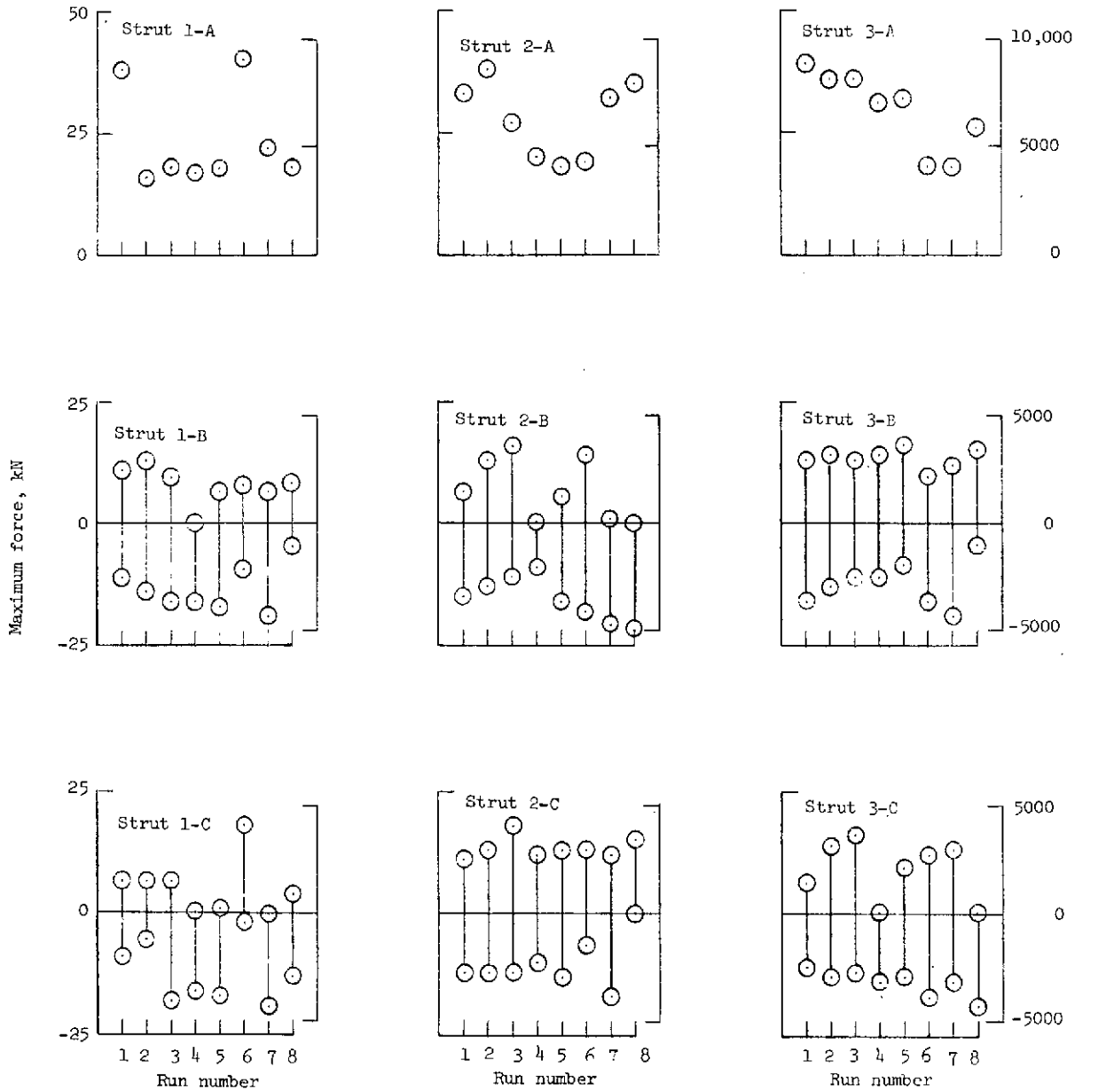

Figure 30.- Maximum force for inverted tripod model. All values are full scale.

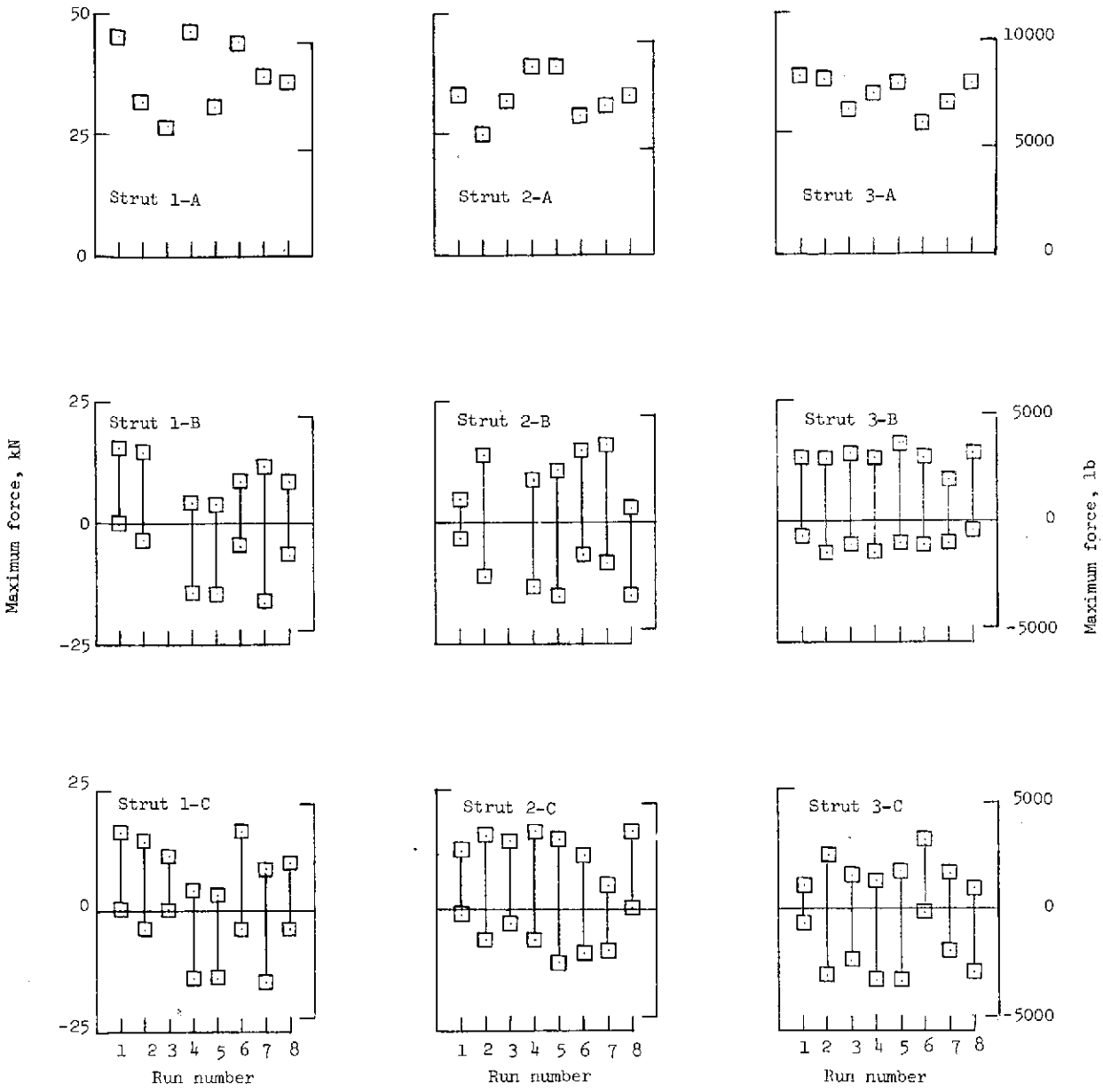

Figure 31.- Maximum force for cantilever model. All values are full scale.

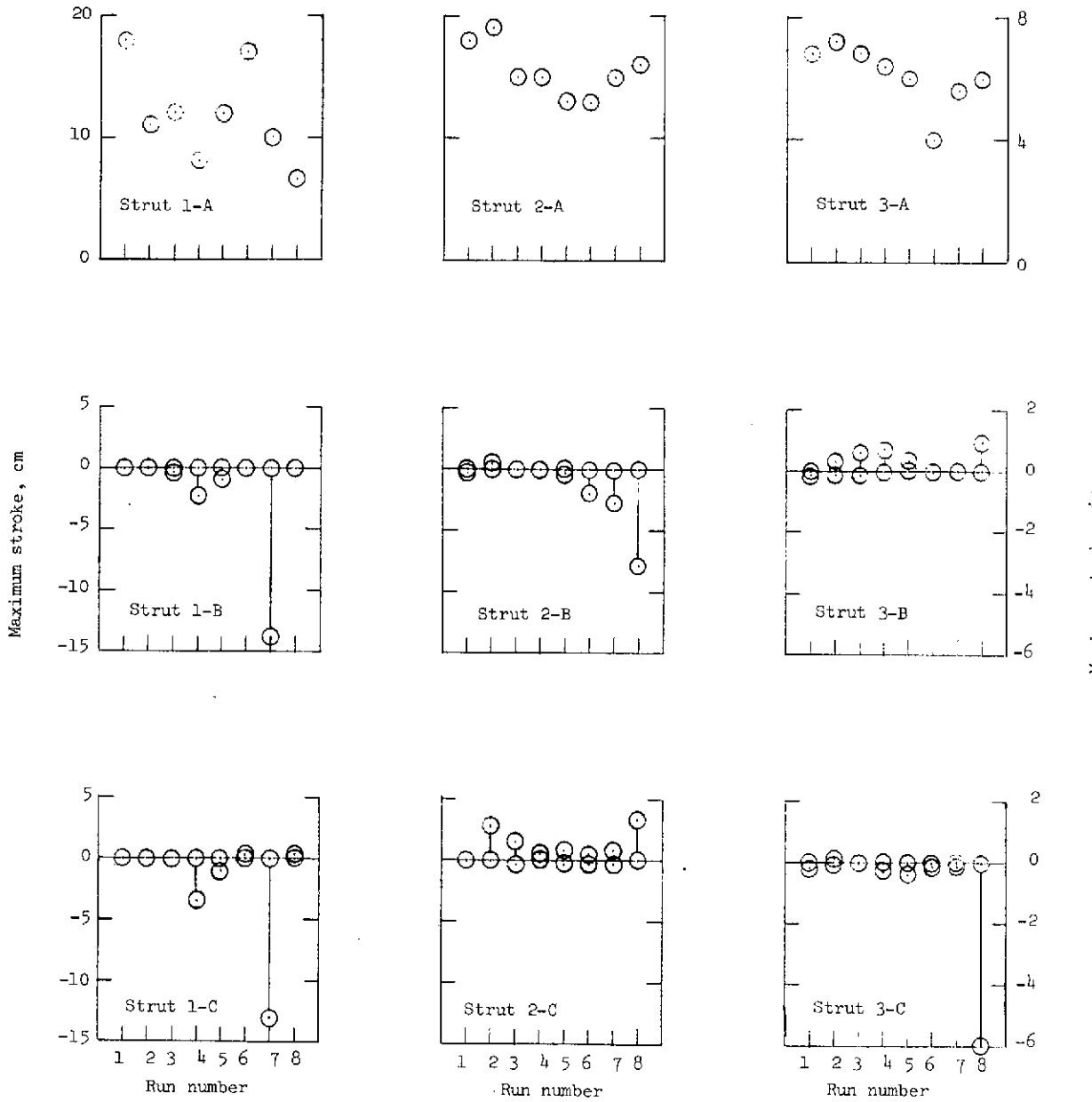

Figure 32.- Maximum stroke values for inverted tripod model. All values are full scale.

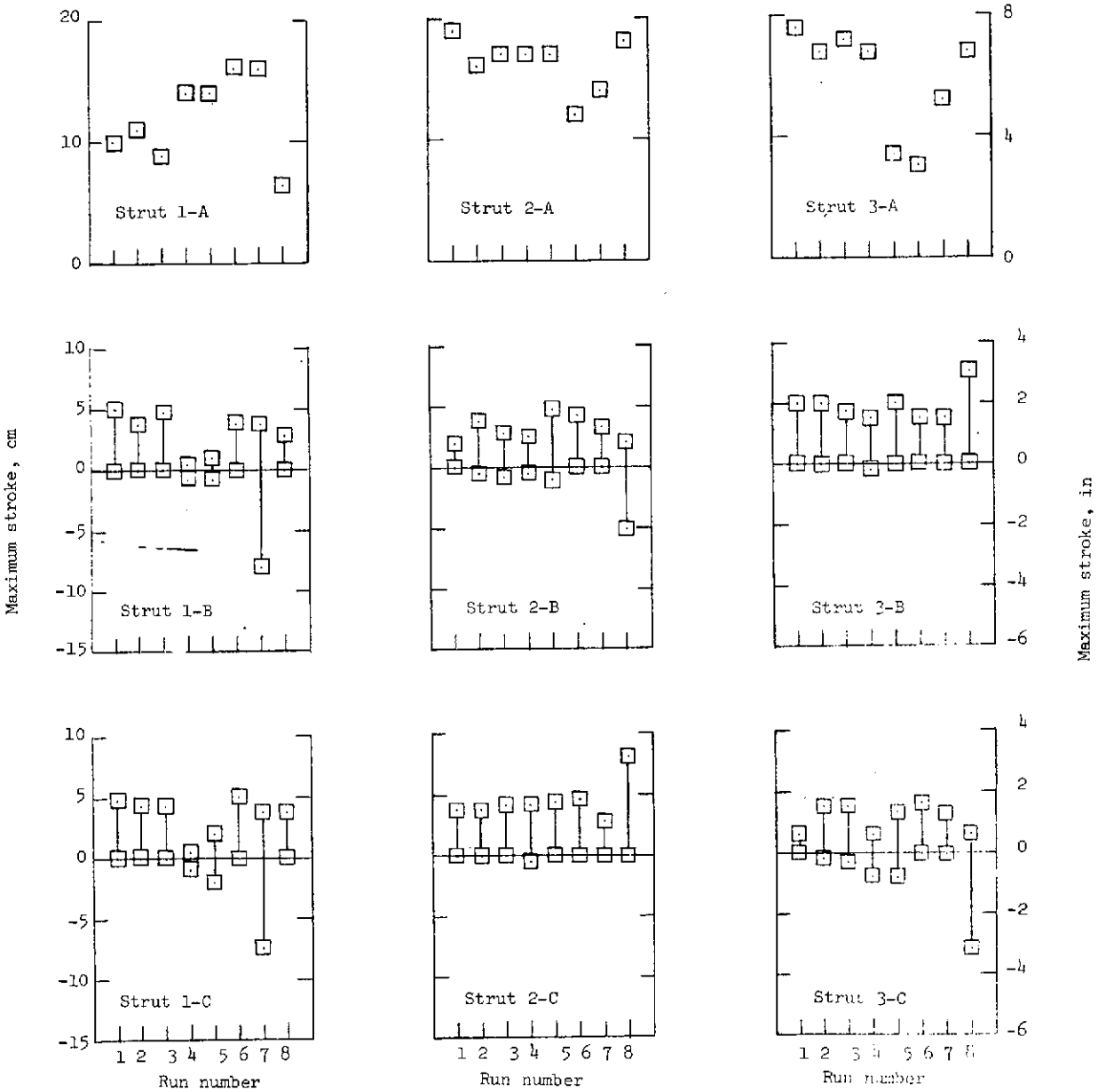

Figure 33.- Maximum stroke values for cantilever model. All values are full scale.

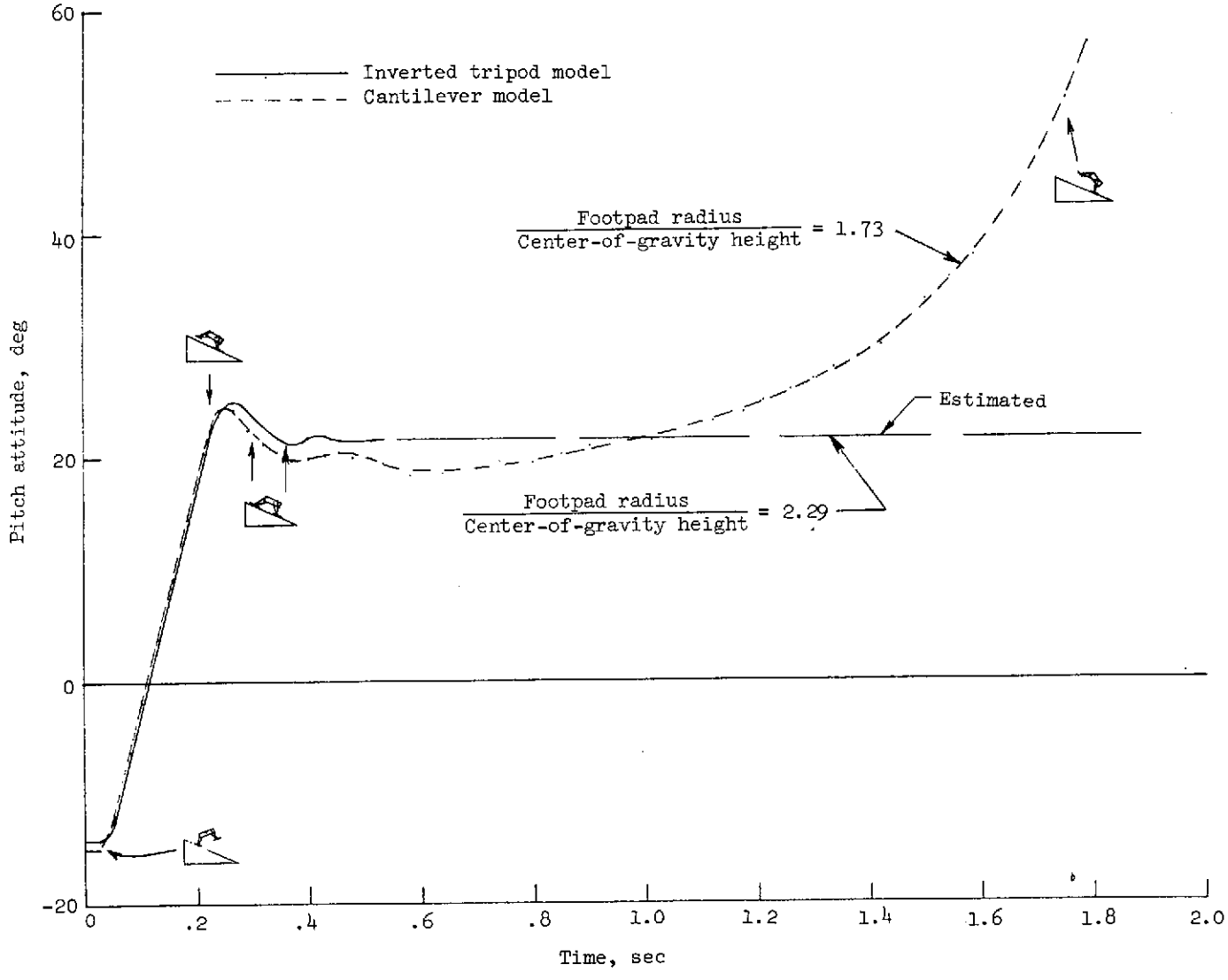

Figure 34.- Pitch-attitude time histories for inverted tripod and cantilever models landed at case 5 conditions. V_v = 6.85 m/sec (22.5 ft/sec); V_h = 2 m/sec (6 ft/sec); pitch, -15°; roll, 180°; yaw, 1° right; μ = 0.8; slope, -20°. All values are full scale.